

December 2019

Characterizing the Material Properties of Abdominal Organs

Blake Allen Johnson
University of Wisconsin-Milwaukee

Follow this and additional works at: <https://dc.uwm.edu/etd>



Part of the [Biomechanics Commons](#)

Recommended Citation

Johnson, Blake Allen, "Characterizing the Material Properties of Abdominal Organs" (2019). *Theses and Dissertations*. 2314.
<https://dc.uwm.edu/etd/2314>

This Dissertation is brought to you for free and open access by UWM Digital Commons. It has been accepted for inclusion in Theses and Dissertations by an authorized administrator of UWM Digital Commons. For more information, please contact open-access@uwm.edu.

CHARACTERIZING THE MATERIAL PROPERTIES OF ABDOMINAL ORGANS

by

Blake Johnson

A Dissertation Submitted in

Partial Fulfillment of the

Requirements for the Degree of

Doctor of Philosophy

in Engineering

at

The University of Wisconsin-Milwaukee

December 2019

ABSTRACT

CHARACTERIZING THE MATERIAL PROPERTIES OF ABDOMINAL ORGANS

by

Blake Johnson

The University of Wisconsin-Milwaukee, 2019
Under the Supervision of Dr. Naira Campbell-Kyureghyan

Understanding the behavior of abdominal organs under load will greatly improve several fields involving injury biomechanics. In order to determine the behavior of abdominal organs under load and be able to predict the response, the mechanical properties need to be properly characterized. The characterization of these properties will provide researchers the ability to create finite element models that will provide a better understanding of the mechanism of injury resulting from traumatic events.

Finite element models of today, that simulate traumatic injuries, lack properly characterized material properties. The current body of literature contains a large range of material property values which could be the result of the wide range of testing methodologies used. Because of this lack of consistency among research, several gaps in knowledge exist for many of the abdominal organs regarding material properties. The gaps in literature were found to be the feasibility of using porcine organ material properties instead of human, the quantification of the effect of strain rate, and the impact of using different testing methodologies on the same organ. Therefore this project quantified the relationship between the elastic modulus, failure stress, and failure strain and strain rate and determined the feasibility of using porcine instead of human organ material properties for the liver, kidney, spleen, prostate, bladder, gallbladder, and intestine. A comparison between the elastic modulus found using a

probing protocol and using an unconfined compression protocol was also made for the liver, kidney, spleen, and prostate. These gaps in literature are addressed through four manuscripts: three regarding solid organs that were tested in compression, and one regarding fluid filled/pressurized organs that were tested in tension.

The elastic modulus, failure stress, and failure strain was found for the prostate, liver, kidney, and spleen at rates ranging from 1%/s to 1000%/s using unconfined compression testing. A strain rate dependency was found for the elastic modulus of all tested solid organs. The failure stress was observed to be strain rate dependent for the liver, kidney, and spleen, while the failure strain was found to be strain rate dependent for only the liver. A numerical model was created to estimate the relationship between these material properties and strain rate. The elastic modulus was also measured using a probing protocol and the human liver, kidney, and spleen were found to be stiffer using the probing method versus unconfined compression testing. Porcine failure stress for the prostate, kidney, liver, and spleen were comparable to that of the human host. The elastic modulus of the porcine liver and spleen were found to be a feasible substitute for the respective organ from the human host.

In tension, the elastic modulus, failure stress, and failure strain of the gallbladder, bladder, and intestines were measured at various rates. The elastic modulus and failure stress were found to be strain rate dependent for all organs measured in tension. A numerical model was created to quantify this strain rate dependency. Porcine tissue was determined to be a feasible substitute for the elastic modulus and failure stress for human intestines and gallbladder. In addition, the failure strain was comparable between human and porcine gallbladder.

The knowledge gained from this research provides useful information that can lead to the improvement of finite element models. Creating models with higher fidelity will produce results with higher accuracy and greater applicability. Advancements in modeling from the current characterization of abdominal material properties will have a positive impact on such areas as forensics, diagnostics, injury prediction, personal protective equipment development, and many other fields.

©Copyright by Blake Johnson, 2019
All Rights Reserved

DEDICATION

This dissertation is dedicated to my Mother, Father, and Brother
for always supporting me in all my endeavors

TABLE OF CONTENTS

Chapter 1 : Introduction	1
1.1 Motivation	1
1.2 Material Testing Methods	7
1.2.1 Unconfined compression	7
1.2.2 Tension	11
1.3 Research Objectives	16
1.4 References	18
 Chapter 2 : Critical Review of Organ Material Properties.....	21
2.1 Liver	22
2.2 Kidney	29
2.3 Spleen	34
2.4 Intestines.....	40
2.5 Bladder	45
2.6 Prostate	49
2.7 Gallbladder	51
2.8 Stomach	52
2.9 Literature Gaps	53
2.10 References	57
 Chapter 3 : Research Scope.....	66
3.1 Research Aims	66
3.2 Experimental Requirements.....	68
3.3 Overview of Experimental Design and Protocols.....	70
 Chapter 4 : Compression Testing.....	75
4.1 Prostate Manuscript.....	75
4.2 Liver and Kidney Manuscript	99
4.3 Spleen Manuscript	140

Chapter 5 : Tension Testing	163
5.1 Tension Testing Manuscript.....	163
Chapter 6 : Conclusion	194
6.1 Summary	194
6.2 Future Work.....	198
6.3 Research Significance/Contributions to the Field	199
Chapter 7 : Curriculum Vitae	204

LIST OF FIGURES

Figure 1-1: Human liver.....	8
Figure 1-2: Human kidney	9
Figure 1-3: Human spleen.....	10
Figure 1-4: Human intestine with lining cut and laid flat	13
Figure 1-5: Picture of human bladder segmented for testing.....	14
Figure 1-6: Human gallbladder	15
Figure 1-7: Human stomach.....	16
Figure 3-1: Flow chart of experimental process.....	72
Figure 4-1: Elastic modulus of human prostate measured at various strain rates and with different testing methods	83
Figure 4-2: Stress versus strain curve of human and porcine prostate under unconfined compression using two testing methodologies	84
Figure 4-3: Elastic modulus of porcine prostate measured at various strain rates and with different testing methods	85
Figure 4-4: The measured elastic modulus of the porcine prostate in unconfined compression at varying rates (shading indicates the range of data).....	86
Figure 4-5: Comparison of measured and predicted relationship between elastic modulus and strain rate of porcine prostate using compression method	88
Figure 4-6: Failure stress of human and porcine prostate at various strain rates using unconfined compression	89

Figure 4-7: Failure strain of human and porcine prostate at various strain rates using unconfined compression	90
Figure 4-8: Porcine kidney placed in MTS	103
Figure 4-9: Stress versus strain curve of liver and kidney specimens from both human and porcine showing failure/yield point.....	105
Figure 4-10: Porcine kidney and liver placed on graph paper	107
Figure 4-11: Stress versus strain of representative samples from the compression and probing protocols for both human and porcine kidney specimens.....	109
Figure 4-12: Experimental and modeled stress-strain curve for both human and porcine kidney specimens at 25%/s strain rate	111
Figure 4-13: Elastic modulus of both human and porcine kidneys in the nondestructive compression protocol at various strain rates. * denotes statistically significant differences	112
Figure 4-14: Average and range of elastic modulus for the porcine kidneys at all rates investigated	113
Figure 4-15: Measured and model predicted elastic modulus of the porcine kidney	114
Figure 4-16: Kidney elastic modulus measured in the probing protocol for both human and porcine specimens at various rates	115
Figure 4-17: Failure stress of the human and porcine kidney measured at various rates	116
Figure 4-18: Average and range of failure stress for the porcine kidney measured at all rates investigated.....	116
Figure 4-19: Measured and model predicted failure stress of the porcine kidney	117

Figure 4-20: Failure strain for both human and porcine specimens measured at various rates	118
Figure 4-21: Stress versus strain of representative samples from the compression and probing protocols for both human and porcine liver specimens at 1%/s strain rate.....	119
Figure 4-22: Experimental and modeled stress-strain curve for both human and porcine kidney specimens	121
Figure 4-23: Elastic modulus of both human and porcine livers at various strain rates	122
Figure 4-24: Average and range of elastic modulus for the porcine livers at all rates investigated	122
Figure 4-25: Measured and model predicted elastic modulus of the porcine liver	123
Figure 4-26: Elastic modulus measured in the probing protocol for both human and porcine liver specimens at various rates	124
Figure 4-27: Failure stress of the human and porcine liver measured at various rates	125
Figure 4-28: Measured and model predicted failure stress of the porcine liver.....	126
Figure 4-29: Failure strain for both human and porcine liver specimens measured at various rates	127
Figure 4-30: Measured and model predicted failure strain of the porcine liver	128
Figure 4-31: Current probing locations for the a) human liver and b) porcine liver and proposed probing location to address limitation	134
Figure 4-32: Human spleen placed between the compression plates of an MTS	145

Figure 4-33: Human spleen placed on the Mark 10-EML test stand for the probing protocol.....	146
Figure 4-34: Representative measured and modeled stress-strain curves of the human and porcine spleen in unconfined compression at a rate of 25%/s.....	148
Figure 4-35: Average elastic modulus for both human and porcine spleen tissue under full unconfined compression at a quasi-static and dynamic rate.....	150
Figure 4-36: Average and range of elastic modulus results for porcine spleen under full unconfined compression at each strain rate.....	151
Figure 4-37: Measured and modeled elastic modulus of the porcine specimens at different strain rates.....	152
Figure 4-38: Failure stress of human and porcine spleen at various rates under unconfined compression	153
Figure 4-39: Measured and modeled failure stress at various strain rates.....	154
Figure 4-40: Failure strain of porcine spleen at various rates under unconfined compression	155
Figure 5-1: A dog-bone shaped specimen from the stomach	168
Figure 5-2: Intestine mounted in MTS system.....	169
Figure 5-3: Intestines tested at 50%/s.....	170
Figure 5-4: Predicted porcine and measured human and porcine gallbladder elastic modulus at each rate tested	172
Figure 5-5: Predicted porcine and measured human and porcine gallbladder failure stress at each rate tested	174

Figure 5-6: Average human and porcine gallbladder failure strain at each rate tested .	175
Figure 5-7: Predicted porcine and measured human and porcine bladder elastic modulus at each rate tested	176
Figure 5-8: Predicted porcine and measured human and porcine bladder failure stress at each rate tested.....	177
Figure 5-9: Average failure strain of human and porcine bladder specimens performed in uniaxial tension testing	178
Figure 5-10: Predicted porcine and measured human and porcine intestine elastic modulus at each rate tested	179
Figure 5-11: Predicted porcine and measured human and porcine intestine failure stress at each rate tested.....	180
Figure 5-12: Average failure strain of porcine and human intestine specimens performed in uniaxial tension testing	181

LIST OF TABLES

Table 2-1: Literature review of the material properties of the liver	25
Table 2-2: Literature review table for kidney material properties	32
Table 2-3: Literature review of Spleen material properties	38
Table 2-4: Literature review table of intestine material properties	43
Table 2-5: Literature review table of bladder material properties	48
Table 2-6: Overview of the literature review of material properties for each organ of interest	56
Table 3-1: Number of experiments completed in nondestructive compression testing protocol.....	72
Table 3-2: Number of experiments completed in destructive compression testing protocol.....	73
Table 3-3: Overview of number of tests completed in probing testing protocol	73
Table 3-4: Overview of number of tests completed in uniaxial tension testing protocol	74
Table 4-1: Tested strain rates for each method and host	81
Table 4-2: Model parameters at tested strain rates for each host.....	87
Table 4-3: Parameters for the material model that describes the relationship between strain rate and elastic modulus	88
Table 4-4: Strain rates used in each of the protocols in the kidney experimental testing	105

Table 4-5: Strain rates used in each of the protocols in the liver experimental testing	106
Table 4-6: Average and standard deviation of the model parameters and R^2 of model fit to experimental results for the kidney at tested strain rates for each host in the nondestructive testing protocol	110
Table 4-7: Parameters for the material model that describes the relationship between strain rate and elastic modulus for porcine kidneys.....	114
Table 4-8: Parameters for the material model that describes the relationship between strain rate and failure stress for porcine kidneys	117
Table 4-9: Model parameters for liver at tested strain rates for each host.....	120
Table 4-10: Parameters for the material model that describes the relationship between strain rate and porcine liver elastic modulus	123
Table 4-11: Parameters for the material model that describes the relationship between strain rate and porcine liver failure stress	126
Table 4-12: Parameters for the material model that describes the relationship between strain rate and porcine liver failure strain	128
Table 4-13: Strain rates used in each of the protocols in the spleen experimental testing (✓ represents that only elastic modulus was measured, and x represents that failure properties were also measured)	144
Table 4-14: Average and standard deviation of the modeled variables for both human and porcine specimens in unconfined compression	149
Table 4-15: Values for the parameters of Eq. 5.....	152
Table 4-16: Values for the parameters of Eq. 5.....	154
Table 5-1: Testing strain rates utilized for different organs and hosts	169

Table 5-2: Values of the model parameters that most accurately predicted elastic modulus	172
Table 5-3: Values of the model parameters that most accurately predicted failure stress	174
Table 5-4: Values of the model parameters that most accurately predicted elastic modulus	176
Table 5-5: Values of the model parameters that most accurately predicted the failure stress of porcine bladder at various rates	177
Table 5-6: Values of the model parameters that most accurately predicted the elastic modulus of porcine intestine at various rates.....	179
Table 5-7: Values of the model parameters that most accurately predicted the failure stress of porcine intestine at various rates	180
Table 6-1: Results to all research objectives for each organ.....	195
Table 6-2: List of peer-reviewed publications, conference presentations/abstracts/papers and technical reports *presented in this dissertation	201
Table 6-3: List of honors and awards since the start of PhD	203

LIST OF DEFINITIONS

ANATOMICAL:

Abdominal organs: The spleen, stomach, small intestine, large intestine, liver, spleen, kidney, etc.

In-situ: Refers to experiments conducted within the host.

In-vitro: Refers to experiments conducted outside the living organism.

In-vivo: Refers to experiments conducted on a living organism.

Capsule: A tough fibrous layer surrounding an organ.

Parenchyma: The bulk of functional substance in an organ.

BIO-MECHANICAL:

Boundary conditions: A condition that is required to be satisfied at all or part of the boundary of a region in which a set of differential equations is to be solved.

Elastic Modulus/Stiffness (E): The ratio of the force exerted upon a substance or body to the resultant deformation.

Failure Strain ($F\varepsilon$): The point where the deformation of a material body results in the structure rupturing.

Failure Stress ($F\sigma$): The point where the force exerted upon a material body results in the structure rupturing.

Strain Rate: The change in strain of a material with respect to time.

Strain (ε): A geometrical measure of deformation representing the relative displacement between particles in a material body.

Stress (σ): Pressure or tension exerted on a material object.

Pressure/pressure wave: A load in which the disturbance varies as it propagates through a medium.

Threshold: The magnitude that must be exceeded in order for a certain reaction to occur.

Probing: Uniaxially compressing a specimen using an object with a surface area that is smaller than the surface area of the object.

Unconfined compression: Uniaxial compressive loading on a specimen that is not bound in any other axes.

Tension: Stretching a specimen in one direction.

ACKNOWLEDGMENTS

I would first like to express my sincerest appreciation for my advisor Dr. Naira Campbell-Kyureghyan for not only providing me the opportunity to pursue a Doctorate in Philosophy, but also for her mentorship and guidance that took me to achievements that I didn't think were possible. For this, I will be forever thankful.

I would also like to thank my committee members Dr. Scott Campbell, Dr. Ronald Perez, Dr. Wilkistar Otieno, and Dr. Hamid Seifoddini for their contributions and guidance throughout my degree. Their comments and suggestions were valuable in strengthening my research. I would also like to express gratitude for my laboratory colleagues. Their support and friendship throughout my time in the lab will be forever remembered.

Chapter 1 : Introduction

1.1 Motivation

Injuries to the abdomen from traumatic situations can often be fatal. The exact mechanisms of injury are not fully known but often speculated. It has been suggested that the organs can rupture due to the force of an impact directly to the abdomen or the resulting compression of the organ against other structures in the cavity. Also, the overpressure/negative pressure from blast injuries can result in the rupture of pressurized organs such as the stomach and intestines. Common sources of abdominal injury are from car accidents and exposure to blast forces. The severity of the injuries in the automotive industry has been well documented. Approximately 9,000 people in the United States sustain moderate to severe abdominal injuries in 2009 [1]. Abdominal injuries sustained from car accidents generally concentrated on the solid organs (61%), but other organs within the digestive system are also commonly affected (17%) [2].

Although the use of explosive devices is a focal point of modern warfare, only recently is the increasing danger of injuries due to blast forces being revealed. In operation Iraqi Freedom the primary threat was improvised explosive devices (IED) [3]. Over 40,000 service members have been wounded and over 5,500 have been killed (Sayer, 2008; Murray, 2005). Eighty percent of the injuries reported by a military medical unit were the result of IEDs [6]. An increase in blast injuries among soldiers is due to the increasing number of explosive devices. Blasts are commonly due to improvised explosive devices (IEDs), as well as rocket and mortar shells, mines, aerial bombs and rocket-propelled grenades (RPGs).

Research has determined that there are multiple mechanisms of injury from blast forces. Because of the variety of mechanisms, these injuries from blasts are described as polytraumatic or causing injury to multiple body systems [7]. Due to the complex nature of the harm, blast injury has been described as the most difficult to manage [8]. There are five mechanisms of injury due to blasts that has been described in the literature: primary, secondary, tertiary, quaternary and quinary [9].

Primary injuries are caused by an over pressure shock wave followed by a negative pressure wave which travels through the body. While the exact mechanism of how a shock wave causes damage to the brain is under investigation, theories include the direct passage of the wave into the brain causing shear forces on the tissues [10]. Tympanic membrane ruptures and lung injuries are also caused by these shock waves [7]. Secondary injuries are created by objects propelled from the explosion and are considered the most common cause of blast-related injury [11]. Penetrating injuries and lacerations are common injuries due to these fragments.

Tertiary injuries are caused by an indirect result from the blast such as the fall to the ground of the victim being thrown back from the blast wave or a wall collapsing on the victim due to the explosion. Blunt and crushing injuries such as fractures, traumatic amputations and compartment syndromes are common tertiary injuries [12]. Quaternary blast injuries are a result of the explosion but not from the force of the blast. An example of a quaternary blast injury is a burn or exposure to a toxic from the exploding element [12].

Due to the nature of the blast, organs that are of primary risk for injury are ones that contain gas such as the lungs and intestines, but injuries to solid organs such as spleen,

kidneys, liver, and testicles have also been described in the literature [12]. Although the lungs are of primary risk, the diagnostic and treatment of such injuries are more readily identifiable [6]. Injuries occurring within the abdomen due to blasts are a diagnostic challenge as symptoms can be clinically silent until complications intensify [12]. Several cases of fatalities from blast injuries occur to people that on the surface were believed to be fine [13].

In order to save these soldiers' lives, better personal protective equipment needs to be created. However, personal protective equipment is only effective if it can lower the exposed forces below the threshold that would cause serious injury or death. For this it is required to know what level of applied force is required to produce serious injury or organ failure. These factors are only found when the mechanisms of injury are known. Since it is impossible to monitor a real-life scenario where *in-situ* organs are subjected to a blast, an alternative method of simulation must be used.

Finite elemental models are a powerful tool with a wide range of applications, and have become popular in the field of biomedical engineering. Finite element modelling can create estimated solutions to questions that otherwise would not be feasible in a laboratory setting. Models incorporate material properties, geometries, and boundary conditions to digitally reconstruct an environment. The ability to recreate an environment digitally means that the type of simulations that can be performed are endless. However, a finite element simulation is literally only as accurate as the sum of its parts. This means that accurate digital geometric reconstruction, accurate boundary conditions, realistic loading scenarios, and accurate material properties are required in order to get the most precise estimations. Accurate geometric reconstruction can be

checked through imaging modalities such as CT and MRI scans [14]. Boundary conditions can be optimized through running simulation on known results [15].

However, correct material properties of the organs of interest can be more difficult to determine. Finite element models need such parameters as the elastic modulus, failure stress, and failure strain, among others. The elastic modulus is a measure of the ratio between a materials stress and strain. It provides useful information to know how the deformation of a body, changes with the applied loading. In a finite element model this information will be a main factor in formulating how the organ deforms when a large force is applied to the abdomen. Failure stress and failure strain are also key material properties as these variables identify how much pressure or how much deformation the tissue can withstand prior to failure. In a model designed to help save lives, a solid understanding of what situations will result in organ structural failure is important. Failure stress and failure strain provide the threshold for organ rupture. In order to determine these material properties mechanical testing must be performed on the tissues of interest.

The simulation tool of finite element analysis uses the material properties and mathematical concepts to predict how the modeled objects will respond to applied force. A few studies have been designed to model the abdominal organ response to blunt trauma and blasts, however there are some common issues with the material properties that are used within these models [16-18]. For example, the properties were found using quasi-static methods when the model is simulating high velocity impacts. Previous articles, which will be further explored in Chapter 2, have shown that the material properties of organs change when tested at different rates [19]. A material property

found using quasi-static testing might not yield accurate results when used in a dynamic simulation. The relationship between different material properties and strain rate has yet to be determined and the point at which this relationship start to saturate has yet to be found.

Additionally, analyzing the various material properties from the published literature, the testing method used to determine the property influences the results. Thus in order to get the most accurate material properties it is suggested that the tissues should be testing in a manner that mimics the force application of the situation. A third issue is the material properties are found using hosts other than humans. For example, models have used material properties of bovine, porcine, or sheep organs. The host from which the tissue came from could impact the material characteristics. Previous literature has shown that the material properties for at least some organs are different from animal tissue and are strain rate dependent [19, 20]. However, these tests were conducted in a way that is not reflective of type of forces these organs would experience in a traumatic situation. Finding the differences and similarities between human and animal hosts, for the testing methods and at the strain rates required, will benefit the scientific community as resources are more readily available for the material testing of animal organs.

The methodology used to determine the material properties is of the upmost importance in determining whether they are appropriate for the intended purpose. As was highlighted earlier, different methodologies can yield different measured material properties. This means that to obtain the most accurate material properties for a finite element model, the methodology should ideally reflect the scenario that the model is

simulating, which often depends on the organ type. In general, the structure of abdominal organs can be separated into two categories, solid organs and fluid filled/pressurized organs. In an impact applied to the anterior or posterior section of the abdomen, the entire body will be subject to compression loading. During this loading condition, solid organs will be placed in compression by either being trapped between other structures in the body or by the two outer walls of the abdomen. Fluid filled/pressurized organs on the other hand generally only consists of a lining and thus rupture will not occur due to compressing the tissue, but by stretching the balloon-like surface. In order to better understand which organ will require what type of testing, and to provide insight on why each tissue behaves in a given way, an overview of the anatomy of the different organs for each of the testing categories is required.

The goal of this research is to characterize the mechanical properties of selected abdominal organ tissue in order to better understand the injury threshold in various traumatic situations. Based on more accurate simulation results, better personal protective equipment may be created that will save more lives. The specific principal aim of this research is to establish the organ material properties under dynamic rates, which can be utilized in the development of a human abdominal model. The primary focus of the model will be organs within the abdominal cavity as the mechanisms to lung injury are known and diagnosis is often clear. A solid understanding of the tissues of interest including the anatomy of the organs inside the abdominal cavity is required to ensure proper material testing methods and to be able to draw proper conclusions based on the results.

1.2 Material Testing Methods

The two main testing methods used in this study, unconfined compression and tension, are investigated along with their relationship to the organ composition and expected *in-vivo* loading. In order to understand the proper testing methodologies that are most realistic form mimicking blunt trauma and to gain greater insight into why specific results were obtained for the different organs an understanding of the anatomy within the abdominal cavity is required. The abdominal cavity is located just below the thoracic cavity, separated by the thoracic diaphragm, and just above the pelvic cavity, separated by the opening of the pelvic inlet. Several vital digestive organs are housed in this cavity which is surrounded by muscle, fat, and peritoneum. The cavity consists of the intestines, stomach, kidney, spleen, liver, gallbladder, pancreas, and adrenal glands. These organs can be separated into two broad classifications: solid organs and fluid/pressurized organs.

The pelvic cavity, which sits just below the abdominal cavity, is the space between the pelvic inlet and the pelvic floor. All the reproductive organs and some of the digestive organs are housed within this cavity. The digestive organs are the urinary bladder, rectum, and colon.

1.2.1 Unconfined compression

The solid organs within the abdominal cavity all share a common attribute, which is that they have a capsule that surrounds the organ, and within the capsule is the parenchyma, which is the functional part of the organ. The members within this group of organs that will be the focus of this study are the liver, kidney, spleen, and prostate.

All these organs will be placed in compression because of the structure and geometry of the abdomen. However, there are some differences between these organs that need to be highlighted, even though the overall organ structure is similar.

The liver (Figure 1-1) is a large organ located in the upper right quadrant of the abdomen. Its main function is to detoxify various metabolites, synthesize proteins, and produce bile. The layers of the liver consist of a double layer capsule, known as the peritoneum, which covers the parenchyma, the functional part of the liver. The liver tissues material properties can be affected by multiple factors, such as alcoholism, which in turn create scarring/hardening of the tissue. The cause or associated factors contributing to the death of the cadaver host should be known prior to the testing of the liver in order to obtain suitable specimens and to potentially compensate for confounding factors [21]. During blast or traumatic accident, the liver will be subject to forces applied from either the posterior or anterior side of the body forcing the organ into compression.



Figure 1-1: Human liver

The normal human body has two kidneys located on the right and left side of the spine, between the twelfth thoracic and third lumbar vertebrae. On the right side of the body the kidney (Figure 1-2) is slightly lower due to the presence of the liver. The main function of this bean shaped organ is to cleanse blood through filtration, reabsorption, secretion, and excretion. A renal capsule surrounds the kidney functional tissue. This layer is constructed of thin fibrous tissue that is also surround by adipose tissue. The first layer of the parenchyma is the renal cortex, a continuous smooth tissue surrounding the kidneys just below the renal capsule. Below this tissue resides the veins, arteries, and tissues that make up the renal medulla. Similarly to the liver, the kidney would be placed in compression when the abdomen is subjected to traumatic forces, and as the force increases on the abdomen the kidney will be further compressed by portions of the ribcage as well as the anterior and posterior portions of the body. Therefore, in order to test this kidney in a manner similar to the injury scenario, the kidney should be tested under compression.



Figure 1-2: Human kidney

The human spleen (Figure 1-3) is located in the upper left-hand side of the abdominal cavity between the 9th and 11th rib, just behind the stomach. Blood filtration is the primary role of the spleen. It is surrounded by a connective tissue capsule which holds the parenchyma. Two different types of tissue makeup the parenchyma, red pulp and white pulp. The soft pulpy structure of the spleen is similar to that of a lymph node. Pulp is viscous in nature and thus the spleen can resemble a fluid filled sack. Due to the location of the spleen, it is susceptible to compressive forces during a traumatic blunt force impact to the abdomen. The spleen will be compressed against the ribcage by other surrounding organs or the outer body.



Figure 1-3: Human spleen

The prostate sits within the pelvic girdle and is connected to both the urethra, which runs through the prostate, and the bladder. All three structures are a part of the digestive system of the male body, but the prostate's main function is in aiding

reproduction. The main functional tissue of the prostate is called the stroma which is made up of connective tissues and muscle fibers. Like all solid organs, the prostate has a surrounding tissue called the capsule made up of only connective tissue. Although the prostate is protected by the pelvic girdle, there exists the potential of being placed in compression if the abdomen is impacted with a large force. The compressive load would be placed parallel to the urethra and push the prostate against the pelvis and sacrum. Testing of this tissue should be similar, with the load being placed parallel to the urethra on the anterior/posterior sides of the prostate.

Similarities in the solid organs include the structure of a parenchyma housed within a capsule. It has been found that each of these structures can result in their own material properties, but these individual component material properties might not reflect how the structure behaves as a whole. In order to understand the material properties of solid organs, these structures must remain intact. Previous literature split a single organ into multiple samples for testing in order to increase sample size and obtain statistical significance. However, based on the structure of these organs, if these organs are segmented into smaller pieces the capsule will be destroyed and thus only the parenchyma is essentially being tested. Therefore, only the incisions necessary to separate the organ from the host should be made when harvesting for testing.

1.2.2 Tension

Due to the lack of internal solid material, gas/liquid filled organs can compress with little resistance. However, when loaded in tension, either from internal pressure or due to external loads, injury and failure are possible. Therefore, these organs are

typically tested in tension. This section discusses each gas/liquid filled organ, their internal structure, and the relationship with tension testing.

The intestines (Figure 1-4) are separated into two different sections, the small and large intestine. Although larger in diameter, the large intestine is smaller in surface area, 2 m^2 , in relation to the small intestine. The main function of the large intestine is to absorb water. With an area of approximately 30 m^2 , the small intestine is split into three different sections: the jejunum, ileum, and duodenum. This section of the intestines is responsible for absorbing carbohydrates, proteins, fats, vitamins, etc. into the blood stream. Both portions of the intestines have a similar structure. The outer structure consists of five layers: the mucosa, submucosa, thick muscle, subserosa, and serosa. Digested food travels through the intestines and thus it is considered a pressurized/hollow organ. Because of the pressure within the intestines, this organ will act in a manner similar to a balloon when subjected to an external load. If a compressive load is placed on the structure, the air within the balloon or intestine will expand, placing the lining of the structure in tension. In order to obtain accurate material properties of the intestine during a blunt force impact, the organ should be tested under tension.



Figure 1-4: Human intestine with lining cut and laid flat

The function of the bladder is to store urine prior to the process of urination. It is located in the base of the pelvic girdle just posterior and superior of the pubic symphysis. Similar to a balloon, the bladder will expand based on the level of urine deposited into this organ, or in response to internal or external pressure. The lining (functional part of the tissue) is made up of several layers of muscle tissue which allows the organ to contract to force urine out of the bladder in the process of urination. The pressure within the hollow organ is dependent on the amount of urine, however the forces that the bladder tissue will experience is similar to the intestine. Force placed on the abdomen will translate to tensile forces on the bladder tissue and thus the organ should be tested by being segmented into a dog bone shape specimen (Figure 1-5) and loaded using uniaxial tension methods.



Figure 1-5: Picture of human bladder segmented for testing

The gallbladder (Figure 1-6) is a hollow organ that is located posterior and inferior of the liver. A digestive enzyme called bile is stored within the gallbladder. During the digestive process, the gallbladder is required to contract and secrete bile into the small intestine in order to absorb the fat that has been consumed. Due to the unique function of the gallbladder, the lining is a complex structure of several different layers. The inner most layer is made of microvilli that is similar to the walls of the intestine. A layer of muscle tissue follows which provides the ability for the gallbladder to contract. The outer most layer is made up of a serosa layer that contains blood vessels and lymphatics. The balloon like structure of the gallbladder is very similar to the urinary bladder. The gallbladder will most likely be compressed by the liver and ribcage, but this compressive load will translate into a tensile load that is placed on the structure of the gallbladder.



Figure 1-6: Human gallbladder

The stomach is a thick-walled organ essential for digestion and is the second stop for food in the digestion process after the mouth. During digestion, food enters through the esophagus and is housed in the stomach. Food is broken down through the secretion of several enzymes into the stomach. The stomach is a hollow organ with a multilayered structure for a lining (Figure 1-7). The lining of the stomach broken down into four layers, the mucosa, submucosa, muscularis externa, and serosa. The first layer is the rugae which is used in digestion. The submucosa, muscularis externa, and serosa are involved in the process of contracting the stomach to turn food which helps digestion. This hollow organ will be subject to tension during traumatic loading, and thus tension testing is appropriate for determining material properties.



Figure 1-7: Human stomach

Each of the hollowed/fluid filled organs structure is comprised of an outer tissue structure surrounding the hollow interior. However, each organ differs with respect to the number of layers and types of tissues that are within these layers. The material properties of these organs are dependent on all layers working together as a complete structure. Testing that would reflect these organs being subjected to large forces placed on the abdomen should have each layer of the lining remain intact and use a tension protocol.

1.3 Research Objectives

The overall goal of this research is to either establish or improve the characterization of the material properties of human abdominal organs. In order to accomplish this goal, a series of research studies have been performed. This dissertation will be split into five different chapters and within those chapters, the goals and

outcomes of each study are compiled into manuscripts. Thus, each research study will be a part an independent paper. The current chapter introduces the readers to the motivation of the project, provides a brief overview of organ anatomy, and includes the rationale for the testing methods that will be used. Chapter 2 will be an overview of the current body of literature which will determine the state of knowledge for the organ material properties. The literature review will also highlight the research gaps, which vary for each organ, that will be addressed in this dissertation. Chapter 3 addresses the specific scope of the project and provides a brief overview of the breadth of work that was accomplished. Chapter 4 covers the research conducted on organs that were in the compression testing category while Chapter 5 covers the research conducted on organs that required tension testing. Finally, Chapter 6 summarizes the research results and the novel information that was found for all organs of interest.

1.4 References

- [1] MacKenzie, E. J., and Fowler, C. J. (2008). Epidemiology. In D. V. Feliciano, K. L. Mattox, and E. E. Moore (Eds.), *Trauma, 6th Edition* (pp. 25-40). New York: The McGraw-Hill Companies, Inc.
- [2] Yoganandan, N., Pintar, F. A., Gennarelli, T. A., and Maltese, M. R. (2000). Patterns of Abdominal Injuries i Frontal and Side Impacts. *Annals of Advances in Automotive Medicine*, 44, 17-36.
- [3] Gondusky, J. S., & Reiter, M. P. (2005). Protecting Military Convoys in Iraq: An Examination of Battle Injuries Sustained by a Mechanized Battalion During Operation Iraqi Freedom II. *Military Medicine*, 170(6), 546-549.
- [4] Sayer, N. A., Chiros, C. E., Sigford, B., Scott, S., Clothier, B., Pickett, T., & Lew, H. L. (2008). Characteristics and Rehabilitation Outcomes Among Patients with Blast and Other Injuries Sustained During The Global War on Terror. *Archives of Physical Medicine and Rehabilitation*, 89(1), 163-170.
- [5] Murray, C. K., Reynolds, J. C., Schroeder, J. M., Harrison, M. B., Evans, O. M., & Hospenthal, D. R. (2005). Spectrum of Care Provided at an Echelon II Medical Unit During Operation Iraqi Freedom. *Military Medicine*, 170(6), 516-520.
- [6] Mackenzie, I. M., & Tunnicliffe, B. (2011). Blast Injuries to the Lung: Epidemiology and Management. *Philosophical Transactions of the Royal Society B: Biological Sciences*, 366(1562), 295-299.
- [7] Champion, H. R., Holcomb, J. B., & Young, L. A. (2009). Injuries from Explosions: Physics, Biophysics, Pathology, and Required Research Focus. *Journal of Trauma and Acute Care Surgery*, 66(5), 1468-1477.
- [8] Gawande, A. (2004). Casualties of War—Military Care for the Wounded from Iraq and Afghanistan. *New England Journal of Medicine*, 351(24), 2471-2475.
- [9] DePalma, R. G., Burris, D. G., Champion, H. R., & Hodgson, M. J. (2005). Blast Injuries. *New England Journal of Medicine*, 352(13), 1335-1342.

- [10] Leung, L. Y., VandeVord, P. J., Dal Cengio, A. L., Bir, C., Yang, K. H., & King, A. I. (2008). Blast Related Neurotrauma: A Review of Cellular Injury. *Molecular and Cellular Biomechanics*, 5(3), 155-168.
- [11] Warden, D. (2006). Military TBI During the Iraq and Afghanistan Wars. *The Journal of Head Trauma Rehabilitation*, 21(5), 398-402.
- [12] Horrocks, C. L. (2001). Blast Injuries: Biophysics, Pathophysiology and Management Principles. *Journal of the Royal Army Medical Corps*, 147(1), 28-40.
- [13] Yeh, D. D., & Schechter, W. P. (2012). Primary Blast Injuries—An Updated Concise Review. *World Journal of Surgery*, 36(5), 966-972.
- [14] Chauhan, N., Badgurjar, M. K., & Saxena, P. (2019). A Prospective Study Of Assessment of Solid Organs in Cases of Blunt Abdominal Trauma. *International Journal of Scientific Research*, 8(3).
- [15] Martelli, S., & Viceconti, M. (2010) Mechanical Testing Of Bones: The Positive Synergy Of Finite-Element Models And In Vitro Experiments. *Philosophical Transactions of the Royal Society: Mathematical, Physical, and Engineering Sciences*, 368(1920), 2725-2763.
- [16] Stuhmiller, J. H., Chuong, C. J., Phillips, Y. Y., & Dodd, K. T. (1988). Computer Modeling of Thoracic Response to Blast. *The Journal of Trauma*, 28(supp1), 132-139.
- [17] Roberts, J. C., O'Connor, J. V., & Ward, E. E. (2005). Modeling the Effect of Nonpenetrating Ballistic Impact as a Means of Detecting Behind-Armor Blunt Trauma. *Journal of Trauma and Acute Care Surgery*, 58(6), 1241-1251.
- [18] Shen, W., Niu, Y., Mattrey, R. F., Fournier, A., Corbeil, J., Kono, Y., & Stuhmiller, J. H. (2008). Development and Validation of Subject-Specific Finite Element Models for Blunt Trauma Study. *Journal of Biomechanical Engineering*, 130(2), 1-13.
- [19] Kemper, A. R., Santago, A. C., Stitzel, J. D., Sparks, J. L., & Duma, S. M. (2010, January). Biomechanical Response of Human Liver in Tensile Loading. *Advances in Automotive Medicine/Annual Scientific Conference*, (54), 15.

- [20] Brunon, A., Bruyere-Garnier, K., & Coret, M. (2010). Mechanical Characterization of Liver Capsule Through Uniaxial Quasi-Static Tensile Tests Until Failure. *Journal of Biomechanics*, 43(11), 2221-2227.
- [21] Srinivasa Babu, A., Wells, M. L., Teytelboym, O. M., Mackey, J. E., Miller, F. H., Yeh, B. M., ... & Venkatesh, S. K. (2016). Elastography In Chronic Liver Disease: Modalities, Techniques, Limitations, and Future Directions. *Radiographics*, 36(7), 1987-2006.

Chapter 2 : Critical Review of Organ Material Properties

Understanding the material properties of abdominal organs is of particular importance for many fields. Characterizing the mechanical behavior of these tissues can advance the fields of biomedicine such as diagnostics, forensics, surgical simulations, and injury prediction. The various uses for material properties leads to multiple methodologies being used to derive these characteristics. In order to devise a research program to expand the knowledge in the area of abdominal organ material properties and mechanical behavior, a critical review is needed to establish the current state of literature.

This critical review was restricted to the abdominal organs such as intestines, stomach, prostate, gallbladder, bladder, liver, kidney, and spleen in keeping with the research purpose. Databases such as google scholar, ebsco, and science direct were used to search for existing literature. The aim of this review is to capture the current state of knowledge in regard to the material properties of abdominal organs tested mechanically. Specifically, the material properties of interest are the elastic modulus (stiffness), shear modulus, bulk modulus, toughness, ultimate strength, and ultimate. These material properties will be used as key words for the search. Particular methods will also be of interest and thus key works like dynamic, quasi-static, tension, and compression were included. All of these key words and other common parameters found in articles for each organ are outlined in the tables below.

2.1 Liver

The liver is the most extensively researched abdominal organ in terms of material property characterization. A wide variety of methodologies and factors have been utilized for liver testing. Eleven of the articles subjected liver tissue to tensile loads. All of the articles that used this methodology prepared samples of the liver by dissecting the whole organ into several bone shaped specimens. Although the sample preparation was similar, the methodology for all of the research projects differed in various ways.

Brunon et al. investigated the effect of freezing the specimen prior to testing for the stiffness and failure properties [1]. In vitro quasi-static tensile testing of both human and porcine liver capsules was performed on fresh tissue and tissue that was frozen prior to testing. Brunon et al. concluded that human and porcine tissue was statistically different for all variables, and only the ultimate strain of porcine liver tissue was statistically different from the fresh versus frozen specimens [1]. Duong et al. conducted a similar study, but focused on porcine liver parenchyma, that investigated the difference between fresh and refrigerated tissue material properties tested under tension [2]. The quasi-static tensile testing revealed that the liver parenchyma is not affected by freezing or refrigerating the tissue.

Another tension testing study investigated the effect of heat on the material properties of bovine liver parenchyma. Santiago et al. determined that testing at a room temperature versus a temperature of 98 degrees Fahrenheit had no impact on the failure properties of the organ [3]. In another similar study by the same author, the effect of freezing the liver parenchyma was once again investigated [4]. The bovine tissue in this study performed similarly to the porcine liver parenchyma. Santiago et al. concluded

that freezing did not change the failure stress but lowered the failure strain of the parenchyma when placed under quasi-static tensile loading [4].

Lu et al. conducted two studies investigating the effect of freezing and refrigerating bovine tissue for up to 60 days on the properties tested at different tensile rates [5,6]. In the first study by Lu et al., human parenchyma was tensile tested fresh and frozen for 20 days [5]. Failure stress and strain were observed to be significantly less when tested at quasi-static rates under tension after being frozen. Lu et al. performed similar testing but utilized different rates [6]. Fresh, 30-day, and 60-day frozen human liver parenchyma samples were placed under tensile loads performed at strain rates of 0.01 /s, 0.1 /s, and 1 /s. Lu et al. found that only the failure strain was effected by freezing the specimen, and liver parenchyma failure properties did not change based on rate [6].

The only other study to investigate the strain rate dependency of the liver was conducted by Kemper et al. [7]. Tension tests of human liver parenchyma were conducted at the rates of 0.008/s, 0.08/s, 0.8/s, 8/s. A strain rate dependency was observed with failure stress being significantly higher at the rate of 8/s versus 0.008/s and 0.08/s, while failure strain was lower for the fastest rate than the slowest rate tested.

Six studies utilized a compression testing methodology (Table 2-1). Of the six studies, four studies tested the liver under quasi-static rates [8-11]. Only one study, however, reported the material properties, while the rest utilized the results to fit a mathematical material model. Umale et al., investigated the elastic modulus of the kidney, liver, and spleen using various methodologies [12]. The liver testing consisted of

quasi-static compression loading on cylindrical porcine liver samples and found the elastic modulus of porcine parenchyma to be 1.98 kPa for strains less than 10% and 0.75 kPa for strains between 35% and 40% under quasi-static compressive loading [12]. Only one study performed dynamic compression testing on the liver [13]. However, the results were used for an Ogden elastic curve fitting model and the material properties were not directly reported.

The rest of the techniques that were used ranged from elastography, indentation, and inflation with different research goals. Evaluating the results for different organ hosts and different testing techniques, it can be concluded that the measured material properties differ based on testing methodology and it is still unclear on whether the material properties from an animal host is a feasible substitute for human. Furthermore, the methodology that would be optimal for the assessment of organs under impact loads is the quantification of the whole, undissected, liver material properties tested at various rates. To date no research has been performed that directly compares protocols using the same organ, directly compares human versus porcine liver tissue, and tests using a whole organ in unconfined compression at various rates (Table 2-2).

Table 2-1: Literature review of the material properties of the liver

Author	Year	Rate	Human	Animal	Shear Modulus	Elastic Modulus	Bulk Modulus	Tension	Compression	Other Methods	Failure Stress	Failure Strain	Curve Fit
SARAF	2007	1-20m/s (not specifically recorded)	Parenchyma		0.005 to 0.035 MPa					Kolsky bar			
GAO	2010	125mm/s		Porcine Parenchyma				x	x				x
BRUNON	2010	0.5mm/s	Capsule	Porcine Capsule		16.9+/19.9MPa Fresh Human 27.5+/-22.7MPa Frozen human 11.6+/-19.2 mPA fresh pig 7.8+/-10.5Mpa frozen pig		x			1.85+/1.18MPa Fresh Human 2.77+/-2.69MPa Frozen human 2.03+/-2.44 mPA fresh pig 1.22+/-1.12Mpa frozen pig	32.6+/13.8% Fresh Human 43.9+/-24.2% Frozen human 43.3+/-25.4% fresh pig 62.9+/-35.4% frozen pig	
BRUNON	2011	0.1/s	Capsule							Inflation		50.5%+/-10.8%	
PERVIN	2011	3000/s	Parenchyma		37kPa		0.25 GPa			Kolsky Bar			
LU	2012	0.5mm/s		Porcine	3.406+/- .819kPa Cooling, 5.33+/- 1.349 day 20;3.93+/-0.962 frozen 3.651+/- 0.708					Indentation			
GOKOL	2012	3mm/s		Bovine						Indentation			
LU	2014	0.01/s,0.1/s,1/s		Bovine				x			0.01:43 kPa; 0.1:50 kPa; 1:57kPa	0.01:0.38; 0.1: 0.37; 1:0.35	
LU	2013	0.01/s, 0.1/s,0.1/s,1/s, 10/s	Parenchyma					x			0.01:41.32(13.87)kPa; 0.1:44.72(7.08)kPa; 1:46.25(11.49)kPa; 10:56.89(15.48)kPa	0.01:0.305(0.088); .1:0.275(0.064); 1:0.264(0.055); 10:0.245(0.034)	
Umale	2013	0.007/s		Porcine Parenchyma		Low:1.98 (.84)kPa; High: .75(.15)kPa			x				
WEX	2014	Quasi-static		Porcine		0.02: .21(0.06); 0.05:0.24(0.09); 0.2:0.34(0.09); 0.5:0.35(0.08); 2:0.44(0.14); 5:0.52(0.09)				Indentation			
DUONG	2015	0.083/s		Porcine Parenchyma				x			Fresh:0.509(0.164)MPa; FreezeThaw:0.345(0.142)MPa; Cooled:0.359(0.169)MPa	Fresh:1.756(0.165); FreezeThaw:1.335(0.1); Cooled:1.339(0.097)	
UNTAROIU	2015	0.01/s, 0.1/s, 1/s, 10/s	Parenchyma										x
ROAN	2007	0.01/s		Porcine Parenchyma					x				x

OCAL	2010	48mm/s	Porcine Parenchyma					Impact Hammer	x
OZCAN	2011	1 to 80Hz	Parenchyma	10 to 80 kPa				Impact Hammer	
CHUI	2007	10 mm/s	Porcine Capsule		x	x			x
YEH	2002	0.12mm/s	Parenchyma	800 Pa to 2500 Pa		x			
CHATELIN	2011		Porcine		x			Transient Elastography	x
KEMPER	2010	0.01/s, 0.1/s, 1/s, 10/s	Parenchyma		x			0.01:40.21(21.39)kPa; 0.1:46.79(24.81)kPa; 1:52.61(25.73)kPa; 10:61.02(24.89)kPa	0.01:0.34(0.12); 0.1:0.32(0.05); 1:0.30(0.1); 10:0.24(0.07)
BARNES	2007	0.05mm step increments	Murine	x					x
CARTER	2001	4mm/s	Intact					Indentation	x
CONSTANTINIDES	2008	Quasi-static	x	x				Indentation	
CHEN	1996	5 cm/min		0.43 to 1.68 kPa		x			x
SANTAGO	2009		Bovine	x	x			19(4.74)kPa	0.33(0.05)
TAMURA	2002	60mm/s	Porcine			x			
TAY	2006	Quasi-static	Porcine	13 kPa				Indentation	
YOMADA	1970	Quasi-static	Rabbit	5.6 kPa				Indentation	
MILLER	2000	0.225/s, 11.25/s, 22.5/s	Porcine			x			
SCHWARTZ	2002	10mm/s	Deer	25 kPa				Indentation	
HOLLENSTEIN	2006	Quasi-static	Bovine Capsule	1.1 (0.2) MPa to 38.5 (4.9) MPa	x			Shear wave Elastography	9.2(0.7)MPa

Table 2-2: Summary of research topics of interest addressed in literature

AUTHOR	YEAR	HUMAN	ANIMAL	STATIC	DYNAMIC	STRAIN RATE DEPENDENCY	HUMAN VS PORCINE	COMPRESSION	INTACT ORGAN	ELASTIC MODULUS	FAILURE STRESS	FAILURE STRAIN
SARAF	2007	√			√			√				
GAO	2010		√					√				
BRUNON	2010	√	√	√			√			√	√	√
BRUNON	2011	√										√
PERVIN	2011	√			√							
LU	2012		√	√								
GOKOL	2012		√	√					√			
LU	2014		√	√	√	√					√	√
LU	2013	√		√	√	√					√	√
UMALE	2013		√	√				√				
WEX	2014		√	√					√	√		
DUONG	2015		√								√	√
UNTAROIU	2015	√		√	√	√						
ROAN	2007		√	√				√				
OCAL	2010	√			√							
OZCAN	2011		√	√	√					√		
CHUI	2007		√	√				√				
YEH	2002	√		√				√		√		
CHATELIN	2011		√									
KEMPER	2010	√		√	√	√					√	√
BARNES	2007		√	√						√		
CARTER	2001	√		√					√			
CONSTANTINIDES	2008		√						√	√		
CHEN	1996		√					√				
SANTAGO	2009									√	√	√
TAMURA	2002		√		√			√				
TAY	2006		√	√						√		

YOMADA	1970	√	√					√	
MILLER	2000	√	√	√	√		√		
SCHWARTZ	2002	√	√					√	
HOLLENSTEIN	2006	√	√					√	√

2.2 Kidney

Overall, 11 studies were found that involved the material testing of kidneys (Table 2-3). Three of these studies were performed under quasi-static tension testing. Herbert et al. was the first study of its kind to investigate the mechanical properties of kidney renal capsule through quasi-static tension tests using a canine model [32]. Failure stress, failure strain, and elastic modulus of different portions of the renal capsule were measured and compared to a dog aorta within this study. The major finding from this study is that the anterior-posterior portion of the kidney was significantly stiffer and stronger than the lateral portions of the kidney.

Karimi et al. performed also performed quasi-static tension testing, but on human kidney renal capsules [33]. The purpose of this study was to investigate the differences in the elastic modulus, failure stress, and failure strains between axial and transverse tested specimens. Karimi et al. found that the elastic modulus and failure stresses were significantly higher when tested axially versus transversely [34]. Results from this study have determined that the kidney renal capsule is anisotropic under tension at quasi-static rates.

Umale et al. performed quasi-static tension and compression testing, but on porcine kidney capsules [12]. The elastic modulus and ultimate stress were much higher with the elastic modulus being 7.1 MPa at low strain and 16.34 MPa at high strain and failure stress at 4.78 MPa. Umale et al. also performed compression testing on the cortex of the porcine kidney, measuring the elastic modulus to be 15 MPa at 10% strain and 1.16 MPa at 35% strain [12]. These differences in values between methods highlights the importance of methodology for measuring material properties. Researchers should strive to derive material properties in a way that most closely resembles the intended application that will use said characteristics.

Snedeker et al. was the only other study to perform compression testing on the kidney [34]. Experiments were carried out on both human and porcine kidney parenchyma. The measured stiffness at a quasi-static rate for the porcine specimens were 40 kPa at low strains and 1,470 kPa at high strains while the human kidney modulus was measured to be 19 kPa at low strains and 530 kPa at high strains. Failure

stresses were also observed to be lower in the human specimens while the failure strains were comparable. Falling weight and projectile tests were also carried out on whole porcine kidneys to investigate a rate dependency. This study found that the material properties did not differ between the rates of 5 m/s to 25 m/s. However, the dynamic tests were carried out by repeating drop tests on the same specimen at increasing rates until the specimen failed. This methodology is testing impact and if no ruptures were observed a test is repeated on the same organ. The study ignores the effect of the several preceding impact that may have weakened the organ, which will not accurately depict the strain rate dependency. Snedeker et al. however did highlight the differences between species [34].

Umale et al. also performed dynamic compression testing on the whole porcine kidney [35]. Kidneys were placed in an impacting device that subjected the specimens to compressive loads at rates of 1.5 to 2 m/s. This study did not investigate the effects of strain rate, and thus kept the impact velocity constant. Results were used to develop and validate a material model with the aim of describing kidney behavior during an impact and did not report any of the material parameters directly. The goal of this paper was to develop a model for the kidney that could be used in conjunction with a comprehensive human body model to assess impact trauma.

One study performed material characterization tests using an indentation technique. Lu et al. performed quasi-static indentation tests to investigate the effect of tissue storage on the material properties [5]. Two kidneys were cooled to 4 degrees Celsius and two kidneys were frozen to -20 degrees Celsius and stored for 20 days. Specimens were then brought back to room temperature and a compressive load at a quasi-static rate was placed on the center of the kidney using a cylindrical probe. This study found that the stiffness was significantly higher in the specimens subject to freezing.

The rest of the studies used various other testing techniques such as aspiration, torque, radio frequency, and perfusion [36-39]. Overall, the research regarding the material properties of the kidney does not address whether or not a porcine host is able to be substituted for human, the effect of using a probing protocol versus an unconfined

compression protocol, and the rate dependency on the material properties of whole, undamaged, kidneys (Table 2-4).

Table 2-3: Literature review table for kidney material properties

AUTHOR	YEAR	RATE	DYNAMIC	HUMAN	ANIMAL	SHEAR MODULUS	ELASTIC MODULUS	TENSION	COMPRESSION	FAILURE STRESS	FAILURE STRAIN	ENERGY	OTHER	CURVE FITTING
HELFENSTEIN	2015	Stepwise pressure increase			Porcine	Cortex: 4.9-18 kPa Medulla:3-16.8 kPa							Perfusion	
NASSERI	2012	100 rad/s			Porcine	1kPa to 10 kPa							Torque	x
SNEDEKER	2005	0.005/s up to 25 m/s		Parenchyma	Porcine		Static (kPa): Human: E1:19(6), E2:530(130), Pig: E1:40, E2:1470		x	Static (kPa): Human: 116(28), Pig:245 20 kPa	Static: Human:63(6.3), Pig:57	Static(kJ/m3): 17.1(4.4), Pig: 23; Dynamic: 15 kJ/m3	Kolskey bar	
KARIMI	2017	5 mm/min		Parenchyma			180 kPa	x						
UMALE	2017	1.5 to 2 m/s			Porcine					X				x
UMALE	2013	0.05 mm/s			Porcine Parenchyma		Cortex: 10%: 15(7.20 35%:1.16(.1) MPa Para: 10%:1.98(0.84)kPa, 45%:0.75(0.15) MPa Probe: 10%:14(1.8)kPa, 50%: 35(11)kPa Capsule: low:7.1(3.75)MPa, High:16.35(4.52)MPa	X		X	Tension: 4.78(1.05) MPa	Tension: 36(8.3)%		
NAVA	2004			Intact									Aspiration	x
BRACE	2009			Intact									Radio frequency Indentation	
LU	2012	0.5mm/s			Porcine	3.603 (0.504) kPa								

Table 2-4: Summary of research topics of interest addressed in literature

AUTHOR	YEAR	HUMAN	ANIMAL	STATIC	DYNAMIC	STRAIN RATE DEPENDENCY	HUMAN VS PORCINE	COMPRESSION	INTACT ORGAN	ELASTIC MODULUS	FAILURE STRESS	FAILURE STRAIN	PROBING VS COMPRESSION
HELFENSTEIN	2015		√	√									
NASSERI	2012		√		√								
SNEDEKER	2005		√	√	√	√		√		√	√	√	
KARIMI	2017		√	√						√			
UMALE	2017		√					√					
UMALE	2013		√	√				√		√	√	√	
NAVA	2004	√		√					√				
BRACE	2009	√							√				
LU	2012		√	√					√				

2.3 Spleen

A total of nine studies were found that investigated the mechanical behavior of splenic tissue (Table 2-5). The most popular technique used to characterize the splenic tissue was indentation which was used by three studies. Carter et al. performed ex-vivo indentation of porcine splenic tissue at quasi-static rates and compared the results to porcine liver [40]. The results were used to create a material model to aid in the estimation of human spleen mechanical behavior placed under indentation. It was found that the porcine spleen tissue was more compliant than liver tissue under compressive forces using a probe. Umale et al. also used a probing methodology to characterize the material properties of the porcine spleen [12]. Quasi-static indentation was performed on intact spleens to quantify the stress and strain relationship. The goal of this paper was to compare the results with other porcine tissue, and it was found that the spleen was the least stiff tissue when compared to the kidney and liver. However, this study changed the methodology between the different organs of interest and earlier studies have already identified that different testing techniques result in different material properties.

Lu et al. also performed quasi-static indentation tests of the porcine spleen but had a different goal [41]. This study was primarily interested in the effect of the storage methods on the material properties. Porcine splenic tissue was indented immediately after it was harvested, after 20 days of refrigeration, and after 20 days of freezing. Lu et al. concluded that under quasi-static compressive indentation, the spleen stiffness was significantly reduced by freezing and cooling versus testing immediately after harvest [41].

Three of the nine studies performed tension testing on the spleen. Duong et al. performed quasi-static tension testing of the porcine spleen parenchyma. The goal of the study was to investigate the storage effects on the spleen failure material properties [2]. It was found that the freezing and refrigerating the spleen tissue caused a significant decrease in the failure parameters used for the material model. Similar results were found in a study that utilized an indentation protocol.

Stingl et al. (2002) also performed tension testing but used human spleens and a dynamic loading rate [42]. The goal of the study was to determine the morphological and mechanical behavior of the spleen and compare the results to the forces measured on a test dummy subjected to frontal impacts. Human spleen tissue was harvested and segmented into dog bone shape specimens. The collagen and elastin content was measured for each organ, and then specimens were dynamically tested until failure. From the resulting forces, a theoretical value of critical acceleration was obtained and used for comparison to recorded sled impact forces. No statistically significant conclusions were drawn from this study, which can highlight that impact of sex, age, and other biological factors can play.

Kemper et al. utilized a tension testing protocol on human spleens [43]. The goal of the study was to investigate the strain rate dependency on the failure properties of splenic parenchyma and capsule. Human spleens were separated into several bone-shaped samples, some specimens with and without the capsule, and placed in tension at strain rates ranging from 0.1 /s to 10/s. Kemper et al. found that the strain was significantly lower, and stress were significantly higher between the slowest and fastest rate for the parenchyma and the stress was significantly higher for the capsule samples

[43]. The ultimate strength of spleen parenchyma ranged from 16.5 kPa at 0.1 /s to 33.8 kPa at 10 /s and the capsule strength ranged from 43.6 kPa at 0.1 /s to 65.3 kPa at 10 /s [43]. The ultimate strain from this study ranged from 1.26 at 0.1 /s to 1.18 at 10 /s for the parenchyma and 1.23 at 0.1 /s to 1.17 at 10 /s for the capsule [43].

Only one study tested the spleen tissue under compressive loading. Tamura et al. performed compression testing on porcine spleens at strain rates of 0.005/s, 0.05/s, and 0.5/s [25]. The study investigated the strain rate dependency of the failure strength, failure strain, and stiffness of cubic samples of the spleen parenchyma. In the study by Tamura et al. the ultimate strength and ultimate strain remained constant, ranging from 0.420 to 0.438 kPa and 1.81 to 1.83 [25].

The last two studies utilized less conventional testing methods and also utilized the experimental testing to curve fit a material model. Rosen et al. performed cyclic testing of porcine spleen, and other organs, at a quasi-static rate. The goal of the study was to compare the viscoelastic behavior abdominal organs tested in-vivo. The study found that after repeated tests the spleen tissue became less stiff and was the least stiff organ among the small intestine, stomach, and liver. Another less conventional method that was studied is the use of rotary motion. Nicolle et al. segmented porcine spleen tissue into cylindrical samples and subjected the samples to rotary motion at different frequencies [44]. The rheometric tests were conducted between the frequencies of 0.1 Hz and 1 Hz. A weak frequency dependence of the shear mechanical properties was found within this study. This type of behavior is typically characteristic of biological tissue. In an earlier study conducted by Kemper et al. a strain rate dependency on the mechanical properties of the spleen was already observed [43].

Overall, major gaps in the literature regarding the material properties of the spleen were found (Table 2-6). None of the research studies investigated the material properties of a whole organ placed in unconfined compression at various rates. Also, it is clear that the use of different protocols can have an impact on the results and no studies have directly compared two different methods like a probing protocol and an unconfined compression testing protocol. Only one study compared the human tissue to the porcine spleen, but it further stated that assumptions were made between the two studies that were in comparison and thus was not a direct comparison.

Table 2-5: Literature review of Spleen material properties

AUTHOR	YEAR	RATE	HUMAN	ANIMAL	ELASTIC MODULUS	TENSION	COMPRESSION	OTHER	FAILURE STRESS	FAILURE STRAIN	ENERGY	CURVE FIT
LU DUONG	2013	0.5mm/s		Porcine				Indentation				x
	2015	0.0823/s		Porcine		x			Fresh:0.509(0.164)MPa; FreezeThaw:0.345(0.142)MPa; Cooled:0.359(0.169)MPa	Fresh:1.756(0.165); FreezeThaw:1.335(0.1); Cooled:1.339(0.097)		x
KEMPER	2012	0.01/s- 10/s	Parenchyma and capsule			x			Para (kPa): 0.01:16.5(13.1; 0.1:23.9(10.3); 1:31.5(16.3); 10:33.8(15.9); Cap (kPa): 0.01:43.6(18.1; 0.1:46.1(15.5); 1:68.4(33.1); 10:65.3(24.3);	Para: 0.01:0.26(.08; 0.1:0.21(.05); 1:0.19(.08); 10:0.18(.02); Cap: 0.01:0.23(.04; 0.1:0.2(.04); 1:0.19(.05); 10:0.17(.02);		
Umale	2013	0.003/s		Porcine	14(1.8) kPa- 35(11) kPa		x					x
Carter Stingl	2001 2002	1 mm/s (33- 149g)	Parenchyma	Porcine	0.11 MPa 0.14 to 2.99 MPa		x	Indentation	0.077 to 1 MPa			x
Tamura	2002	0.005/s 0.05/s 0.5/s		Porcine			x		(kPa) 0.005:0.432(.026) 0.05:0.420(.038) 0.5:0.438(.040)	0.005:0.825(.041) 0.05:0.809(.04) 0.5:0.834(.012)	(kJ/m3) 0.005:22.51(3.55) 0.05:24.46(3.17) 0.5:32.55(3.44)	x
Rosen	2008	Quasi- static		Porcine				Mechanical grasper				x
Nicolle	2012	0.1 to 1 Hz		Porcine				Rotary Motion				x

Table 2-6: Summary of research topics of interest addressed in literature

AUTHOR	YEAR	HUMAN	ANIMAL	STATIC	DYNAMIC	STRAIN RATE DEPENDENCY	HUMAN VS PORCINE	COMPRESSION	INTACT ORGAN	ELASTIC MODULUS	FAILURE STRESS	FAILURE STRAIN	PROBING VS COMPRESSION
LU	2013		√	√									
DUONG	2015		√	√							√	√	
KEMPER	2012	√		√	√	√	√				√	√	
UMALE	2013		√	√				√					
CARTER	2001		√	√									
STINGL	2002	√			√	√		√			√		
TAMURA	2002		√	√	√	√		√			√	√	
ROSEN	2008		√	√									
NICOLLE	2012		√		√								

2.4 Intestines

The most popular method used to investigate the mechanical behavior of the small intestine was through inflation of the tissue (Table 2-7). A total of five studies were found that utilized this methodology. Storkholm et al. performed step-wise inflation tests on the small intestine of guinea pigs [46]. The goal of the study was to characterize the stiffness of different areas of the small intestine. It was found that the stiffness of the small intestine was significantly higher in the ileum than the duodenum portion. The significance of this study highlights how different portions of the same organ can have different material properties. Furthermore, special attention to the portion of the intestine that is being tested is required to insure accurate and repeatable results.

Duch et al. researched the passive wall mechanics of rat small intestine using inflation [47]. Fifteen small intestines from rats were harvested and through a probe were subjected to step increases in pressure. The stress and cross-sectional area were recorded with each pressure step for each of the different segments of the intestine. Similar to the study above it was found that the stiffness and cross-sectional area was higher in the ileum versus the jejunum and duodenum. Even between different hosts, the effect of testing location on the material properties of the small intestine remained constant. Gregersen et al. also performed inflation tests on guinea pig jejunum with the goal to characterize the history dependent mechanical behavior [48]. Three different pressure loading protocols were used in this study. Each protocol involved increasing and relieving the pressure in 5 different increments, but one of the protocols involved repeated inflations to the midrange pressure, and the last protocol involved repeated

inflation to the peak pressure. It was concluded that the small intestine softened with repeated inflation to the same pressure. The softening was more pronounced for repeated lower pressure inflation. The significance of this research is that the intestine is poor at retaining its structure once expanded passed the elastic region.

Roeder et al. investigate the stiffness and the failure properties of the small intestine through an inflation protocol [49]. The small intestine from adult pigs were inflated at a constant pressure until rupture, and the compliance, elastic modulus, and failure pressure was recorded. It was found that the compliance and elastic modulus increased exponentially as pressure was increased. This further highlights the nonlinear nature of the small intestine tissue behavior.

Ergorov et al. investigated the failure properties of human cadaveric and surgically removed small intestine using dynamic tensile loading [50]. Failure stress and failure strain were not statistically different between human cadaveric and surgically removed intestines nor between specimens with fibers running longitudinal and transversely. The results indicated the intestines obtain at the time of death or through a gastrectomy have similar failure properties, and that the direction of which the fibers are running during tension testing is not consequential.

Bourgouin et al. tension tested human intestines at a rate of 1 m/s [51]. The goal was to categorize the mechanical properties of fresh and embalmed human small intestine. It was found that embalmed tissue was stiffer and yielded a higher failure stress than fresh cadaveric tissue. This study hypothesized that the embalming strengthened the organs, and the fresh tissue resulted in more accurate values of failure stress, 1.18 MPa, and failure strain, 148.5%.

Rosen et. al. utilized three different methodologies to characterize the material properties of the small and large porcine intestine [52]. A mechanical grasper was used to measure the force and deformation while being clamped in both in-vivo and ex-corpus conditions. Tension testing of the small and large intestine was conducted using a material testing system. All tests were carried out using a quasi-static rate. This study used the resulting stress and strain data to develop and curve fit a material model. The main finding from this research is that the small and large intestine material model parameters were not significantly different from each other.

Overall, two major knowledge gaps were found in the review of intestine material properties. Although some of the studies utilized animal tissue, none of the studies performed a comparison between an animal and human host. In addition, the effect of strain rate was also not investigated throughout the current body of literature (Table 2-8). Determining the impact of strain rate on material properties and whether or not an animal tissue, such as porcine, is a feasible substitute for human tissue would improve the current finite element models involving this tissue.

Table 2-7: Literature review table of intestine material properties

AUTHOR	YEAR	RATE	HUMAN	ANIMAL	DELTA RATE	ELASTIC MODULUS	TENSION	COMPRESSION	OTHER	FAILURE STRESS	FAILURE STRAIN	CURVE FIT
BOURGOUIN	2012	1m/s	x			5.16 (3.03) MPa	x			1.18 (0.41) MPa	48.5 (17.4)	
GREGERSEN	1998	15 mmHg in 3 mm Hg		Guinea pigs					Inflation			x
ROEDER	1999			Porcine		4106 g/cm2 (1348 to 5601			Inflation	3517 mmHg		
EGOROV	2002	0.04/min to 20/min	x		19		x					
ROSEN	2008	5.4 mm/s		Porcine					Grasper			x
DUCH	1996	0.1 mm2/s		Rat					Inflation			x
GAO	2000	0.007 mm2/s		Rat					Inflation			x
STORKHOLM	1995	1 mm2/s		Guinea pig					Inflation			x

Table 2-8: Summary of research topics of interest addressed in literature											
AUTHOR	YEAR	HUMAN	ANIMAL	STATIC	DYNAMIC	STRAIN RATE DEPENDENCY	HUMAN VS PORCINE	TENSION	ELASTIC MODULUS	FAILURE STRESS	FAILURE STRAIN
BOURGOUIN	2012	✓			✓			✓	✓	✓	✓
GREGERSEN	1998		✓	✓							
ROEDER	1999		✓						✓	✓	
EGOROV	2002	✓		✓	✓			✓			
ROSEN	2008		✓	✓							
DUCH	1996		✓	✓							
GAO	2000		✓	✓							
STORKHOLM	1995		✓	✓							

2.5 Bladder

Eight studies were found that investigated the mechanical behavior of the bladder tissue (Table 2-9). Five of the eight studies tested the bladder in tension. A study by Dahms et al. investigated the biological properties of human, porcine, and rat bladders subject to tensile forces [53]. Quasi-static tensile tests were performed on the various animal bladders as well as bladder acellular matrix grafts. It was found that the graft material properties were not significantly different from the animal hosts. No statistical comparisons were performed between the different animal tissue, but it was found that rat bladders had the highest failure stress, failure strain, and elastic modulus followed by the porcine bladder and the human bladder. Pedro et al. also performed quasi-static tension tests but only on human bladders [54]. The goal of the study was to correlate stiffness and failure stress as well as compare the stiffness and failure stress with hosts over the age of 50 versus younger. It was concluded that stiffness and failure stress was correlated and bladders from hosts over the age of 50 were stiffer than younger specimens. No statistical difference was observed between failure stress and age. Zanetti et al. performed a similar test on porcine bladders to investigate the effect of fiber orientation, strain rate, and loading history [55]. The stress and strain results of the tension testing was used to create a material model. Based on the material parameters, all of the factors of fiber orientation, strain rate, and loading history had influenced the bladder behavior.

Griffiths et al. put tensile load on human bladder tissue but utilized the body's own muscular system [56]. Strips of human bladder were placed in a device to measure tensile forces and electrodes were attached to the bladder. The contractile forces were

recorded and used to compare to a Hill muscle model in order to characterize the tissue. It was found that the contractile properties of the human bladder are not similar to those of regular muscle.

Barnes et al. used two different methods of sectioning the bladder tissue for tensile testing [57]. The goal of this study was to investigate the differences between methodology and the frequency dependent effects on porcine bladder stiffness. No differences were found between testing with looped specimens and rectangular specimens. The storage and loss stiffness were observed to increase as the frequency increased from quasi-static to 1 Hz, but then the stiffness decreases above 1 Hz and returns to similar values to quasi-static as the rate approaches 10 Hz [57].

Coolsaet et al. used a less conventional stepwise cystometry method to characterize the mechanical behavior of bladder tissue [59]. The study was conducted on living canines placed under anesthetic and involved increasing the pressure within the bladder using a tube that was inserted through the urethra. Overall the study concluded that this technique was not suitable for characterizing the viscoelastic behavior of the bladder tissue. This study suggests that the results from the study by Klevmark et al. are not valid as the same technique was used on feline bladders [60]. The conclusions from this study also interjects skepticism regarding other protocols that use inflation for determining the viscoelastic behavior of tissue.

Nenadic et al. also conducted an inflation experiment to characterize the behavior of porcine bladder and compared the results with patients [61]. Fluid was filled inside the porcine bladder and the expansion was measured using ultrasound. A model to describe the material behavior was developed and implemented through ultrasound

measurement of human patients. The study concluded that the model and the ultrasound technique was a valid method for assessing bladder compliance.

Overall it was found that there are gaps in knowledge within the current body of literature regarding bladder material properties (Table 2-10). Unlike most organs, one research study attempted to compare human bladder to animal host tissue, however, this was only done at one loading rate [53]. Furthermore, only one study used a dynamic testing rate, but did not vary the rate [57]. More research needs to be conducted to not only determine if there is a strain rate dependency for the bladder tissue, but also if porcine tissue is similar to human at multiple loading rates. Characterizing the bladder material properties and understanding these factors will enable researchers to incorporate this often overlooked organ in finite element models of the human abdomen.

Table 2-9: Literature review table of bladder material properties

AUTHOR	YEAR	RATE	HUMAN	ANIMAL	SHEAR MODULUS	ELASTIC MODULUS	FAILURE STRESS	FAILURE STRAIN	TENSION	OTHER	CURVE FITTING	
BARNES COOLASET GRIFITHS NENADIC	2015	10 Hz		Porcine	1.89 N/mm				x			
	1975	Stepwise		Canine						Inflation	x	
	1979	0.6 mm/s		Porcine	x				x		x	
	2016		x	Porcine	50 kPa – 400 kPa					Ultrasound		
PEDRO ZANETTI DAHMS	2011	0.083 mm/s	x		1.9 (0.2)MPa		0.9 (0.1)MPa		x			
	2012	0.16 mm/s		Porcine	0.5 to 4 MPa				x			
	1998	0.3mm/s	x	Porcine, Rat	Rat: 0.76(0.44)MPa, Porcine:0.26(0.18)MPa, Human:0.25(0.18)MPa		Rat: 0.72(0.21) MPa, Porcine:0.32(0.1)MPa, Human:0.27(0.14)MPa		Rat: 2.03(0.44), Porcine:1.66(0.31), Human:0.69(0.17)			
KLEVMARK	1974	.26ml/kg/day		Feline							Inflation	

Table 2-10: Summary of research topics of interest addressed in literature

AUTHOR	YEAR	HUMAN	ANIMAL	STATIC	DYNAMIC	STRAIN RATE DEPENDENCY	HUMAN VS PORCINE	TENSION	ELASTIC MODULUS	FAILURE STRESS	FAILURE STRAIN
BARNES	2015		√		√			√	√		
COOLASET	1975		√	√							
GRIFITHS	1979		√					√	√		
NENADIC	2016		√								
PEDRO	2011	√		√				√	√	√	
ZANETTI	2012		√	√				√	√		
DAHMS	1998	√	√	√			√	√	√	√	√
KLEVMARK	1974		√	√							

2.6 Prostate

The material characterization of the human prostate has been conducted with the primary focus of improving prostate cancer diagnosis. Many of the studies used imaging methodology because of this reason. Twenty studies were found that determined the stiffness of the prostate through sono-elastography, using sonar to image the organ [61-80]. Six more studies were found that used magnetic resonance elastography to characterize the stiffness of the prostate [81-86]. Only seven studies were found that used mechanical methods to determine the material stiffness of the prostate, and none of these studies determined the failure properties.

Three out of the seven studies used a compressive probing protocol. Ahn et al. investigated the stiffness of cancerous and noncancerous human prostate tissue in six different regions of the organ [87]. The elastic modulus was found to be statistical stiffer in regions of the prostate with cancerous tissue versus areas without. The Ahn et al. study demonstrates that the material stiffness of prostate tissue changes with the presence of cancer when compressed using a probe at a quasi-static rate [87]. This study also explains that different portions of the prostate resulted in statistically different stiffnesses, however the technique to prevent slipping of the prostate when testing on the lateral portions of the organ were not defined and could influence the results.

Carson et al. performed a similar study as above but used a spherical indenter instead of a probe with a flat end and performed indentation on whole-mounted prostates as well as sections dissected from the prostates [88]. The findings of the study concluded that diseased tissue is statistical stiffer than normal prostate tissue, the

stiffness within different regions of noncancerous tissue is not statistically different, and the measured elastic modulus between specimens contains large variations.

Phipps et al. investigated the phase difference and amplitude ratios of sectioned benign and malignant prostate tissue using a dynamic compression protocol [89]. The study found statistical differences between the phases with respect to benign and malignant tissue. However, the methodology within the paper does not detail the rates used, the size of the specimens, or the compressed strain. No information regarding the strain rate dependency of the non-diseased prostate tissue was able to be extracted.

Hoyt et al. investigated the effect of cancerous prostate tissue on the stiffness of cylindrical samples subjected to unconfined compression at various loading rates [90]. Non-statistically significant differences in stiffness were found between cancerous and normal prostate tissue samples at each tested rate. Hoyt et al. has provided the first evidence of the rate dependency behavior of the prostate tissue, however these compression tests were performed on prostates that were dissected in order to create a geometrically uniform sample [90].

Zhang et al. performed a similar study investigating prostate stiffness of cancerous and normal prostate tissue under dynamic compressive loading [91]. Prostate samples were cored to produced geometrically uniform specimens and tested at a constant dynamic rate. Similarly, this study also found differences between the stiffness of cancerous prostate tissue versus noncancerous tissue at the specified rate.

The final study that used the mechanical technique of compression probing was performed by Krouskop et al. [92]. The viscoelasticity of the prostate tissue under compression probing conditions was investigated at 3 different strain rates: 0.1 Hz, 1

Hz, and 4 Hz. Results from the study determined that sectioned cancerous prostate tissue was statistically stiffer than sectioned noncancerous tissues at all rates, but not between rates. Krouskop et al. provided evidence that the prostate tissue is not rate dependent at these measured rates, however the strain at which the tissue is compressed to is not published and varied with each test [92]. Due to the nonlinear nature of the response, a varying strain within the compression probing protocol between tests would result in different strain rates if the frequency is kept constant.

2.7 Gallbladder

The current state of research in the area of gallbladder material properties is scarce. Currently only 4 research articles were found, none of which perform direct measurement. The bulk of the literature is focused on the diagnosis and treatment of gallstones and thus are based on imaging and modeling methods. Genovese et al. investigated the heterogeneity of a single lamb gallbladder using an inflation protocol and inverse stress analysis [93]. In an incremental step-protocol, pressure within the gallbladder was increased and the resulting tissue expansion was imaged. These measured variables were then used in conjunction with a material model and finite element analysis to determine that the stiffness in the hepatic region differs from the serosal surface. However, this study bases the conclusion of a sample size of one and uses an estimate with the aid of a computer model.

Li et al. used a material model and finite element analysis to estimate the mechanical properties of the human gallbladder [94]. In conjunction with the material model that was validated through ten Cholecystokinin provocation tests, it was concluded that the gallbladder peak stress is 1.6 times greater than previously reported

using linear models. Although estimates of the peak stress that is observed in functional gallbladders was found, no direct measurement of failure stress, failure strain, or elastic modulus was determined.

Li et al. investigated the stiffness properties of the human gallbladder through means of ultrasound and the use of a material model [95]. Based on the material models estimation, it was concluded that the human bladder is both anisotropic and patient dependent. However, this study uses an ultrasound technique to estimate the material stiffness, and no direct mechanical measurement was used. In an extension of the previous study, Li et al. investigated the heterogeneity of the human gallbladder material model parameters during the filling and refilling phases of gallbladder function [95]. Based on the validation on a single lamb gallbladder and on ten human gallbladder ultrasounds, Li et al. determined that the model parameters were indeed different for different portions of the gallbladder during the different functional states.

2.8 Stomach

Ergorov et al. investigated the failure properties of human cadaveric and surgically removed stomach through dynamic tensile loading [50]. Failure stress and failure strain were not statistically different between human cadaveric and surgically removed stomach nor between specimens with fibers running longitudinal and transversely. The results indicated the stomach specimens obtain at the time of death or through a gastrectomy have similar failure properties. It was also found that the direction of the stomach fibers during tension testing does not impact the failure results under dynamic loading.

Zao et al. found conflicting results from the study above. This study investigated the factor of the stomach layer, tension testing direction, and tissue location [97]. Five porcine stomachs were dissected into different portions and different submucosa layers and tensile tested uniaxially in both longitudinal and transverse directions. The results of this study concluded that the stiffness of the porcine stomach differed significantly between all the factors investigated when tested at quasi-static rates.

Jia et al. performed stress relaxation and creep tests of porcine stomach tissue under uniaxially loading [98]. The results of this study found that under quasi-static tension testing the orientation, layer of the stomach, and location of the gastric wall effected the stiffness and failure properties of the porcine stomach tissue. Conclusions from the previous two studies demonstrated that under quasi-static conditions, the stomach tissue is anisotropic, viscoelastic, and the properties differ from layer to layer. However, none of the studies investigated the effect of strain rate on the viscoelastic properties of the stomach.

2.9 Literature Gaps

The gaps in literature vary from organ to organ as different studies had different focuses. For example, the bulk of the mechanical characterization for the purpose of developing a model to assess traumatic injuries has been performed on the kidney, spleen, and liver. This could be due to applicability as these organs are often injured in traumatic events or due to the more abundant resources to obtain such organs from various hosts. On the other hand, virtually no research has been performed on the mechanical characterization of the material properties of the prostate. The purpose being that this organ is not as often injury in traumatic scenarios, however the focus of

the research has been on the improvement of diagnosis of prostate cancer as this is has been a more pressing issue for this organ. For some of the abdominal organs, there is a void in establishing basic mechanical properties such as the elastic modulus, failure stress, and failure strain which can be observed in Table 2-11. However, there are some common gaps in literature that applies to all abdominal organs.

A major gap in knowledge that is common among the solid organs is the material properties of a complete intact organ. Most literature highlighted the differences between the individual structures of the organs such as the parenchyma and the capsule, meaning these structures were mechanically tested individually. However, only a few studies look at the material properties of an intact solid organ, and none looked at this aspect with special reference to varying strain rate. Understandably, there is difficulty of acquiring resources for this type of research on human cadaver organs, and thus it is clear why researchers would increase sample size through sectioning the organ into several individual samples. However, the understanding of how an intact organ reacts to forces is essential for the development and use of multi-organ human models.

Another a major gap in the literature is quantifying the effect of strain rate on the material properties of abdominal organs. Several studies have investigated the effect of strain rate for such organs as the intestines, stomach, kidney, liver, and spleen. However, these studies have only determined that there is a statistical difference between two different rates. No studies have fully characterized how the material properties change as the rate increases from quasi-static to dynamic. Several articles have suggested a potential saturation of the strain rate dependency but the point at which this saturation occurs has yet to be determined. A gap in literature exists in

quantifying the by what factor mechanical properties change due to increasing strain rate and fully establish if this relationship is linear or nonlinear.

This critical review of the mechanically characterized material properties of various abdominal organs has highlighted a clear need for research that will help push the area tissue mechanics forward. Establishing characteristics of lesser researched organs and expanding on the research regarding the effects of strain rate will provided necessary information that will expand the knowledge in this area.

Table 2-11: Overview of the literature review of material properties for each organ of interest

Article Topics			Prostate	Liver	Kidney	Spleen	Intestines	Stomach	Bladder	Gallbladder	
Compression	Static	Stiffness		X	X	X					
		Failure Stress			X						
		Failure Strain			X						
	Dynamic	Stiffness		X	X	X					
		Failure Stress				X					
		Failure Strain				X					
Tension	Static	Stiffness		X	X	X			X		
		Failure Stress		X		X			X		
		Failure Strain		X		X			X		
	Dynamic	Stiffness							X		
		Failure Stress				X	X				
		Failure Strain				X	X				
Probing	Static	Stiffness				X	N/A	N/A	N/A	N/A	
		Failure Stress					N/A	N/A	N/A	N/A	
		Failure Strain					N/A	N/A	N/A	N/A	
	Dynamic	Stiffness					N/A	N/A	N/A	N/A	
		Failure Stress					N/A	N/A	N/A	N/A	
		Failure Strain					N/A	N/A	N/A	N/A	
Probing versus compression						N/A	N/A	N/A	N/A		
Intact organ						N/A	N/A	N/A	N/A		

2.10 References

- [1] Brunon, A., Bruyere-Garnier, K., & Coret, M. (2010). Mechanical Characterization Of Liver Capsule Through Uniaxial Quasi-Static Tensile Tests Until Failure. *Journal Of Biomechanics*, 43(11), 2221-2227.
- [2] Dương, M. T., Nguyễn, N. H., Trần, T. N., Tolba, R., & Staat, M. (2015). Influence Of Refrigerated Storage On Tensile Mechanical Properties Of Porcine Liver And Spleen. *International Biomechanics*, 2(1), 79-88.
- [3] Santago, A., Kemper, A., McNally, C., Sparks, J., & Duma, S. (2009). Freezing Affects The Mechanical Properties Of Bovine Liver. *Biomed. Sci. Instrum*, 45, 24-29.
- [4] Santago, A., Kemper, A., McNally, C., Sparks, J., & Duma, S. (2009). The effect of temperature on the mechanical properties of bovine liver. *Biomed Sci Instrum*, 45, 376-81.
- [5] Lu, Y. C., & Untaroiu, C. D. (2013). Effect of storage methods on indentation-based material properties of abdominal organs. *Proceedings of the Institution of Mechanical Engineers, Part H: Journal of Engineering in Medicine*, 227(3), 293-301.
- [6] Lu, Y.-C., Kemper, A. R., & Untaroiu, C. D. (2014). Effect Of Storage On Tensile Material Properties Of Bovine Liver. *Journal Of The Mechanical Behavior Of Biomedical Materials*, 29, 339-349.
- [7] Kemper, A. R., Santago, A. C., Stitzel, J. D., Sparks, J. L., & Duma, S. M. (2010). *Biomechanical Response Of Human Liver In Tensile Loading*. Paper Presented At The Annals Of Advances In Automotive Medicine/Annual Scientific Conference.
- [8] Roan, E., & Vemaganti, K. (2007). The Nonlinear Material Properties Of Liver Tissue Determined From No-Slip Uniaxial Compression Experiments. *Journal Of Biomechanical Engineering*, 129(3), 450-456.
- [9] Chui, C., Kobayashi, E., Chen, X., Hisada, T., & Sakuma, I. (2007). Transversely Isotropic Properties Of Porcine Liver Tissue: Experiments And Constitutive Modelling. *Medical & Biological Engineering & Computing*, 45(1), 99-106.
- [10] Chen, E. J., Novakofski, J., Jenkins, W. K., & O'Brien, W. D. (1996). Young's Modulus Measurements Of Soft Tissues With Application To Elasticity Imaging. *IEEE Transactions On Ultrasonics, Ferroelectrics, And Frequency Control*, 43(1), 191-194.

- [11] Yeh, W.-C., Li, P.-C., Jeng, Y.-M., Hsu, H.-C., Kuo, P.-L., Li, M.-L., . . . Lee, P. H. (2002). Elastic Modulus Measurements Of Human Liver And Correlation With Pathology. *Ultrasound In Medicine And Biology*, 28(4), 467-474.
- [12] Umale, S., Deck, C., Bourdet, N., Dhumane, P., Soler, L., Marescaux, J., & Willinger, R. (2013). Experimental Mechanical Characterization Of Abdominal Organs: Liver, Kidney & Spleen. *Journal Of The Mechanical Behavior Of Biomedical Materials*, 17, 22-33.
- [13] Saraf, H., Ramesh, K., Lennon, A., Merkle, A., & Roberts, J. (2007). Mechanical Properties Of Soft Human Tissues Under Dynamic Loading. *Journal Of Biomechanics*, 40(9), 1960-1967.
- [14] Gao, Z., Lister, K., & Desai, J. P. (2010). Constitutive Modeling Of Liver Tissue: Experiment And Theory. *Annals Of Biomedical Engineering*, 38(2), 505-516.
- [15] Brunon, A., Bruyere-Garnier, K., & Coret, M. (2011). Characterization Of The Nonlinear Behaviour And The Failure Of Human Liver Capsule Through Inflation Tests. *Journal Of The Mechanical Behavior Of Biomedical Materials*, 4(8), 1572-1581.
- [16] Pervin, F., Chen, W. W., & Weerasooriya, T. (2011). Dynamic Compressive Response Of Bovine Liver Tissues. *Journal Of The Mechanical Behavior Of Biomedical Materials*, 4(1), 76-84.
- [17] Wex, C., Arndt, S., Brandstädter, K., Herrmann, L., & Bruns, C. (2014). Biomechanical Characterization Of Material Properties Of Porcine Liver After Thermal Treatment. *Soft Materials*, 12(4), 411-419.
- [18] Roan, E., & Vemaganti, K. (2007). The Nonlinear Material Properties Of Liver Tissue Determined From No-Slip Uniaxial Compression Experiments. *Journal Of Biomechanical Engineering*, 129(3), 450-456.
- [19] Ocal, S., Ozcan, M. U., Basdogan, I., & Basdogan, C. (2010). Effect Of Preservation Period On The Viscoelastic Material Properties Of Soft Tissues With Implications For Liver Transplantation. *Journal Of Biomechanical Engineering*, 132(10), 101007.
- [20] Ozcan, M. U., Ocal, S., Basdogan, C., Dogusoy, G., & Tokat, Y. (2011). Characterization Of Frequency-Dependent Material Properties Of Human Liver And Its Pathologies Using An Impact Hammer. *Medical Image Analysis*, 15(1), 45-52.
- [21] Chatelin, S., Oudry, J., Périchon, N., Sandrin, L., Allemann, P., Soler, L., & Willinger, R. (2011). In Vivo Liver Tissue Mechanical Properties By Transient Elastography: Comparison With Dynamic Mechanical Analysis. *Biorheology*, 48(2), 75-88

- [22] Kemper, A. R., Santago, A. C., Stitzel, J. D., Sparks, J. L., & Duma, S. M. (2012). Biomechanical Response Of Human Spleen In Tensile Loading. *Journal Of Biomechanics*, 45(2), 348-355.
- [23] Barnes, S. L., Lyshchik, A., Washington, M. K., Gore, J. C., & Miga, M. I. (2007). Development Of A Mechanical Testing Assay For Fibrotic Murine Liver. *Medical Physics*, 34(11), 4439-4450.
- [24] Carter, F. J., Frank, T. G., Davies, P. J., Mclean, D., & Cuschieri, A. (2001). Measurements And Modelling Of The Compliance Of Human And Porcine Organs. *Medical Image Analysis*, 5(4), 231-236.
- [25] Constantinides, G., Kalcioglu, Z. I., Mcfarland, M., Smith, J. F., & Van Vliet, K. J. (2008). Probing Mechanical Properties Of Fully Hydrated Gels And Biological Tissues. *Journal Of Biomechanics*, 41(15), 3285-3289.
- [26] Tamura, A., Omori, K., Miki, K., Lee, J. B., Yang, K. H., & King, A. I. (2002). *Mechanical Characterization Of Porcine Abdominal Organs*. Paper Presented At The SAE CONFERENCE PROCEEDINGS
- [27] Tay, B. K., Kim, J., & Srinivasan, M. A. (2006). In Vivo Mechanical Behavior Of Intra-Abdominal Organs. *IEEE Transactions On Biomedical Engineering*, 53(11), 2129-2138
- [28] Yamada, H., & Evans, F. G. (1970). *Strength Of Biological Materials*. United States: Lippincott Williams & Wilkins.
- [29] Miller, K. (2000). Constitutive modelling of abdominal organs. *Journal of biomechanics*, 33(3), 367-373.
- [30] Schwartz, J.-M., Dellinger, M., Rancourt, D., Moisan, C., & Laurendeau, D. (2002). *Modelling Liver Tissue Properties Using A Non-Linear Viscoelastic Model For Surgery Simulation*. Paper Presented At The ESAIM: Proceedings.
- [31] Hollenstein, M., Nava, A., Valtorta, D., Snedeker, J. G., & Mazza, E. (2006). *Mechanical Characterization Of The Liver Capsule And Parenchyma*. Paper Presented At The International Symposium On Biomedical Simulation.
- [32] Herbert, L. A., Chen, W. C., Hartmann, A. L. O. I. S., & Garancis, J. C. (1976). Mechanical properties of the dog renal capsule. *Journal of applied physiology*, 40(2), 164-170.
- [33] Karimi, A., & Shojaei, A. (2017). Measurement Of The Mechanical Properties Of The Human Kidney. *IRBM*, 38(5), 292-297.
- [34] Snedeker, J., Niederer, P., Schmidlin, F., Farshad, M., Demetropoulos, C., Lee, J., & Yang, K. (2005). Strain-Rate Dependent Material Properties Of The Porcine And Human Kidney Capsule. *Journal Of Biomechanics*, 38(5), 1011-1021.

- [35] Umale, S., Deck, C., Bourdet, N., Diana, M., Soler, L., & Willinger, R. (2017). Experimental and finite element analysis for prediction of kidney injury under blunt impact. *Journal of biomechanics*, 52, 2-10.
- [36] Nava, A., Mazza, E., Furrer, M., Villiger, P., & Reinhart, W. H. (2008). In vivo mechanical characterization of human liver. *Medical image analysis*, 12(2), 203-216.
- [37] Brace, C. L. (2009). Radiofrequency and microwave ablation of the liver, lung, kidney, and bone: what are the differences?. *Current problems in diagnostic radiology*, 38(3), 135-143.
- [38] Nasser, S., Bilston, L. E., & Phan-Thien, N. (2002). Viscoelastic Properties Of Pig Kidney In Shear, Experimental Results And Modelling. *Rheologica Acta*, 41(1), 180-192.
- [39] Helfenstein, C., Gennisson, J.-L., Tanter, M., & Beillas, P. (2015). Effects Of Pressure On The Shear Modulus, Mass And Thickness Of The Perfused Porcine Kidney. *Journal Of Biomechanics*, 48(1), 30-37.
- [40] Carter, F. J., Frank, T. G., Davies, P. J., Mclean, D., & Cuschieri, A. (2001). Measurements And Modelling Of The Compliance Of Human And Porcine Organs. *Medical Image Analysis*, 5(4), 231-236.
- [41] Lu, Y.-C., Kemper, A. R., Gayzik, S., Untaroiu, C. D., & Beillas, P. (2013). Statistical Modeling Of Human Liver Incorporating The Variations In Shape, Size, And Material Properties. *Stapp Car Crash Journal*, 57, 285.
- [42] Stingl, J., Báča, V., Čech, P., Kovanda, J., Kovandova, H., Mandys, V., ... & Sosna, B. (2002). Morphology and some biomechanical properties of human liver and spleen. *Surgical and radiologic anatomy*, 24(5), 285-289.
- [43] Kemper, A. R., Santiago, A. C., Stitzel, J. D., Sparks, J. L., & Duma, S. M. (2012). Biomechanical Response Of Human Spleen In Tensile Loading. *Journal Of Biomechanics*, 45(2), 348-355.
- [44] Nicolle, S., Noguer, L., & Palierne, J.-F. (2012). Shear Mechanical Properties Of The Spleen: Experiment And Analytical Modelling. *Journal Of The Mechanical Behavior Of Biomedical Materials*, 9, 130-136.
- [45] Rosen, J., Brown, J. D., De, S., Sinanan, M., & Hannaford, B. (2008). Biomechanical Properties Of Abdominal Organs In Vivo And Postmortem Under Compression Loads. *Journal Of Biomechanical Engineering*, 130(2), 021020.
- [46] Storkholm, J. H., Villadsen, G. E., Jensen, S., & Gregersen, H. (1995). Passive Elastic Wall Properties In Isolated Guinea Pig Small Intestine. *Digestive Diseases And Sciences*, 40(5), 976-982.

- [47] Duch, B., Petersen, J., VINTER-JENSEN, L., & Gregersen, H. (1996). Elastic Properties In The Circumferential Direction In Isolated Rat Small Intestine. *Acta Physiologica*, 157(2), 157-163.
- [48] Gregersen, H., Emery, J., & McCulloch, A. (1998). History-Dependent Mechanical Behavior Of Guinea-Pig Small Intestine. *Annals Of Biomedical Engineering*, 26(5), 850-858.
- [49] Roeder, R., Wolfe, J., Lianakis, N., Hinson, T., Geddes, L., & Obermiller, J. (1999). Compliance, Elastic Modulus, And Burst Pressure Of Small-Intestine Submucosa (SIS), Small-Diameter Vascular Grafts. *Journal Of Biomedical Materials Research Part A*, 47(1), 65-70.
- [50] Egorov, V. I., Schastlivtsev, I. V., Prut, E. V., Baranov, A. O., & Turusov, R. A. (2002). Mechanical Properties Of The Human Gastrointestinal Tract. *Journal Of Biomechanics*, 35(10), 1417-1425.
- [51] Bourgouin, S., Bège, T., Masson, C., Arnoux, P.-J., Mancini, J., Garcia, S., . . . Berdah, S. V. (2012). Biomechanical Characterization Of Fresh And Cadaverous Human Small Intestine: Applications For Abdominal Trauma. *Medical & Biological Engineering & Computing*, 50(12), 1279-1288.
- [52] Rosen, J., Brown, J. D., De, S., Sinanan, M., & Hannaford, B. (2008). Biomechanical Properties Of Abdominal Organs In Vivo And Postmortem Under Compression Loads. *Journal Of Biomechanical Engineering*, 130(2), 021020.
- [53] Dahms, S., Piechota, H., Dahiya, R., Lue, T., & Tanagho, E. (1998). Composition And Biomechanical Properties Of The Bladder Acellular Matrix Graft: Comparative Analysis In Rat, Pig And Human. *British Journal Of Urology*, 82, 411-419.
- [54] Martins, P. A., Silva Filho, A. L., Fonseca, A. M. R. M., Santos, A., Santos, L., Mascarenhas, T., ... & Ferreira, A. J. (2011). Uniaxial mechanical behavior of the human female bladder. *International urogynecology journal*, 22(8), 991-995.
- [55] Zanetti, E. M., Perrini, M., Bignardi, C., & Audenino, A. L. (2012). Bladder tissue passive response to monotonic and cyclic loading. *Biorheology*, 49(1), 49-63.
- [56] Griffiths, D. J., van Mastrigt, R., Van Duyl, W. A., & Coolsaet, B. L. R. A. (1979). Active mechanical properties of the smooth muscle of the urinary bladder. *Medical and Biological Engineering and Computing*, 17(3), 281-290.
- [57] Barnes, S., Shepherd, D., Espino, D., & Bryan, R. (2015). Frequency Dependent Viscoelastic Properties Of Porcine Bladder. *Journal Of The Mechanical Behavior Of Biomedical Materials*, 42, 168-176.
- [58] Coolsaet, B., Van Duyl, W., Van Mastrigt, R., & Van Der Zwart, A. (1975). Visco-Elastic Properties Of The Bladder Wall. *Urologia Internationalis*, 30(1), 16-26.

- [59] Klevmark, B. (1974). Motility of the urinary bladder in cats during filling at physiological rates: I. intravesical pressure patterns studied by a new methods of cystometry. *Acta Physiologica Scandinavica*, 90(3), 565-577.
- [60] Nenadic, I., Mynderse, L., Husmann, D., Mehrmohammadi, M., Bayat, M., Singh, A., . . . Fatemi, M. (2016). Noninvasive Evaluation Of Bladder Wall Mechanical Properties As A Function Of Filling Volume: Potential Application In Bladder Compliance Assessment. *Plos One*, 11(6), E0157818.
- [61] Cochlin, D. L., Ganatra, R. H., & Griffiths, D. F. R. (2002). Elastography in the detection of prostatic cancer. *Clinical radiology*, 57(11), 1014-1020.
- [62] Pallwein, L., Aigner, F., Faschingbauer, R., Pallwein, E., Pinggera, G., Bartsch, G., ... & Frauscher, F. (2008). Prostate cancer diagnosis: value of real-time elastography. *Abdominal imaging*, 33(6), 729-735.
- [63] Nelson, E. D., Slotoroff, C. B., Gomella, L. G., & Halpern, E. J. (2007). Targeted biopsy of the prostate: the impact of color Doppler imaging and elastography on prostate cancer detection and Gleason score. *Urology*, 70(6), 1136-1140.
- [64] Kamoi, K., Okihara, K., Ochiai, A., Ukimura, O., Mizutani, Y., Kawauchi, A., & Miki, T. (2008). The utility of transrectal real-time elastography in the diagnosis of prostate cancer. *Ultrasound in medicine & biology*, 34(7), 1025-1032.
- [65] Ferrari, F. S., Scorzelli, A., Megliola, A., Drudi, F. M., Trovarelli, S., & Ponchiatti, R. (2009). Real-time elastography in the diagnosis of prostate tumor. *Journal of ultrasound*, 12(1), 22-31.
- [66] Romagnoli, A., Autieri, G., Centrella, D., Gastaldi, C., Pedaci, G., Rivolta, L., ... & Roggia, A. (2010). Real-time elastography in the diagnosis of prostate cancer: personal experience. *Urologia Journal*, 77(4), 248-253.
- [67] Giurgiu, C. R., Manea, C., Crisan, N., Bungardean, C., Coman, I., & Dudea, S. M. (2011). Real-time sonoelastography in the diagnosis of prostate cancer. *Medical ultrasonography*, 13(1), 5-9.
- [68] Sumura, M., Shigeno, K., Hyuga, T., Yoneda, T., Shiina, H., & Igawa, M. (2007). Initial evaluation of prostate cancer with real-time elastography based on step-section pathologic analysis after radical prostatectomy: A preliminary study. *International Journal of Urology*, 14(9), 811-816.
- [69] Zhang, Y., Tang, J., Li, Y. M., Fei, X., Lv, F. Q., He, E. H., ... & Shi, H. Y. (2012). Differentiation of prostate cancer from benign lesions using strain index of transrectal real-time tissue elastography. *European Journal of Radiology*, 81(5), 857-862.
- [70] Miyagawa, T., Tsutsumi, M., Matsumura, T., Kawazoe, N., Ishikawa, S., Shimokama, T., ... & Akaza, H. (2009). Real-time elastography for the diagnosis

- of prostate cancer: evaluation of elastographic moving images. *Japanese journal of clinical oncology*, 39(6), 394-398.
- [71] Brock, M., von Bodman, C., Palisaar, R. J., Löppenber, B., Sommerer, F., Deix, T., ... & Eggert, T. (2012). The impact of real-time elastography guiding a systematic prostate biopsy to improve cancer detection rate: a prospective study of 353 patients. *The Journal of urology*, 187(6), 2039-2043.
 - [72] Barr, R. G., Memo, R., & Schaub, C. R. (2012). Shear wave ultrasound elastography of the prostate: initial results. *Ultrasound quarterly*, 28(1), 13-20.
 - [73] Correias, J. M., Khairoune, A., Tissier, A. M., Vassiliu, V., Eiss, D., & H  l  non, O. (2011, March). Trans-rectal quantitative shear wave elastography: application to prostate cancer—a feasibility study. In *Proceedings of the European Congress of Radiology* (Vol. 10).
 - [74] Teng, J., Chen, M., Gao, Y., Yao, Y., Chen, L., & Xu, D. (2012). Transrectal sonoelastography in the detection of prostate cancers: A meta-analysis. *BJU international*, 110(11b), E614-E620.
 - [75] Pallwein, L., Mitterberger, M., Struve, P., Pinggera, G., Horninger, W., Bartsch, G., ... & Frauscher, F. (2007). Real-time elastography for detecting prostate cancer: preliminary experience. *BJU international*, 100(1), 42-46.
 - [76] Sumura, M., Shigeno, K., Hyuga, T., Yoneda, T., Shiina, H., & Igawa, M. (2007). Initial evaluation of prostate cancer with real-time elastography based on step-section pathologic analysis after radical prostatectomy: A preliminary study. *International Journal of Urology*, 14(9), 811-816.
 - [77] Salomon, G., K  llerman, J., Thederan, I., Chun, F. K., Bud  us, L., Schlomm, T., ... & Graefen, M. (2008). Evaluation of prostate cancer detection with ultrasound real-time elastography: a comparison with step section pathological analysis after radical prostatectomy. *European urology*, 54(6), 1354-1362.
 - [78] Walz, J., Marcy, M., Pianna, J. T., Brunelle, S., Gravis, G., Salem, N., & Bladou, F. (2011). Identification of the prostate cancer index lesion by real-time elastography: considerations for focal therapy of prostate cancer. *World journal of urology*, 29(5), 589-594.
 - [79] Tsutsumi, M., Miyagawa, T., Matsumura, T., Endo, T., Kandori, S., Shimokama, T., & Ishikawa, S. (2010). Real-time balloon inflation elastography for prostate cancer detection and initial evaluation of clinicopathologic analysis. *American journal of roentgenology*, 194(6), W471-W476.
 - [80] Aboumarzouk, O. M., Ogston, S., Huang, Z., Evans, A., Melzer, A., Stolzenberg, J. U., & Nabi, G. (2012). Diagnostic accuracy of transrectal elastosonography (TRES) imaging for the diagnosis of prostate cancer: a systematic review and meta-analysis. *BJU international*, 110(10), 1414-1423.

- [81] Sahebjavaher, R. S., Nir, G., Honarvar, M., Gagnon, L. O., Ischia, J., Jones, E. C., ... & Kozlowski, P. (2015). MR elastography of prostate cancer: quantitative comparison with histopathology and repeatability of methods. *NMR in Biomedicine*, 28(1), 124-139. Li, 2011
- [82] Sinkus, R., Nisius, T., Lorenzen, J., Kemper, J., & Dargatz, M. (2003). In-vivo prostate MR-elastography. In *Proc. Intl. Soc. Mag. Reson. Med* (Vol. 11, p. 586).
- [83] Dresner, M. A., Rossman, P. J., Kruse, S. A., & Ehman, R. L. (2002). MR elastography of the prostate. In *Proceedings of the 10th Annual Meeting of ISMRM* (p. 526).
- [84] Dresner, M. A., Cheville, J. C., Myers, R. P., & Ehman, R. L. (2003). MR elastography of prostate cancer. In *Proceedings of the 11th Annual Meeting of ISMRM* (p. 578).
- [85] McGrath, D. M., Foltz, W. D., Samavati, N., Lee, J., Jewett, M. A., van der Kwast, T. H., ... & Brock, K. K. (2011). Biomechanical property quantification of prostate cancer by quasi-static MR elastography at 7 tesa of radical prostatectomy, and correlation with whole mount histology. In *Proc Intl Soc Mag Res Med* (Vol. 19, p. 1483).
- [86] Ahn, B. M., Kim, J., Ian, L., Rha, K. H., & Kim, H. J. (2010). Mechanical property characterization of prostate cancer using a minimally motorized indenter in an ex vivo indentation experiment. *Urology*, 76(4), 1007-1011.
- [87] Carson, W. C., Gerling, G. J., Krupski, T. L., Kowalik, C. G., Harper, J. C., & Moskaluk, C. A. (2011). Material characterization of ex vivo prostate tissue via spherical indentation in the clinic. *Medical engineering & physics*, 33(3), 302-309.
- [88] Phipps, S., Yang, T. H., Habib, F. K., Reuben, R. L., & McNeill, S. A. (2005). Measurement of tissue mechanical characteristics to distinguish between benign and malignant prostatic disease. *Urology*, 66(2), 447-450.
- [89] Hoyt, K., Castaneda, B., Zhang, M., Nigwekar, P., di Sant'Agnese, P. A., Joseph, J. V., ... & Parker, K. J. (2008). Tissue elasticity properties as biomarkers for prostate cancer. *Cancer Biomarkers*, 4(4-5), 213-225.
- [90] Zhang, M., Nigwekar, P., Castaneda, B., Hoyt, K., Joseph, J. V., di Sant'Agnese, A., ... & Parker, K. J. (2008). Quantitative characterization of viscoelastic properties of human prostate correlated with histology. *Ultrasound in medicine & biology*, 34(7), 1033-1042.
- [91] Krouskop, T. A., Wheeler, T. M., Kallel, F., Garra, B. S., & Hall, T. (1998). Elastic moduli of breast and prostate tissues under compression. *Ultrasonic imaging*, 20(4), 260-274.

- [92] Genovese, K., Casaletto, L., Humphrey, J. D., & Lu, J. (2014). Digital image correlation-based point-wise inverse characterization of heterogeneous material properties of gallbladder in vitro. *Proceedings of the Royal Society A: Mathematical, Physical and Engineering Sciences*, 470(2167), 20140152.
- [93] Li, W. G., Luo, X. Y., Hill, N. A., Ogden, R. W., Smythe, A., Majeed, A. W., & Bird, N. (2012). A Quasi-Nonlinear Analysis of the Anisotropic Behaviour of Human Gallbladder Wall. *Journal of biomechanical engineering*, 134(10), 101009.
- [94] Li, W. G., Hill, N. A., Ogden, R. W., Smythe, A., Majeed, A. W., Bird, N., & Luo, X. Y. (2013). Anisotropic behaviour of human gallbladder walls. *journal of the mechanical behavior of biomedical materials*, 20, 363-375.
- [95] Li, W., Bird, N. C., & Luo, X. (2017). A Pointwise Method for Identifying Biomechanical Heterogeneity of the Human Gallbladder. *Frontiers in Physiology*, 8, 176.
- [96] Zhao, J., Liao, D., Chen, P., Kunwald, P., & Gregersen, H. (2008). Stomach stress and strain depend on location, direction and the layered structure. *Journal of biomechanics*, 41(16), 3441-3447.
- [97] Jia, Z. G., Li, W., & Zhou, Z. R. (2015). Mechanical characterization of stomach tissue under uniaxial tensile action. *Journal of biomechanics*, 48(4), 651-658.

Chapter 3 : Research Scope

3.1 Research Aims

Several gaps in knowledge regarding material properties of the abdominal organs have been identified from a state-of-the-art literature review. One of areas identified as having insufficient data is the quantification of the relationship between strain rate and material properties, such as the elastic modulus, failure stress, and failure strain. This lack of data exists for all the organs included in this study. Several organs, the kidney, liver, and spleen, have some testing results available at different strain rates, but the results only established that strain rate was a factor that effected the material properties but did not firmly establish the nature of that relationship.

Therefore, the first aim of this study is to quantify the effect of strain rate on the elastic modulus, failure stress, and failure strain of the major abdominal organs through testing at various rates ranging from quasi-static to dynamic.

Another gap identified is related to the use of material properties from various animal hosts as substitutes for human tissue properties. This substitution is primarily suggested due to the lack of data for human tissue. It is commonly assumed that material properties derived for animal tissue may be assumed to be equivalent to the properties of human tissue, but this assumption has not been validated for the abdominal organs. For those few studies that have attempted to compare the properties of human and animal organs, the comparisons are based on data derived from different studies. The assumption is made that the two experiments were conducted the exact

same way, and the comparisons are therefore valid, but it is rare that identical protocols were used in the comparison studies.

Therefore, the second aim of this study is to address this knowledge gap through testing animal and human organs under the exact same conditions and using identical protocols. A comparison between the two hosts will be performed and the feasibility of using animal organs as a substitute will be examined.

Finally, many studies use material properties from the literature to examine the effects of extreme incidents such as blunt force trauma or exposure to blast loads. However, these studies often use material properties that were derived using testing methods that do not match what conditions the model is intended to simulate. For example, if the study is investigating blunt force trauma to the organ, the material properties used in a model might have been determined using a probing or grasping methodology. The published literature contains a wide range of material properties for a given organ, potentially due to widely varying testing methodologies. Based on the details contained in the published work it is unclear whether the range of results are due to the testing methodologies or some other factors.

Therefore, the third aim of this study is to perform a comparison between the elastic modulus measured using a probing and an unconfined compression methodology on the same specimens at the same loading rates. A comparison between the two methods using the same organs in the same conditions will provide a quantification on the difference between results obtained based solely on the testing method and identify whether or not the testing method makes a difference for each organ studied.

3.2 Experimental Requirements

As part of conducting a study with such a wide breadth of research goals a large amount of testing must be performed. In order to make the greatest use of the available test specimens the experimental program needs to be carefully designed to obtain the maximum amount of data from each test. The testing requirements for each aim are examined in order to develop an efficient testing program.

Due to the biological similarities between human and porcine abdominal organs, and the ability to easily acquire porcine organs from slaughterhouses, researchers often use porcine specimens as a human substitute. However, the resulting studies often assume that the tissue properties are similar and do not directly compare them, rendering the results questionable. This study will perform material testing on both porcine and human organs in an identical fashion in order to investigate the feasibility of using porcine organ material properties as a substitute for human organ material properties.

In order to characterize the strain rate dependency of the material properties it is necessary to test at a variety of strain rates on the same specimen. Human organs will be tested at both quasi-static and dynamic rates to measure the effect of strain rate on elastic modulus, failure stress, and failure strain. The results will then be compared to porcine tissue properties measured at the same loading rates. The limited number of human specimens available means that statistical validity of the human organ testing results cannot be established. However, sufficient porcine specimens are available to allow for statistical significance of the results, develop valid numerical models, and to allow for failure testing over a wider range of loading rates. Comparing the human organ

material properties with the porcine results for identical strain rates will potentially allow for extrapolation of the human results to additional loading rates.

Due the different physical characteristics and *in-vivo* loading conditions between the organs of interest, the tissues were divided into two different testing categories. Fluid filled/pressurized organs are typically loaded in tension *in-vivo*, either from stretching due to the boundary conditions or from expansion of the fluid/gas inside the organ. Therefore, the material properties will be determined through uniaxial tension testing.

However, the solid organs are typically loaded in compression *in-vivo*, either from direct pressure application or through confinement by other anatomical features. From the literature review, it was found that solid organs have typically been tested using probing, mechanical graspers, uniaxial compression, etc., and that the organs are dissected into several smaller specimens to increase the number of available test specimens, which can affect the measured properties. The experimental protocols will be designed to address the issue of how the elastic modulus changes between probing and uniaxial compression protocols on the same intact organs. Organs will be compressed up to a strain that is lower than the yield point which will allow the organ to recover from the test and obtain results from both protocols and at multiple strain rates. Once both nondestructive protocols are completed the organ will be tested in a destructive compression protocol to obtain failure properties.

3.3 Overview of Experimental Design and Protocols

The experimental flow is depicted in Figure 1. Testing will be conducted from two different hosts: human and porcine. Then, as previously described, the abdominal organs will be classified as either solid or fluid/air filled, each of which requires a different testing protocol to accurately simulate the *in-vivo* conditions. The solid organs will be tested in compression while the fluid/gas filled organs will be tested in tension. Solid organs will have 3 different tests that will happen on the same organ: nondestructive compression, nondestructive probing, and destructive compression. The elastic modulus will be measured from the nondestructive compression and probing protocols while the failure stress and failure strain will be measured from the destructive protocol. Each test in the uniaxial tension testing protocol will be destructive. The elastic modulus, failure stress, and failure strain will be measured from each test. Chapter 4 details the methods, results, and analysis of all organs that were compressed, and Chapter 5 covers the same topics for all the organs tested in tension.

Uniaxial compression testing resulted in 3 different types of testing on 4 different organs (liver, kidneys, spleen, prostate) for both human and porcine specimens, thus required several iterations of testing. The three testing methodologies consisted of nondestructive unconfined compression, destructive (failure) unconfined compression testing, and compression probing. A total of 1,071 tests were conducted using the compression methodologies alone. An overview of the number of tests completed in nondestructive compression, destructive compression, and probing for each organ is contained in Tables 3-1:3-4. Since the probing and nondestructive unconfined compression protocols did not damage the organ, specimens were retested at multiple

loading rates. Fewer tests were conducted using the destructive protocol since the organ was tested until failure and was therefore not reusable for further testing.

The uniaxial tension testing protocol, in contrast, resulted in every test proceeding until failure of the tissue and thus each test represents an individual specimen. An overview of all 160 test tests, 86 of which are presented in this dissertation, conducted on all the organs of interest in tension for both human and porcine specimens is shown in Table 3-5.

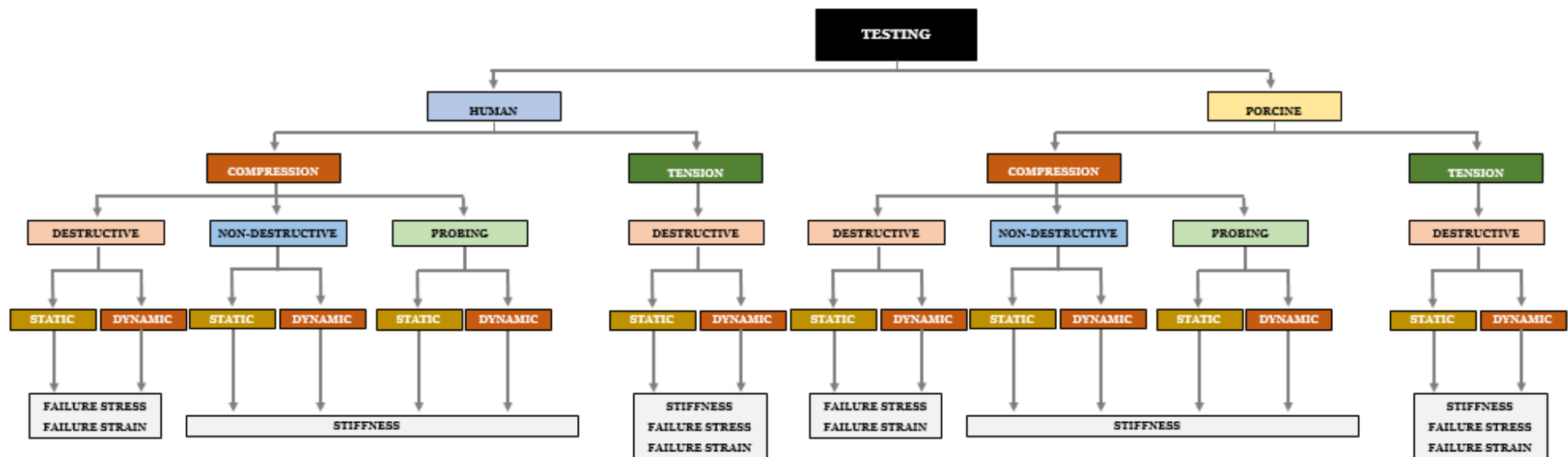


Figure 3-1: Flow chart of experimental process

Table 3-1: Number of experiments completed in nondestructive compression testing protocol

[illegible]

Table 3-2: Number of experiments completed in destructive compression testing protocol

DESTRUCTIVE COMPRESSION TESTING *Not presented in dissertation																
Organ	1%/s		5%/s		25%/s		50%/s		100%/s		250%/s		500%/s		1000%/s	
	Human	Porcine	Human	Porcine	Human	Porcine	Human	Porcine	Human	Porcine	Human	Porcine	Human	Porcine	Human	Porcine
Liver	-	-	1	4	1	4	-	4	-	5	-	-	1	4	-	-
Kidney	-	-	1	5	1	5	1	5	1	5	1	2	1	5	-	3
Spleen	1	6	-	-	1	6	1	6	-	6	-	-	1	6	-	-
Prostate	-	-	-	-	-	2	-	2	1	2	-	2	1	2	-	2
Testicles	-	-	-	-	1*	-	1*	-	1*	-	1*	-	2*	-	-	-

Table 3-3: Overview of number of tests completed in probing testing protocol

NONDESTRUCTIVE PROBING TESTING *Not presented in dissertation				
Organ	1%/s		25%/s	
	Human	Porcine	Human	Porcine
Liver	3	23	3	23
Kidney	6	32	6	32
Spleen	4	32	4	32
Prostate	2	12	2	12
Testicles*	6*	-	6*	-

Table 3-4: Overview of number of tests completed in uniaxial tension testing protocol

Organ	TENSTION TESTING													
	<i>*Not presented in dissertation</i>													
	1%/s		5%/s		25%/s		50%/s		100%/s		500%/s		1000%/s	
	Human	Porcine	Human	Porcine	Human	Porcine	Human	Porcine	Human	Porcine	Human	Porcine	Human	Porcine
<i>Bladder</i>	-	-	6*	-	1	5	2	5	2	5	2	5	-	4*
<i>Gallbladder</i>	-	6*	-	6*	1	6	2	6	1	6	1	6	-	-
<i>Stomach</i>	-	-	-	8*	2*	8*	2*	8*	-	8*	-	11*	-	-
<i>Intestine</i>	-	-	-	5*	2	5	2	5	2	5	1	5	-	-
<i>Penis</i>	-	-	-	-	1*	-	-	-	1*	-	1*	-	-	-

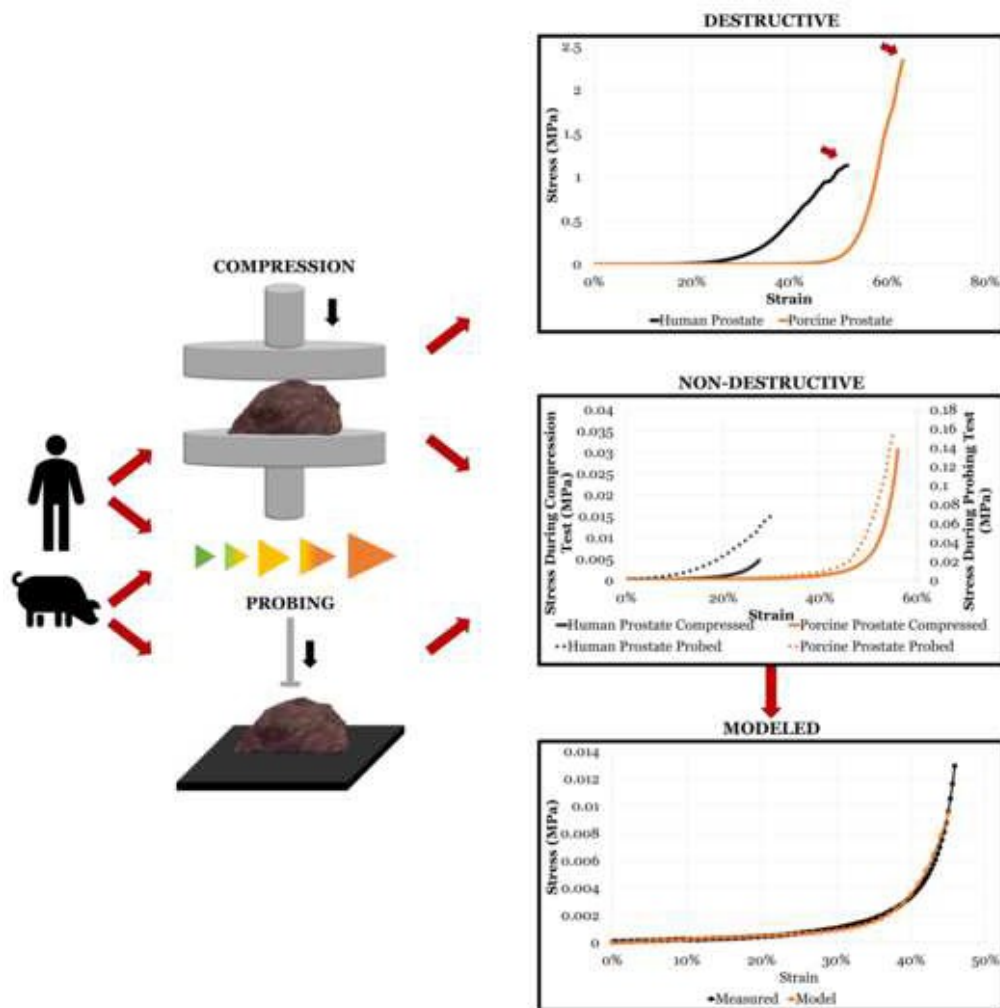
Chapter 4 : Compression Testing

4.1 Prostate Manuscript

THE DIFFERENCES IN MEASURED PROSTATE MATERIAL PROPERTIES BETWEEN PROBING AND UNCONFINED COMPRESSION TESTING METHODS

Blake Johnson, MS¹; Scott Campbell, PhD²; Naira Campbell-Kyureghyan, PhD¹

GRAPHICAL ABSTRACT



ABSTRACT

Characterization of the mechanical properties of organs is important for determining their behavior under load and understanding and predicting their response. In order to appropriately understand behavior, including developing predictive models, the method used to measure the properties should match the application as different testing techniques can yield different results. One of the organs where little mechanical testing has been performed is the prostate. Therefore, the goal of this paper is to expand the knowledge of prostate mechanical behavior by using two different compressive testing methods under various loading rates. No differences were found between the elastic modulus measured using the compression and probing protocols for both human and porcine specimens. A strain rate dependency of the elastic modulus was observed for both the testing methods. The dependency on strain rate started to saturate at higher rates and a material model was created to quantify this dependence as well as the stress-strain behavior. No strain rate dependency was observed for failure stress or failure strain. Overall, similar values of elastic modulus were found for both probing and compression protocols and the relationship developed between elastic modulus and strain rate could be implemented in models of the prostate to aid in understanding the response to dynamic loads.

4.1.1 INTRODUCTION

Characterizing the mechanical properties of abdominal organs is fundamental for advances in numerous areas of biomedicine such as diagnostics, forensics, surgical simulations, and injury prediction [1-5]. Various methods have been used to determine the properties of organs such as tension testing, compression testing, perfusion, probing, aspiration, and imaging [6-10]. However, utilizing multiple methods to determine the material properties of tissues yields a range of results. Examples of the effect of testing methodology on the measured properties include tissues such as the spleen, kidney, and liver [11-14].

Biological tissue, including human organs, is complex, and many factors have been found to impact the measured material properties of human or animal organs such as strain rate, storage method, type of the organ, etc. [12-15]. The range of values obtained for material properties of the same tissue type highlights the importance of matching material testing methodology with the anticipated application of the results.

One instance that illustrates the importance of using the proper testing methodology is developing models intended for use in simulation of traumatic situations like blunt impacts or blast forces on the human body. During these loading conditions organs within the human abdominal cavity will be compressed at a high velocity. Previous research has determined that loading rate significantly effects the mechanical behavior of human organ tissue [12,13]. Thus, simulations should use material properties that were determined using appropriate methodologies. However, material properties found using relevant methods are not always available and the simulations are often performed with whatever data is extant in the literature.

One of the human organs that has been understudied is the prostate. Material testing of the prostate has been predominantly performed using imaging techniques [16-20]. Only a few studies have performed mechanical testing of the prostate tissue. Two studies utilized indentation techniques to test the human prostate, with the elastic modulus determined to be 432 kPa and 20 kPa [21-22]. Ma et al. performed tensile testing of the human prostate and found the elastic modulus to range from 450 kPa to 560 kPa [23]. However, these studies were performed on prostate tissue that had been divided into smaller specimens and at quasi-static rates. The limited research on the

prostate could be the reason why many abdominal organ finite element models do not include the prostate.

Clear gaps exist in the understanding of prostate mechanical properties including elastic modulus and failure stress and strain. First, there are no studies to date that explore the effect of strain rate on the material properties, even though prostate injury often occurs through traumatic incidents [24]. Second, only indentation and tensile testing has been performed on the prostate, while most loading scenarios involve primarily compressive loads. These loads are applied to the intact prostate and testing dissected specimens may affect the measured properties as for the liver [25]. Third, often only limited human prostate specimens are available for study, and no research has compared the properties of human prostate tissue with more readily available animal models. Finally, different testing techniques can lead to a wide range in measured properties and there are no studies examining the effect of testing methodology on the modulus and failure properties.

The goal of this research is therefore to expand the knowledge of prostate mechanical behavior by using two different compressive testing methods under various loading rates. It was hypothesized that the elastic modulus will increase as strain rate increases in both the unconfined compression and probing protocols and that the material properties will differ between these two testing methods. Both human and porcine prostates will be tested in full unconfined compression and using a probing methodology. The mechanical properties of elastic modulus, failure stress, and failure strain will be measured.

4.1.2 METHODS

4.1.2.1 Specimens

Fifteen porcine prostates were procured from an FDA inspected slaughterhouse and were obtained from specimens being harvested for other purposes: no animals were euthanized specifically for this study. The slaughterhouse provided prostate tissues that were still intact to the urethra and bladder. Urethra and bladders were removed in the lab using a scalpel to leave the prostate intact and undamaged. Porcine prostates were 558 (± 76) mm² in surface area and 12.2 (± 1.8) mm in height on average.

Two intact fresh human prostates were procured from cadavers (76 and 89 years). The specimens were tested for and cleared of any transmittable diseases, and had an average surface area of 2025 (± 671) mm² and height of 33 (± 1.9) mm. Tissue testing occurred at room temperature as soon as possible after death of the host.

4.1.2.2 Material Testing Devices

Destructive and nondestructive tissue testing was performed using a Material Testing System (MTS). The compression force and specimen height were sampled at a rate of 4,096 Hz. The load placed on the human tissue was measured using a 15 kN load cell, while the load on the porcine prostate was measured using a 2.5 kN load cell.

The probing methodology utilized a Mark-10 force gauge and EMSL-301 test stand. A probe with a flat circular (4.9 mm diameter) loading surface was used as the indenter. Force and specimen height measurements were collected at a rate of 50 Hz.

4.1.2.3 Experimental Protocol

Nondestructive and destructive testing involved placing the prostate laterally (the urethra canal ran parallel to the compression plate) in the MTS. The plates compressed the human and porcine prostates at the strain rates and to the maximum level of strain (for nondestructive tests) specified in Table 4-1. In nondestructive testing, the prostate was not compressed beyond the elastic region and rested in between each test in order to return to the original height. A minimum of 30 seconds rest occurred after each test. Confirmation of the organ returning to the original height was made prior to the next test. The tests were displacement controlled, and force and displacement were sampled throughout the tests and subsequently transformed into nominal stress and engineering strain using Eq. 1 and 2. The elastic modulus was calculated by taking the secant slope at the most linear portion of the curve at the highest applied strain. Calculating the elastic modulus at that point insured that the entire prostate was evenly compressed. Failure stress and failure strain were recorded during destructive testing. Failure was described as a 10% drop in force or an increase of 3% strain with no resulting increase in force.

Table 4-1: Tested strain rates for each method and host

Strain Rate	Human		Porcine	
	Compression	Probing	Compression	Probing
1 %/s	✓	✓	✓	✓
5 %/s	✓	✓	✓	✓
10 %/s	✓	✓	✓	✓
15 %/s	✓	✓	✓	✓
25 %/s	✓	✓	✓	✓
50 %/s	-	-	✓	-
100 %/s	✓	-	✓	-
250 %/s	-	-	✓	-
500 %/s	✓	-	✓	-
1000 %/s	-	-	✓	-

$$\sigma_{ND} = \frac{Force}{Surface\ Area_{specimen}} \quad (1)$$

$$\varepsilon = \frac{\Delta Height}{Height_{Initial}} \quad (2)$$

The probing methodology oriented the prostate in the ESML-301 test stand in the same direction (lateral) as for compression testing. Human and porcine specimens were indented in the center of the prostate at rates of 1%/s, 25%/s, and 50%/s up to 30% strain. The stress for the probing method was calculated using Eq. 3.

$$\sigma_P = \frac{Force}{Surface\ Area_{probe}} \quad (3)$$

4.1.2.4 Data Analysis

The elastic modulus, failure stress, and failure strain were calculated for each test as appropriate. Mathematical models were developed to describe the stress-strain relationship [26] and the variation of the model parameters with strain rate. The model framework for the strain rate relationship was determined through an optimization process that maximized R^2 .

A one-way ANOVA was conducted on the porcine elastic modulus to test the factors of strain rate for each testing method. Two sample t-test was conducted on each of the individual rates to determine statistical differences between the testing methodologies. An alpha value of 0.05 was set for both statistical tests that were performed.

4.1.3 RESULTS

4.1.3.1 Elastic Modulus

The elastic modulus of the human prostates was similar between the two testing methods, with the measured differences not statistically significant (Figure 4-1). The largest difference in modulus observed between the two methods was a 37% lower stiffness for the probing methodology at a strain rate of 10%/s. Although not statistically significant, an increase in stiffness was observed with each increase in strain rate for both the probing and unconfined compression methods. In both the probing and unconfined compression method, an average increase in stiffness of 28% was measured as rates were increased from 1%/s to 25%/s.

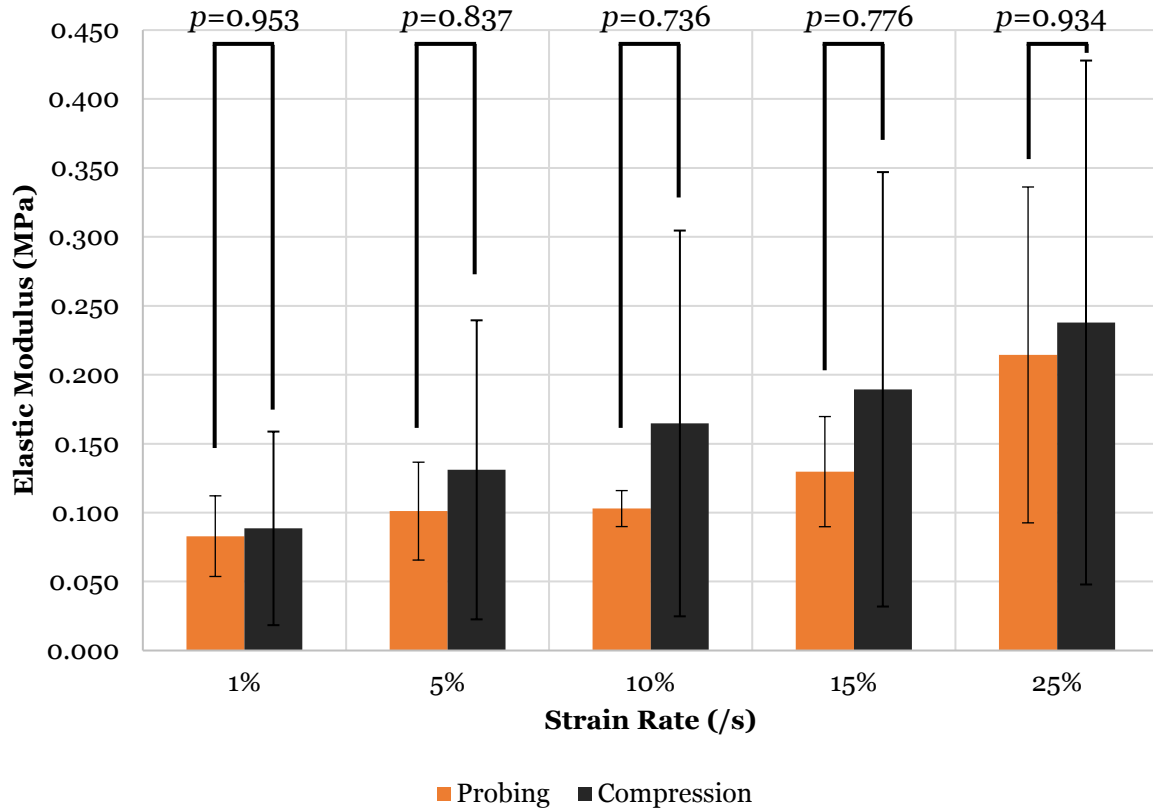


Figure 4-1: Elastic modulus of human prostate measured at various strain rates and with different testing methods

Biological tissue generally has three distinct regions within the stress-strain curve: a toe region at the beginning of the curve where there is a small linear slope (modulus) of the stress versus strain curve, an inflection region where modulus drastically increases, and a terminal region where the stress-strain relationship becomes linear again, but at a larger modulus than the toe region [27]. For both human and porcine specimens the stress strain curves were similar in shape for both testing methods. However, when comparing between the different hosts, the inflection and terminal regions in porcine specimens began at a strain 20% higher than in the human specimens (Figure 4-2).

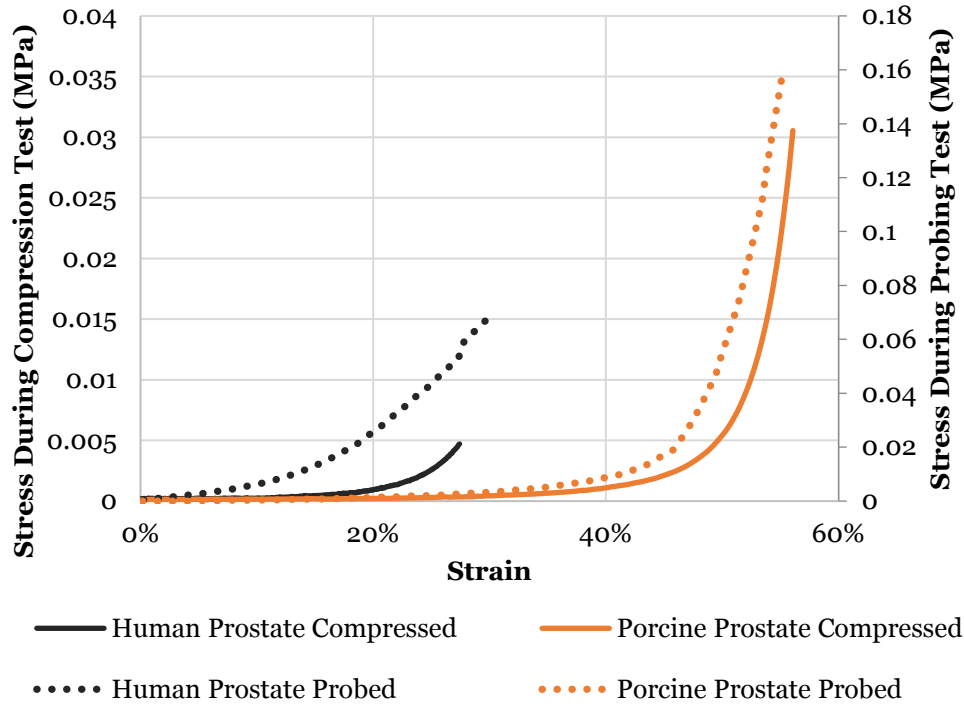


Figure 4-2: Stress versus strain curve of human and porcine prostate under unconfined compression using two testing methodologies

The elastic modulus of the porcine prostates had similar results between the two methods, with no statistically significant differences ($p=0.543$, Figure 4-3). The largest difference observed between the two methods was a 15% smaller stiffness at 10%/s strain rate when tested using the probing methodology versus unconfined compression. Unlike the human prostate, a statistically significant increase in stiffness was observed in the porcine specimens with each increase in strain rate ($p=0.041$). An increase of 102% was observed when the strain rate increased from 1%/s to 25%/s in the probing condition and modulus increased by 115%/s between the same strain rates in the compression method.

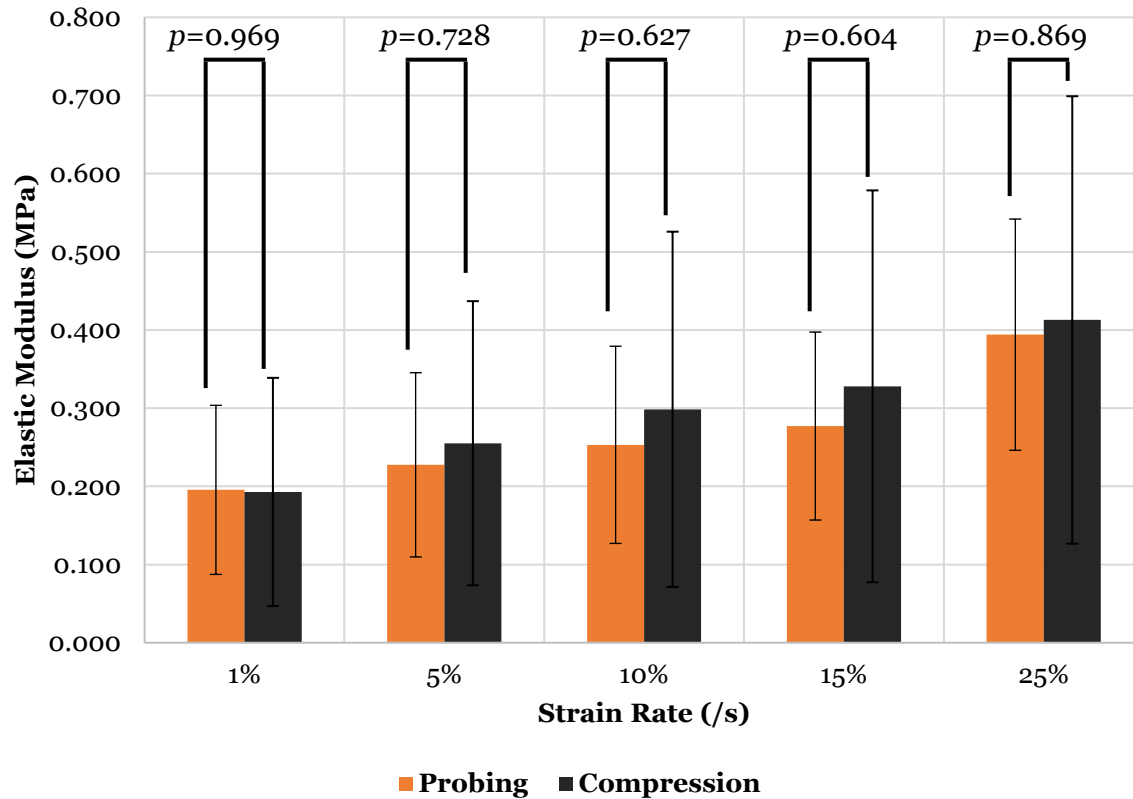


Figure 4-3: Elastic modulus of porcine prostate measured at various strain rates and with different testing methods

The elastic modulus, measured in unconfined compression, was, on average, 88% stiffer in the porcine prostate than the human prostate ($p=0.035$). The differences between the porcine prostate and human prostate stiffness decreased as strain rate increased. The porcine specimen modulus increase over the human specimen modulus was 118% (0.1 MPa) at 1%/s, (0.12 MPa) at 5%/s, (0.13 MPa) at 10%/s, (0.14 MPa) at 15%/s, and (0.18 MPa) at 25%/s. Similar results were observed when comparing the elastic modulus of the two hosts using the probing method. On average, the porcine specimens were measured to be twice as stiff as the human specimens at the same strain rate ($p=0.005$). Both human and porcine tissues were observed to have a strain rate dependency when tested using the probing method ($p=0.612$ and $p=0.15$ respectively).

The porcine prostate was also tested in unconfined compression at higher strain rates and was found to have statistically significant differences between the strain rates. A strain rate of 1%/s resulted in a modulus of 0.19 MPa and 1,000%/s led to a modulus of 1.03 MPa (Figure 4-4) ($p<0.001$). A post-hoc Tukey test revealed two groupings of strain rates that were statistically different from one another. The strain rate of 1%/s is statistically significantly different than rates at and above 250%/s, and strain rates ranging from 5%/s to 250%/s are statistically significantly different from rates at and above 500% ($p<0.05$).

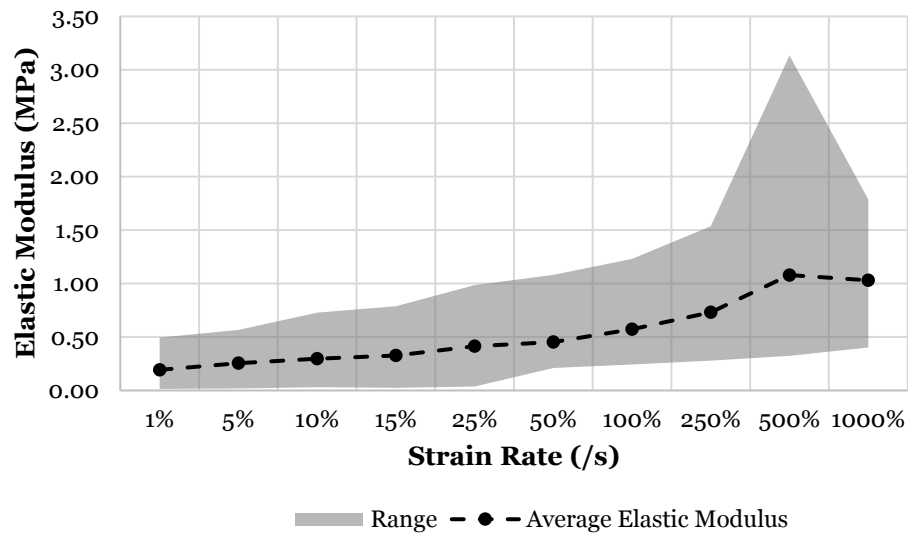


Figure 4-4: The measured elastic modulus of the porcine prostate in unconfined compression at varying rates (shading indicates the range of data)

The stress-strain relationship can be described using Eq. 4. The parameters consist of the elastic modulus in the toe region (E_{toe}), the elastic modulus in the terminal region (E_{term}), the center strain of the inflection region (ϵ_c), and a parameter describing

the curvature of the inflection region (ψ). Values of all four parameters at the tested strain rates for both human and porcine prostates are shown in Table 4-2.

$$E = \{1.0 + \tanh(\psi[\varepsilon - \varepsilon_c])\}(E_{term} - E_{toe})/2.0\} + E_{toe} \quad (4)$$

where E is the current elastic modulus and ε is the current strain.

Table 4-2: Model parameters at tested strain rates for each host

	Strain Rate				
Human	1 %/s	5 %/s	10 %/s	15 %/s	25 %/s
E_{toe} (MPa)	0.0006	0.0006	0.0006	0.0006	0.0006
E_{term} (MPa)	0.0184	0.0260	0.0248	0.0319	0.0472
ε_c	0.0170	0.0180	0.0180	0.0165	0.0180
Ψ	18	18	18	18	17
Porcine					
E_{toe} (MPa)	0.0024	0.0024	0.0024	0.0024	0.0024
E_{term} (MPa)	0.3775	0.4426	0.5057	0.5248	0.6626
ε_c	0.450	0.450	0.445	0.445	0.440
Ψ	14	14	15	14	15

E_{toe} , ε_c , and Ψ were not found to be strain rate dependent for either host.

However, E_{term} was dependent on strain rate, and a model, shown in Eq. 5, was formulated to describe the behavior of the elastic modulus at varying strain rates using unconfined compression on the porcine prostates. Four material constants were used in the equation and $\dot{\varepsilon}$ is the strain rate (Table 4-3).

$$E_{term} = a + b\dot{\varepsilon}^{c-\frac{\varepsilon}{a}} \quad (5)$$

Table 4-3: Parameters for the material model that describes the relationship between strain rate and elastic modulus

Variable	a	b	c	d	$\dot{\epsilon}$
Value	0.20	0.39	0.61	36.66	Strain Rate

The model is plotted against the measured results (Figure 4-5) and has an R^2 of 0.99. The behavior of the prostate elastic modulus is sensitive to the strain rate at low strain rates up to 100%/s and then this dependency starts to saturate. Taken together, Eq. 4 and 5 allow for modeling of the prostate stress-strain behavior at any strain rate.

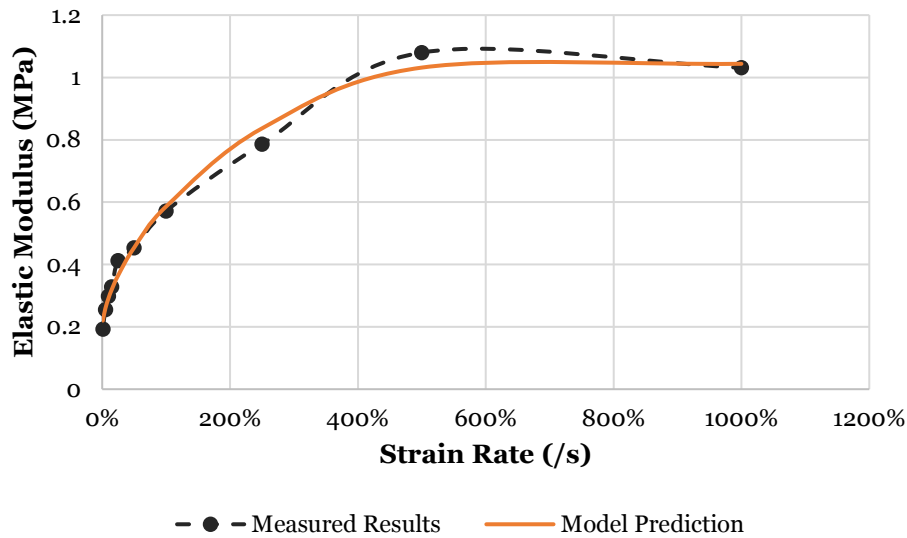


Figure 4-5: Comparison of measured and predicted relationship between elastic modulus and strain rate of porcine prostate using compression method

4.1.3.2 Failure Properties

Both failure stress and failure strain were similar between the porcine and human prostate specimens. In fact, when comparing similar strain rates, the human prostate failure stress was 23% higher than the porcine failure stress at 500%/s, but 23% lower at

100%/s. Although, the human specimen failure stress at 100%/s was 1.13 MPa and increased to 2.08 MPa at a rate of 500%/s the variation observed among the porcine specimen suggests that failure stress is not strain rate sensitive. Porcine failure stress ranged from 0.93 MPa to 1.82 MPa between the rates of 25%/s and 1000%/s (Figure 4-6).

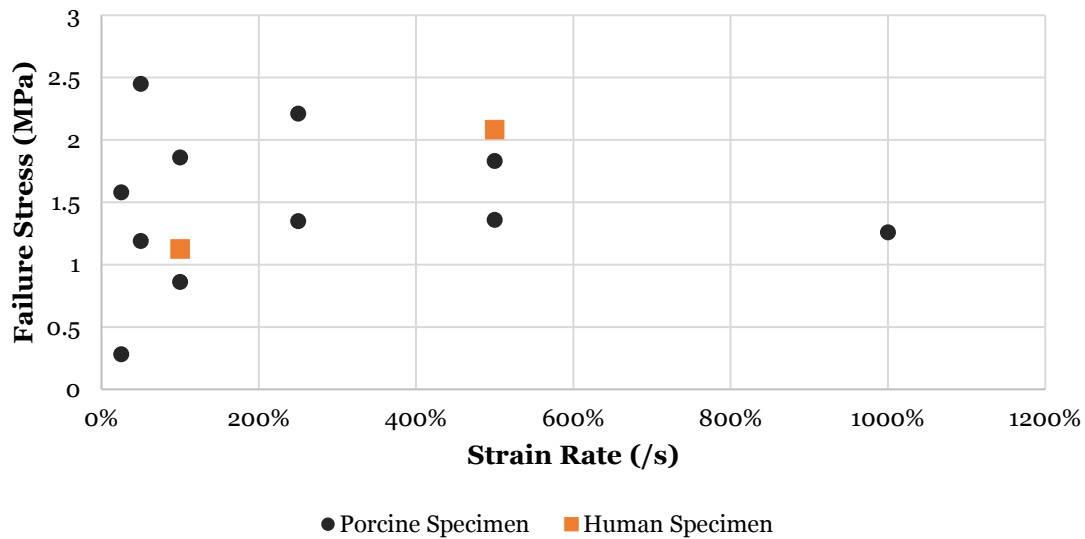


Figure 4-6: Failure stress of human and porcine prostate at various strain rates using unconfined compression

Exhibiting similar trends to failure stress, the failure strain of the human prostate was 53% at 100%/s and increased to 66% at 500%/s. Porcine prostate failure occurred between 59% strain and 65% strain for rates ranging from 25%/s to 1000%/s and demonstrated no strain rate dependency (Figure 4-7).

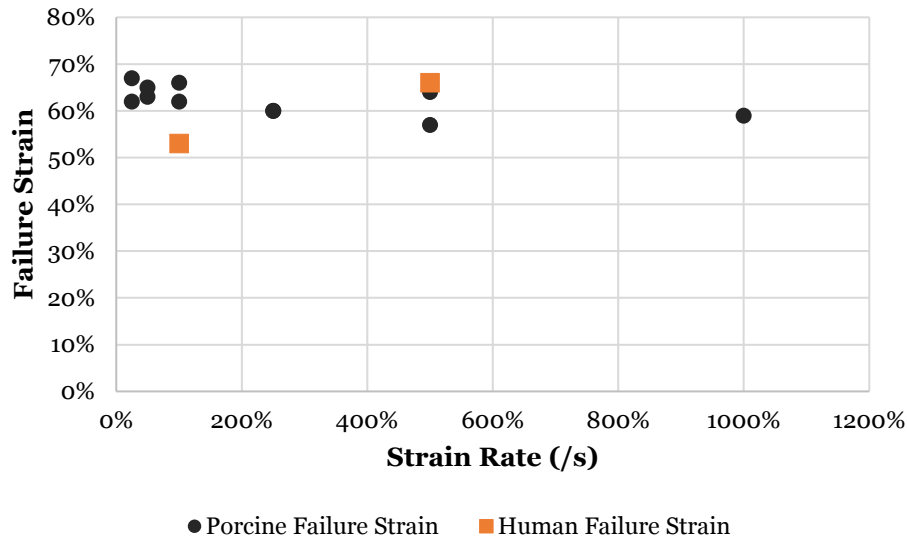


Figure 4-7: Failure strain of human and porcine prostate at various strain rates using unconfined compression

4.1.4 DISCUSSION

Two different testing methodologies were used to determine the structural properties of the prostate tissue: unconfined compression and probing. Identical methods were performed on both human and porcine tissue. Differences in elastic modulus measured using the two different methods varied between 6% and 37% for human specimens and 1% and 15% for porcine specimens, although the differences were not statistically significant. In addition, the differences did not appear to depend on strain rate as no overall patterns were observed. The relative similarity in measured elastic modulus with the two testing methods differs from studies performed on other organs. In a similar study using the kidneys, it was found that probing and unconfined compression yielded elastic moduli that differed by up to 600% [28]. A possible reason for the lack of observed differences between testing methodologies for the prostate is that the prostate is an anatomically heterogeneous organ [29]. Other organs, such as the

kidney and liver, are made up of several different layers that contain tissue of differing cellular structure where the method of testing could have a larger impact on the results. In addition, moduli similar to those obtained using two compression testing methodologies in this study were found in a study using tension testing to characterize the prostate modulus [21].

When comparing the different hosts, it can be argued that for low levels of strain the porcine prostate tissue is not as stiff as the human tissue as the porcine specimens have a longer toe region on the stress-strain curve where the modulus (0.003 MPa for both human and porcine) is relatively low. However, after the inflection point, the porcine tissue is much stiffer than the human specimens (0.3 MPa versus 0.16 MPa). This difference is consistent between the two testing methodologies. A potential reason for the differences could be variations in the elastin and collagen content between human and porcine prostates, and the age-related changes in elastic and collagen behavior [30]. Another factor could be the relative age of the two specimens. The human prostates were harvested after a natural death due to old age of the host. However, the porcine specimens were harvested from hosts that were butchered for consumption at approximately 150 days old when the average natural life is 20 years. After the toe region, the prostate stiffness dramatically increases, which is similar to the behavior of other biological tissues [31-33]. Both hosts exhibited strain rate dependencies for the measured elastic modulus, which is also similar to other abdominal organs [12,13].

This study formulated a material model to aid in describing the relationship of the terminal region elastic modulus of the prostate with strain rate. Material models

published in other studies generally focus on describing the stress-strain relationship, but not the strain rate dependency [8,34,35]. One reason that no other studies used a model to describe this strain rate dependency of modulus could be due to the lack of measured strain rates. Testing the prostate at several different strain rates and formulating the models developed a clear picture of the stress-strain behavior and strain rate dependency, how the terminal modulus saturates at higher strain rates, and allows for prediction of the stress-strain relationship and elastic modulus at other strain rates. Porcine prostate strain rate dependency started to saturate at rates above 100%/s. It is therefore suggested that since the porcine tissue and the human tissue behaved similarly at lower rates that the human tissue would also have a similar saturation of strain rate dependency, although further testing is required to confirm this hypothesis.

Failure stress increased when the loading rate increased from 100%/s to 500%/s in the human specimen, however the porcine specimen failure stress did not exhibit strain rate dependent. Porcine and human prostates exhibited similar behavior regarding elastic modulus strain rate dependence, and thus it was postulated that the human prostate failure properties would behave in a manner similar to the porcine prostates. Similarly, an increase of failure strain was also observed between the two human specimens with increasing strain rate, however the porcine results did not indicate a strain rate dependence for failure strain. This result is unique as studies involving other organs have found strain rate dependency among these failure variables [12,13]. One factor that was not considered that could have affected these results is anisotropy. Other organs, such as the kidneys, have failure properties that are affected by the direction of the organ fibers when loaded [36]. The orientation of the prostate

wall that was in contact with the compression plate, either anterior/posterior or lateral wall, was not considered and could have been different between specimens.

Furthermore, other research articles have established that failure properties of human organs differ between quasi-static testing and dynamic testing, but little difference is observed when comparing properties between dynamic rates [37]. Since all the failure testing in this study was performed at rates greater than quasi-static, the lack of strain rate dependence in the failure properties could be expected.

One of the limitations to this study is characterizing the strain rate dependency of the probing protocol. Equipment limitations prevented investigations of higher strain rates. However, at the tested rates the elastic modulus was similar between the probing and compression tests which suggests that the two methods would also produce similar results at higher strain rates. Another limitation is the lack of sample size for human specimens. Healthy human prostates are difficult to acquire as the prevalence of prostate cancer among cadavers is very high. However, considering the similarity in results between the human and porcine specimens indicates that the results for other strain rates for human specimens could possibly be extrapolated from the porcine specimen results.

4.1.5 CONCLUSION

The elastic modulus was characterized using two different testing methodologies and failure stress and strain were determined using unconfined compression testing. No statistically significant differences were found between the elastic modulus measured using the two test methods for either human or porcine specimens. Elastic modulus for both human and porcine prostates exhibited strain rate dependence for both testing

methods, and the rate dependence of the elastic modulus saturated above 100%/s. The porcine specimens were much stiffer than the human specimens in the terminal phase of the stress-strain curve. Failure stress and strain were not found to have a dependence on strain rate for either the human or porcine prostate.

Overall, the prostate is a unique biological tissue that, unlike other organs, exhibited similar values of elastic modulus when testing using the probing and unconfined compression testing methods. The relationship developed between elastic modulus and strain rate could be implemented in models of the prostate to aid in understanding the response to dynamic loads, while the lack of rate dependence in the failure properties allows for simpler interpretation of tissue damage.

ACKNOWLEDGMENT

The authors would like to acknowledge the tissue donors and the financial support of the US Department of Defense.

FUNDING

This study was funded by the US Department of Defense grant #4892-ARMY-DHP-ELVIS Phase II.

4.1.6 REFERENCES

- [1] Donahue, T. L. H., M. Hull, M. M. Rashid and C. R. Jacobs (2002). "A Finite Element Model of the Human Knee Joint for the Study of Tibio-Femoral Contact." Journal of Biomechanical Engineering **124**(3): pp. 273-280. DOI: 10.1115/1.1470171
- [2] Shen, W., Y. Niu, L. Bykanova, P. Laurence and N. Link (2010). "Characterizing The Interaction Among Bullet, Body Armor, And Human And Surrogate Targets." Journal of Biomechanical Engineering **132**(12): 121001. DOI: 10.1115/1.4002699
- [3] Joldes, G. R., A. Wittek and K. Miller (2009). "Suite of Finite Element Algorithms for Accurate Computation of Soft Tissue Deformation For Surgical Simulation." Medical Image Analysis **13**(6): pp. 912-919. DOI:10.1016/j.media.2008.12.001
- [4] Shen, W., Y. Niu, R. F. Mattrey, A. Fournier, J. Corbeil, Y. Kono and J. H. Stuhmiller (2008). "Development And Validation Of Subject-Specific Finite Element Models For Blunt Trauma Study." Journal of Biomechanical Engineering **130**(2): pp. 21-22. DOI: 10.1115/1.2898723
- [5] Li, P., D. Lai, F. Zhang and T. Feng (2014). "Numerical Modeling and Simulation Based on Finite Element Method for Internal Cardiac Defibrillation in a Human Torso." 2014 7th International Conference on Biomedical Engineering and Informatics (BMEI), IEEE pp 456-460.
- [6] Nava, A., E. Mazza, F. Kleinermann, N. J. Avis, J. McClure and M. Bajka (2004). "Evaluation of The Mechanical Properties of Human Liver and Kidney Through Aspiration Experiments." Technology and Health Care **12**(3): pp. 269-280.
- [7] Gao, Z., K. Lister and J. P. Desai (2010). "Constitutive Modeling of Liver Tissue: Experiment and Theory." Annals of Biomedical Engineering **38**(2): pp. 505-516.
- [8] Umale, S., C. Deck, N. Bourdet, P. Dhumane, L. Soler, J. Marescaux and R. Willinger (2013). "Experimental Mechanical Characterization of Abdominal Organs: Liver, Kidney & Spleen." Journal of the Mechanical Behavior Of Biomedical materials **17**: pp. 22-33.
- [9] Nenadic, I., L. Mynderse, D. Husmann, M. Mehrmohammadi, M. Bayat, A. Singh, M. Denis, M. Urban, A. Alizad and M. Fatemi (2016). "Noninvasive Evaluation of Bladder Wall Mechanical Properties as a Function of Filling Volume: Potential Application in Bladder Compliance Assessment." PloS one **11**(6): e0157818.
- [10] Davis, N. F., J. Mulvihill, S. Mulay, E. M. Cunnane, D. Bolton and M. T. Walsh (2018). "Urinary Bladder vs Gastrointestinal Tissue: A Comparative Study of

- Their Biomechanical Properties for Urinary Tract Reconstruction." Urology **113**: pp. 235-240.
- [11] Nava, A., Mazza E., Furrer, M., Villiger, P., Reinhart, W.H. (2007). "In Vivo Mechanical Characterization of Human Liver." Medial Imaging Analysis **12**: pp. 203-216.
 - [12] Kemper, Andrew R., Anthony C. Santago, Joel D. Stitzel, Jessica L. Sparks, and Stefan M. Duma (2010). "Biomechanical Response of Human Liver in Tensile Loading." Annals of Advances in Automotive Medicine/Annual Scientific Conference, Association for the Advancement of Automotive Medicine **54**: pp. 15-26.
 - [13] Kemper, A. R., A. C. Santago, J. D. Stitzel, J. L. Sparks and S. M. Duma (2013). "Effect of Strain Rate on the Material Properties of Human Liver Parenchyma in Unconfined Compression." Journal of Biomechanical Engineering **135**(10): 104503.
 - [14] Kemper, A. R., A. C. Santago, J. D. Stitzel, J. L. Sparks and S. M. Duma (2012). "Biomechanical Response of Human Spleen in Tensile Loading." Journal of Biomechanics **45**(2): pp. 348-355.
 - [15] Duong, M. T., N. H. Nguyễn, T. N. Trần, R. Tolba and M. Staat (2015). "Influence of Refrigerated Storage on Tensile Mechanical Properties of Porcine Liver and Spleen." International Biomechanics **2**(1): pp. 79-88.
 - [16] Weiss, R. E., V. Egorov, S. Ayrapetyan, N. Sarvazyan and A. Sarvazyan (2008). "Prostate mechanical imaging: a new method for prostate assessment." Urology **71**(3): pp. 425-429.
 - [17] Zhai, L., J. Madden, W.-C. Foo, M. L. Palmeri, V. Mouraviev, T. J. Polascik and K. R. Nightingale (2010). "Acoustic Radiation Force Impulse Imaging of Human Prostates Ex Vivo." Ultrasound in medicine & biology **36**(4): pp. 576-588.
 - [18] Cao, R., Z. Huang, T. Varghese and G. Nabi (2013). "Tissue Mimicking Materials for The Detection Of Prostate Cancer Using Shear Wave Elastography: A Validation Study." Medical physics **40**(2): 022903.
 - [19] Zhang, M., S. Fu, Y. Zhang, J. Tang and Y. Zhou (2014). "Elastic Modulus of The Prostate: A New Non-Invasive Feature to Diagnose Bladder Outlet Obstruction in Patients With Benign Prostatic Hyperplasia." Ultrasound in medicine & biology **40**(7): pp. 1408-1413.
 - [20] Borren, A., G. Groenendaal, M. R. Moman, A. E. Boeken Kruger, P. J. Van Diest, M. Van Vulpen, M. E. Philippens and U. A. Van Der Heide (2014). "Accurate Prostate Tumor Detection with Multiparametric Magnetic Resonance Imaging: Dependence On Histological Properties." Acta Oncologica **53**(1): pp. 88-95.

- [21] Carson, W. C., G. J. Gerling, T. L. Krupski, C. G. Kowalik, J. C. Harper and C. A. Moskaluk (2011). "Material Characterization of Ex Vivo Prostate Tissue Via Spherical Indentation In The Clinic." Medical engineering & physics **33**(3): 302-309.
- [22] Kim, K. H., B. Ahn, S. K. Lim, W. K. Han, J. H. Kim, K. H. Rha and J. Kim (2014). "Indenter Study: Associations Between Prostate Elasticity and Lower Urinary Tract Symptoms." Urology **83**(3): 544-549.
- [23] Ma, J., M. Gharaee-Kermani, L. Kunju, J. M. Hollingsworth, J. Adler, E. M. Arruda and J. A. Macoska (2012). "Prostatic Fibrosis is Associated with Lower Urinary Tract Symptoms." The Journal of urology **188**(4): 1375-1381.
- [24] Durrant, J. J., A. Ramasamy, M. Salmon, N. Watkin and I. Sargeant (2013). "Pelvic Fracture-Related Urethral and Bladder Injury." Journal of the Royal Army Medical Corps **159** (suppl 1): i32-i39.
- [25] Rosen, J., J. D. Brown, S. De, M. Sinanan and B. Hannaford (2008). "Biomechanical Properties of Abdominal Organs In Vivo and Postmortem Under Compression Loads." Journal of Biomechanical Engineering **130**(2): 021020.
- [26] Campbell-Kyureghyan, N. and W. Marras (2009). "Combined Experimental and Analytical Model of the Lumbar Spine Subjected to Large Displacement Cyclic Loads Part II – Model Validation." International Journal of Computational Vision and Biomechanics **2**(1): pp. 95-104.
- [27] Martin, C., and Sun, W. (2012). "Biomechanical Characterization of Aortic Valve Tissue in Humans and Common Animal Models." Journal of Biomedical Materials Research Part A, **100**(6), 1591-1599.
- [28] Sherratt, M. J. (2009). "Tissue Elasticity and the Ageing Elastic Fibre." Age **31**(4): 305-325.
- [29] Roan, E. and K. Vemaganti (2007). "The Nonlinear Material Properties of Liver Tissue Determined from No-Slip Uniaxial Compression Experiments." Journal of Biomechanical Engineering **129**(3): 450-456.
- [30] Wex, C., S. Arndt, K. Brandstädter, L. Herrmann and C. Bruns (2014). "Biomechanical Characterization of Material Properties of Porcine Liver After Thermal Treatment." Soft Materials **12**(4): 411-419.
- [31] Miller, K. (2005). "Method of Testing Very Soft Biological Tissues In Compression." Journal of Biomechanics **38**(1): 153-158.

- [32] Barnes, S. L., A. Lyshchik, M. K. Washington, J. C. Gore and M. I. Miga (2007). "Development of a Mechanical Testing Assay For Fibrotic Murine Liver." Medical physics **34**(11): 4439-4450.
- [33] Lu, Y.-C. and C. D. Untaroiu (2013). "Effect of Storage Methods On Indentation-Based Material Properties of Abdominal Organs." Proceedings of the Institution of Mechanical Engineers, Part H: Journal of Engineering in Medicine **227**(3): 293-301.
- [34] Johnson, B., S. Campbell and N. Campbell-Kyureghyan (2016). "Comparison of Kidney Elastic Modulus Using Full Unconfined Compression and Probing Methods." American Society of Biomechanics. Raleigh, NC. **40**.
- [35] McNeal, J. E. (1981). "The Zonal Anatomy of the Prostate." The prostate **2**(1): 35-49.
- [36] Farshad, M., M. Barbezat, P. Flüeler, F. Schmidlin, P. Graber and P. Niederer (1999). "Material Characterization of The Pig Kidney In Relation With The Biomechanical Analysis Of Renal Trauma." Journal of biomechanics **32**(4): 417-425.
- [37] Snedeker, J. G., M. Barbezat, P. Niederer, F. Schmidlin and M. Farshad (2005). "Strain Energy Density As A Rupture Criterion For The Kidney: Impact Tests On Porcine Organs, Finite Element Simulation, And A Baseline Comparison Between Human And Porcine Tissues." Journal of Biomechanics **38**(5): 993-1001.

4.2 Liver and Kidney Manuscript

CHARACTERIZING THE MATERIAL PROPERTIES OF THE KIDNEY AND LIVER IN UNCONFINED COMPRESSION AND PROBING PROTOCOLS WITH SPECIAL REFERENCE TO VARYING STRAIN RATE

ABSTRACT

The liver and kidneys are the most commonly injured organs due to traumatic impact forces that are applied to the abdomen. These organs pose a challenge to physicians during treatment as they pose a risk of internal bleeding that is hard to diagnose. A better understanding of the mechanism of injury will greatly improve diagnosis, treatment, forensics, and other fields. Finite element modeling is a valuable tool that can aid in this understanding, but accurate material properties are required. Further research regarding the strain rate dependency and the feasibility of using animal tissue instead of human tissue needs to be conducted and is addressed in this manuscript. The elastic modulus in a probing protocol and the elastic modulus, failure stress, and failure strain in a compression protocol were found for both liver and kidney tissue from human and porcine specimens at varying strain rates. Porcine tissue was a feasible substitute for both liver and kidney organs. Increases in the elastic modulus was seen for both the human kidney and liver, but only for the porcine kidney when comparing the unconfined compression and probing protocols. No differences between testing protocols were found between the elastic modulus of porcine liver. A strain rate dependency for both the liver and kidney and was observed to have a larger saturation affect at higher rates for the failure stress than the elastic modulus for both organs. Overall, the material properties of intact liver and kidney were characterized, and the strain rate dependency was numerically modeled. The study findings suggest that porcine liver and kidney tissue is a feasible substitute for human tissue.

4.2.1 INTRODUCTION

Two of the most commonly injured organs due to impact forces in the human abdominal cavity are the kidneys and liver; whether it be from a car accident, explosion, or impact from a projectile [1,2,3]. Due to the quantity of injuries, and the life-threatening impact of these injuries, studies investigating the injury mechanism have become increasingly common. Understanding the behavior of the liver and kidneys subjected to impact loads will provide valuable insight to a variety of fields such as safety, forensics, diagnostic medicine, etc.

A valuable tool that is commonly used to gain insight into the mechanism of abdominal injury is finite element simulation. Many finite element models have been created to aid in investigating abdominal tissue trauma [4-12]. The model results are highly dependent on the tissue material properties, and the models in the literature use properties derived in a variety of methods. However, many times these methods are not reflective of the model application. Since the tissue mechanical properties are highly dependent on the testing methodology, using properties derived from incompatible testing could lead to inaccurate results, invalidating the study. For example, many organs exhibit differing properties when tested in tension and compression [13] and most human tissue shows dependence on the loading rate for stiffness and failure [14;15].

Furthermore, slight variation in similar methodology can have an impact on the material properties. Even different protocols involving compression testing can yield different results. Rosen conducted a study that involved both compression using a mechanical grasper and a probing protocol on the porcine liver [16]. Visible differences

in the stress strain curves and of the parameters of the material model used in the study were found between the different methodologies [Rosen et al., 200816]. Similar results are found for the kidneys. Snedeker determined that falling impact tests required a larger amount of energy to cause failure than using a hail gun protocol [17Snedeker et al., 2005].

During blunt traumatic injury, the liver and kidneys are placed in compression at dynamic rates [18]. Much of the current body of literature involving mechanical testing of the kidneys and liver is not reflective of this reality. Several studies utilize tension testing of these organs [19-28], but test results show significant differences between mechanical properties measured in tension and compression [13,21,22,29,30]. Only a select few studies have investigated the material properties of the liver and kidney under compression and/or at dynamic rates [29,30]. However, these studies did not investigate the properties of a whole intact liver or kidney, and using partial specimens of human organs has been shown to affect the measured properties [14]. Furthermore, several studies utilize organs from hosts other than human, such as bovine or porcine [28,31]. Only one study has investigated the feasibility of using porcine tissue instead of human tissue by comparing the properties of these two tissues [32]. However, this study only investigated the tissue from the two hosts from the perspective of quasi-static tension testing of the kidney capsule. It was found that the elastic modulus differed significantly, but the failure properties did not and that the stress-strain curves were similar, and thus using porcine kidney tissue as a surrogate for human tissue was justifiable [32]. It is still unknown whether these findings hold true at dynamic rates, when tested on an intact organ, and for liver tissue.

The goal of this research is to characterize the material properties of the intact liver and kidney in compression using two protocols, full compression and probing, with special reference to varying strain rate for both human and porcine tissues. Specifically, the aim is to determine the feasibility of using porcine tissue as a model for human tissue as well as quantify the relationship between strain rate and the material properties (elastic modulus, failure stress, failure strain) of the liver and kidney individually. It is hypothesized that there will be little to no differences between the material properties of human and porcine tissues. In addition, it is hypothesized that increasing strain-rate will increase the elastic modulus, failure stress and failure strain. Further characterizing the material properties of these organs will lead to improved blunt force trauma, and other dynamic loading condition, models.

4.2.2 METHODS

4.2.2.1 Specimens

Specimens were obtained from two different hosts, humans and porcine. Three cadavers were procured from the Medical College of Wisconsin. From the three cadavers, six kidneys and three livers were obtained. All cadavers were tested and cleared of any transmittable diseases. A total of 32 fresh kidneys and 23 fresh livers were obtained from porcine. Porcine organs were obtained from a local slaughterhouse and removal of the organs was performed by the butchers. All organs were harvested from porcine that were used for other purposes and thus no animals were euthanized specifically for this study. Specimens were stored in a cooler set to 4 degrees Celsius. Tissue testing occurred as soon as possible after death of the host.

4.2.2.2 Material Testing Devices

Three types of material testing were performed: destructive compression testing, nondestructive compression testing, and probing. A Material Testing System (MTS) was used for both destructive and nondestructive compression testing (Figure 4-8). The compression force and specimen height were sampled at a rate of 4,096 Hz. The load placed on the human tissue was measured using a 15 kN load cell, while the load on the porcine specimens was measured using a 2.5 kN load cell.

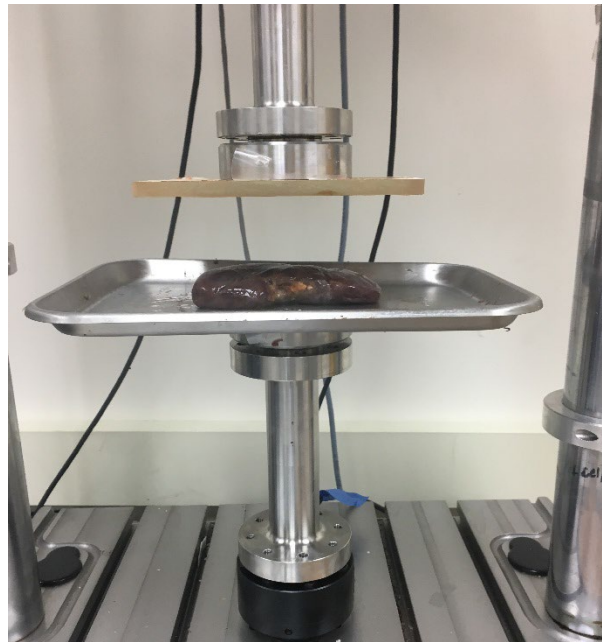


Figure 4-8: Porcine kidney placed in MTS

The third type of material testing was a probing protocol that used a Mark-10 force gauge with an EMSL-301 test stand. Force and displacement data were recorded throughout the tests at a rate of 50 Hz. The end of the probe in contact with the organs was a flat circular (4.9 mm diameter) loading surface.

4.2.2.3 Experimental Protocol

There are two types of testing that utilize the unconfined compression methodology; nondestructive and destructive testing. The compression methodology involved placing the tissue of interest, either liver or kidney, between two compression plates that fully cover the specimen. In nondestructive testing the top compression plate is lowered onto the organ and compresses the tissue up to 30% strain (well below the yield/failure point of the organ as seen in Figure 4-9), while destructive testing compresses the organ until failure. Nondestructive testing tests were repeated at varying strain rates on the same organ, with sufficient time between tests to allow the organ to return to its initial height. Destructive tests were performed at a single strain rate for each specimen, but the strain rate was varied between specimens. All strain rates used in both protocols for the kidneys and livers are given in Tables 4-4 and 4-5. Both testing types were displacement controlled, and force and displacement were sampled throughout the tests and subsequently transformed into stress and strain using equations 1 and 2.

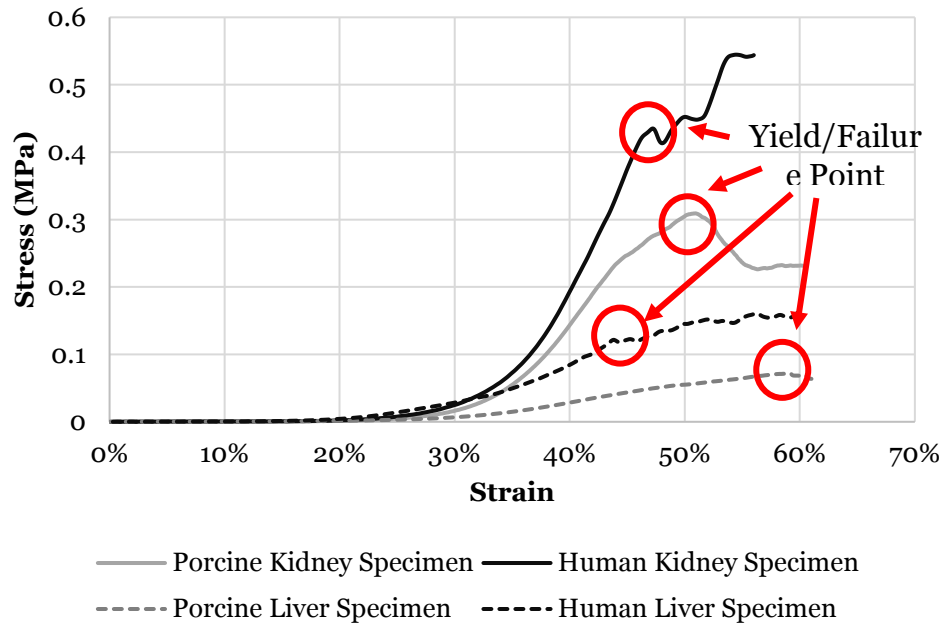


Figure 4-9: Stress versus strain curve of liver and kidney specimens from both human and porcine showing failure/yield point

Table 4-4: Strain rates used in each of the protocols in the kidney experimental testing

Strain Rate	Human Kidney		Porcine Kidney	
	Compression	Probing	Compression	Probing
1 %/s	✓	✓	✓	✓
5 %/s	✓	-	✓	-
25 %/s	✓	✓	✓	✓
50 %/s	✓	-	✓	-
100 %/s	✓	-	✓	-
250 %/s	✓	-	✓	-
500 %/s	✓	-	✓	-
1000 %/s	-	-	✓	-

Table 4-5: Strain rates used in each of the protocols in the liver experimental testing

Strain Rate	Human Liver		Porcine Liver	
	Compression	Probing	Compression	Probing
1 %/s	√	√	√	√
5 %/s	√	-	√	-
25 %/s	√	√	√	√
50 %/s	√	-	√	-
100 %/s	-	-	√	-
500 %/s	√	-	√	-

The surface area of the organs was estimated by placing the organs on graph paper with a known area for each square (Figure 4-10). The elastic modulus was calculated by taking the secant slope at the most linear portion of the curve. Failure stress and failure strain were recorded during destructive testing. Failure was described as a 10% drop in force or an increase of 3% strain with no resulting increase in force.

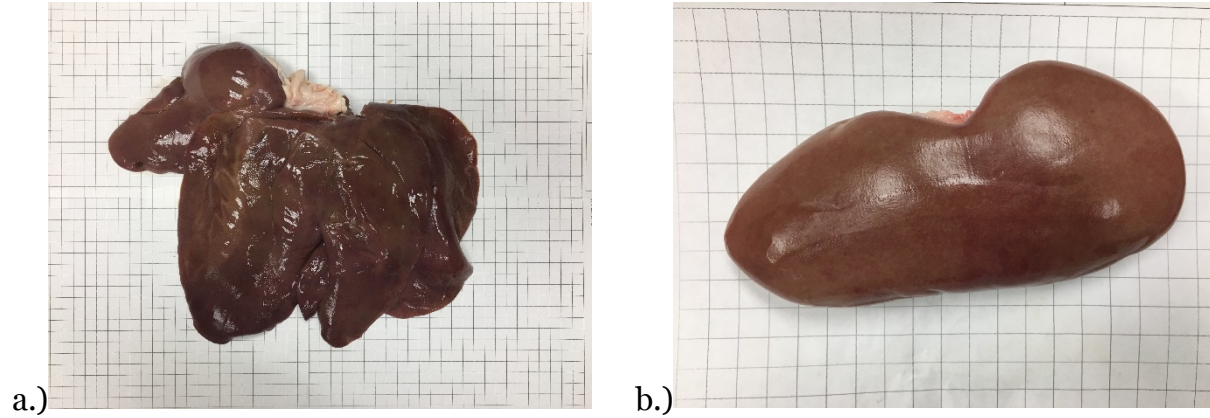


Figure 4-10: Porcine kidney and liver placed on graph paper

$$\sigma_{ND} = \frac{Force}{Surface\ Area_{specimen}} \quad (1)$$

$$\varepsilon = \frac{\Delta Height}{Height_{Initial}} \quad (2)$$

The probing methodology was similar to the nondestructive testing protocol described above. The liver and kidneys were oriented in the ESML-301 test stand in the same direction as for the compression testing. Human and porcine specimens were indented in the center of the organ at rates of 1%/s and 25%/s up to the same specified strain as the nondestructive compression testing. The stress for the probing method was calculated using equation 3.

$$\sigma_P = \frac{Force}{Surface\ Area_{probe}} \quad (3)$$

4.2.2.4 Data Analysis

The material properties were obtained experimentally and calculated based on the equations above. A mathematical model was used to describe the stress-strain relationship that was observed in the experimental testing [33]. The parameters that best fit the experimental curves was found for each of the strain rates. Changes in the

material model parameters between different strain-rates were analyzed. In order to determine the fit of the model with the experimental data, the R^2 of the line produced by comparing the experimental results on the y-axis with the modeled results on the x-axis was found. An equation was also developed to determine the relationship between the material properties with strain rate through an optimization process within Excel (Microsoft, WA) that maximized the R^2 .

The factor of strain rate on the porcine material properties was tested using a one-way ANOVA for each testing method. Two sample t-test was conducted on each of the individual rates to determine statistical differences between human and porcine results. An alpha value of 0.05 was set for both statistical tests that were performed.

4.2.3 RESULTS

4.2.3.1 Kidney

4.2.3.1.1 Stress vs Strain

Different stress versus strain curves were observed for the human and porcine kidney specimens (Figure 4-11). Human specimens had a shorter toe region before the inflection point than the porcine kidneys in both the compression and probing protocols. For both human and porcine specimens a higher stress before the yield point was observed in the probing tests than the compression tests.

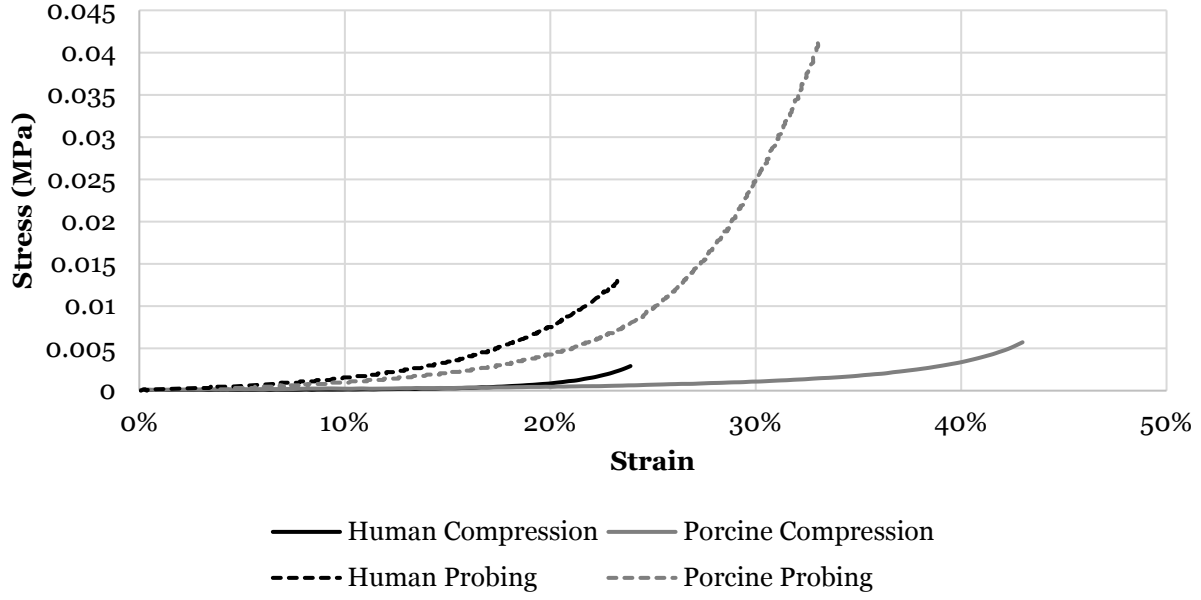


Figure 4-11: Stress versus strain of representative samples from the compression and probing protocols for both human and porcine kidney specimens

A material model (Eq. 4) was used to describe the stress versus strain relationship of both human and porcine kidneys. The parameters consist of the elastic modulus in the toe region (E_{toe}), the elastic modulus in the terminal region (E_{term}), the center strain of the inflection region (ε_c), and a parameter describing the curvature of the inflection region (ψ). Table 4-6 contains the values of all parameters between the rates of 1%/s and 25%/s for the kidney specimens of both human and porcine hosts. An example of the stress strain curve of the experimental versus the modeled results are in Figure 4-12.

$$E = \{1.0 + \tanh(\psi[\varepsilon - \varepsilon_c])\} \{(E_{term} - E_{toe})/2.0\} + E_{toe} \quad (4)$$

where E is the current elastic modulus and ε is the current strain.

Table 4-6: Average and standard deviation of the model parameters and R^2 of model fit to experimental results for the kidney at tested strain rates for each host in the nondestructive testing protocol

Human	Strain Rate		
	1 %/s	5 %/s	25 %/s
E_{toe} (MPa)	0.0008 (± 0.0007)	0.0013 (± 0.0006)	0.00015 (± 0.001)
E_{term} (MPa)	0.0064 (± 0.0012)	0.0093 (± 0)	0.0132 (± 0.000043)
ϵ_c	0.083 (± 0.019)	0.089 (± 0.046)	0.122 (± 0.04)
Ψ	72.16 (± 39.67)	161.01 (± 119.22)	28.22 (± 18.04)
R^2	0.919 (± 0.08)	0.9339 (± 0.06)	0.917 (± 0.046)
Porcine			
E_{toe} (MPa)	0.0003 (± 0.00025)	0.00005 (± 0.00003)	0.00021 (± 0.00012)
E_{term} (MPa)	0.036 (± 0.011)	0.039 (± 0.014)	0.047 (± 0.017)
ϵ_c	0.191 (± 0.012)	0.19 (± 0.015)	0.195 (± 0.014)
Ψ	18.7 (± 2.96)	19.63 (± 1.59)	20.01 (± 1.84)
R^2	0.994 (± 0.006)	0.997 (± 0.003)	0.993 (± 0.008)

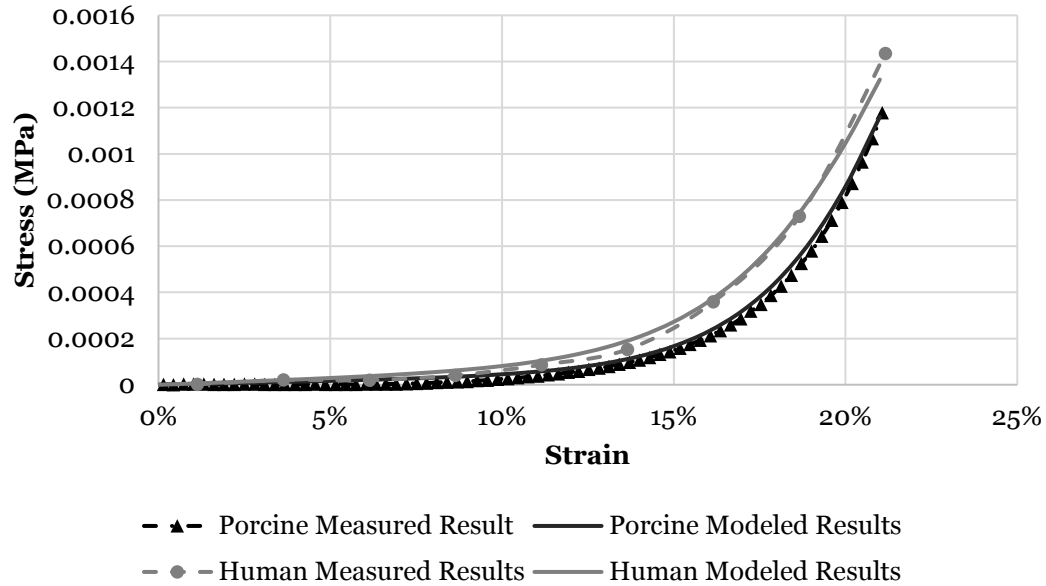
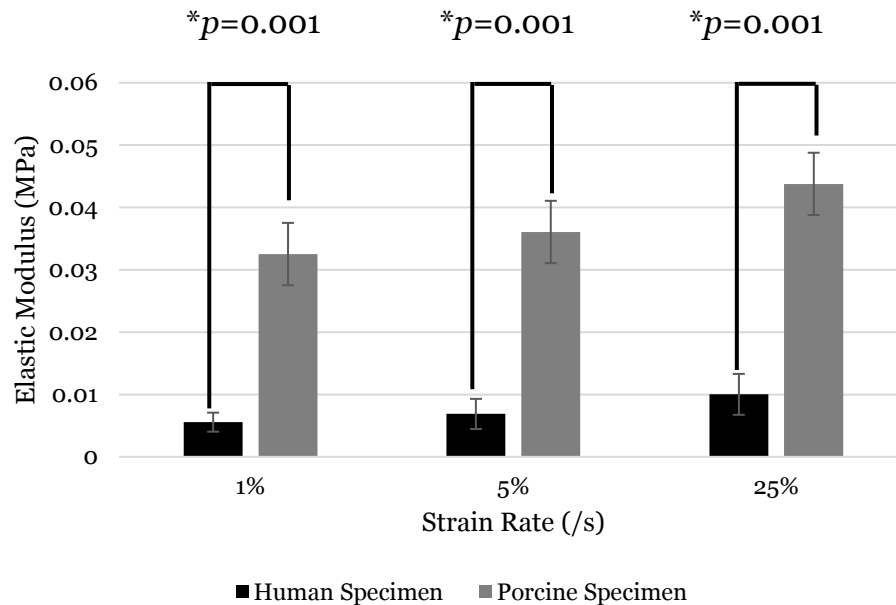


Figure 4-12: Experimental and modeled stress-strain curve for both human and porcine kidney specimens at 25%/s strain rate

A dependency in strain rate was only observed in the model once the strain rate increased from 5%/s to 25%/s for both human and porcine kidney. The parameter that was affected the most was the E_{term} which increased by approximately 0.04 MPa for the human host results and by 0.01 MPa for the porcine host. The curvature of the inflection region slightly dropped as the rates increased for the human kidneys starting at a value of 17.8 at 1%/s and dropping to 17 at 25%/s. Porcine kidneys did not have a consistent change in the curvature of the inflection region between rates but also exhibited a larger standard deviation than was observed in the human specimens. Overall the rest of the parameters were unaffected by the strain rate.

3.1.2 Elastic Modulus

In the nondestructive testing protocol the porcine kidney was measured to be stiffer at all rates in comparison to the human kidney ($p < 0.05$) (Figure 4-13). Human kidney elastic modulus ranged from 0.005 MPa at 1%/s to 0.01 MPa at 25%/s on average in the nondestructive compression protocol. Porcine kidney elastic modulus ranged from 0.03 MPa at 1%/s to 0.045 MPa at 25%/s. Although not statistically significant, the human elastic modulus increased with every increase in strain rate (Figure 6).



*Figure 4-13: Elastic modulus of both human and porcine kidneys in the nondestructive compression protocol at various strain rates. * denotes statistically significant differences*

The elastic modulus of the porcine kidney was measured at rates ranging from 1 %/s to 1000 %/s (Figure 4-14). On average, the specimens became stiffer as the strain

rate increased ($p < 0.001$). From a strain rate of 1%/s to 100%/s there was no statistical difference found between the measured stiffnesses. However, the modulus at rates above 100%/s were statistically higher than at 1%/s and 5%/s, and the modulus at 1000%/s was statistically different from at all rates below 500%/s.

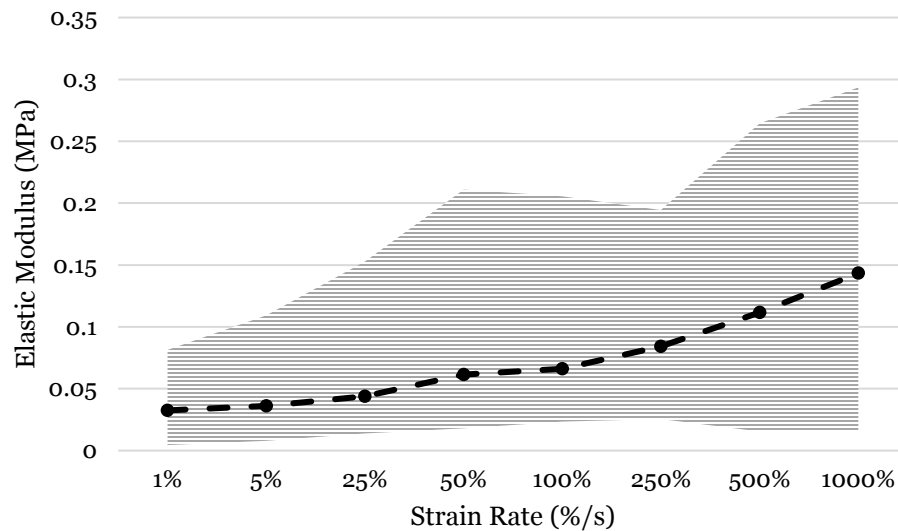


Figure 4-14: Average and range of elastic modulus for the porcine kidneys at all rates investigated

The model relating elastic modulus to strain rate (Equation 5) is plotted against the measured results (Figure 4-15) and has an R^2 of 0.98. Due to limited human specimens, only the porcine results were modeled. The model parameters for porcine kidneys are shown in Table 4-7. The behavior of the kidney elastic modulus is sensitive to the strain rate at low strain rates up to 100%/s and then this dependency starts to saturate. Using the model and parameters an estimate of the elastic modulus can be estimated for a wide range of strain rates.

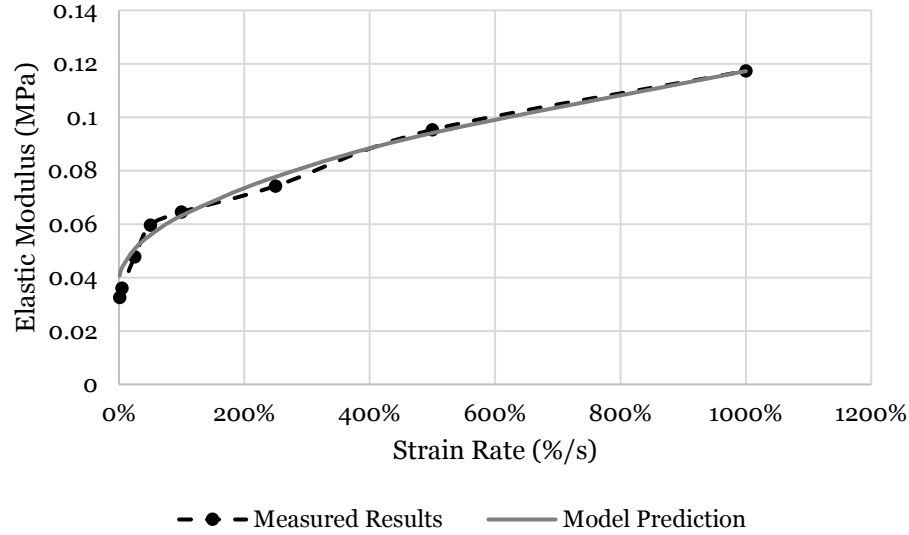


Figure 4-15: Measured and model predicted elastic modulus of the porcine kidney

$$E_{term} = a + b\dot{\epsilon}^{c-\frac{\dot{\epsilon}}{d}} \quad (5)$$

Table 4-7: Parameters for the material model that describes the relationship between strain rate and elastic modulus for porcine kidneys

Variable	a	b	c	d	$\dot{\epsilon}$
Value	0.038	0.025	0.5	1919803	Strain Rate

No differences were observed in the elastic modulus of the two hosts when tested at 1%/s and 25%/s (Figure 4-16). A 95% increase in stiffness was measured in the human kidney when testing at 25%/s versus 1%/s ($p=0.006$). Only a 30% increase was observed between the same rates for the porcine specimens ($p>0.05$).

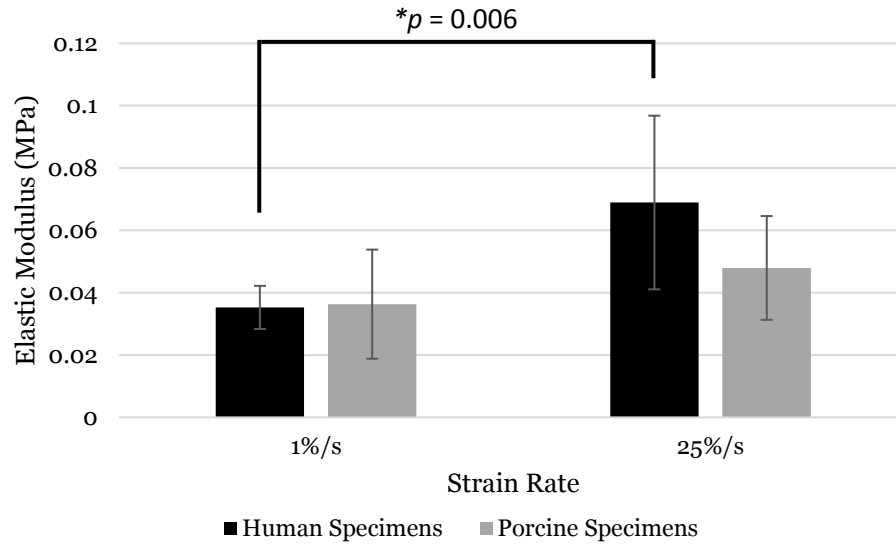


Figure 4-16: Kidney elastic modulus measured in the probing protocol for both human and porcine specimens at various rates

4.2.3.1.3 Failure Properties

Overall the human kidney was stronger than the porcine kidney (Figure 4-17). Other than at a relative low strain rate (5%/s), the human specimens had a failure stress 16% to 25% higher than the porcine specimens. The largest difference was at the rate of 100%/s where the human kidney failed at 0.36 MPa while the porcine kidney failed at 0.26 MPa. The average and range of failure stress at each rate for the porcine destructive testing is presented in Figure 4-18. An increase of 0.13 MPa was observed between the rates of 100%/s and 500%/s for the porcine specimens which was the largest increased observed between all rates.

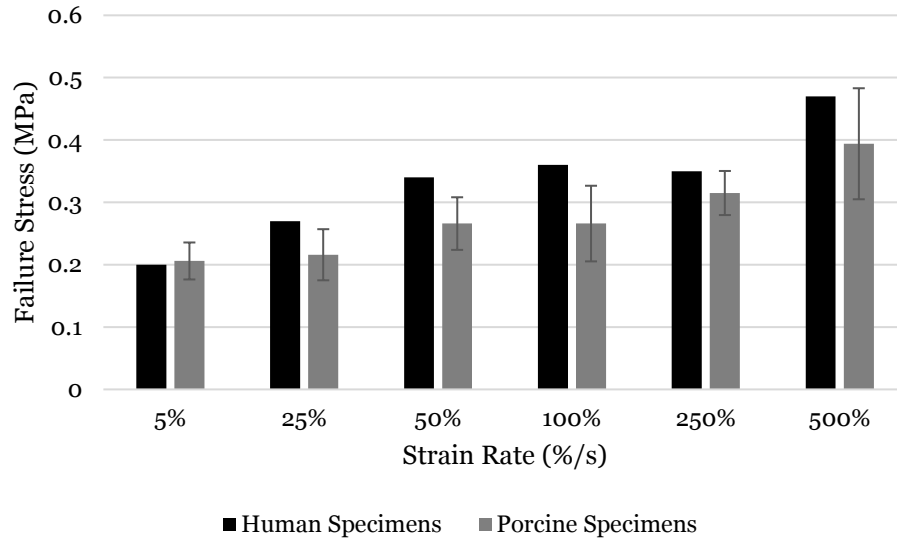


Figure 4-17: Failure stress of the human and porcine kidney measured at various rates

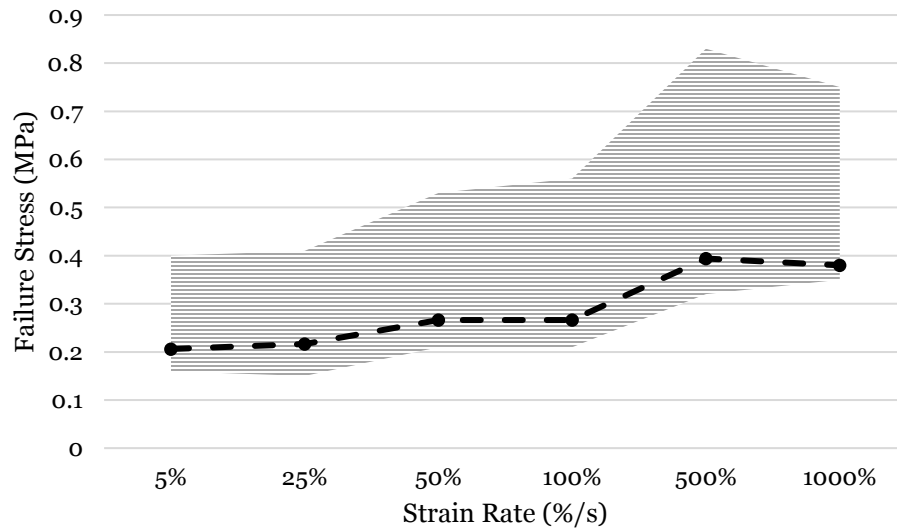


Figure 4-18: Average and range of failure stress for the porcine kidney measured at all rates investigated

Failure stress was observed to be generally dependent on strain rate for both human and porcine specimens (Figure 4-19). The strain-rate dependence model (Equation 5) for porcine specimens is plotted against the measured results in Figure 12

and has an R^2 of 0.97. Due to limited human specimens, only the porcine results were modeled. The behavior of the kidney elastic modulus is sensitive to the strain rate at low strain rates up to 100%/s and then this dependency starts to saturate. Through this model and the parameters found in Table 4-8, an estimate of the failure stress can be obtained at various strain rates.

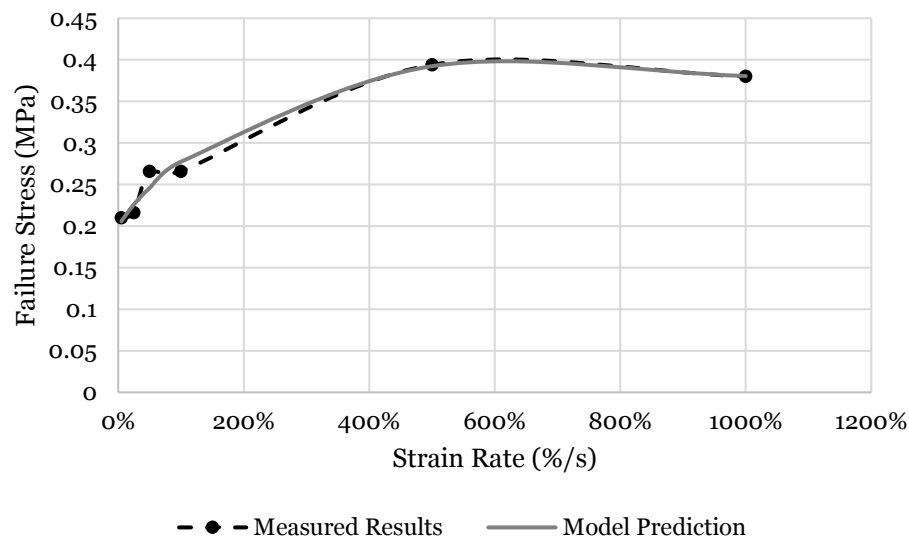


Figure 4-19: Measured and model predicted failure stress of the porcine kidney

Table 4-8: Parameters for the material model that describes the relationship between strain rate and failure stress for porcine kidneys

Variable	a	b	c	d	ϵ
Value	0.196	0.081	0.74	25.92	Strain Rate

Failure strain was nearly identical between the two hosts. Both human and porcine failure strain was observed to be independent of strain rate (Figure 4-20). On average the failure strain was 49% and ranged from 41% to 57%.

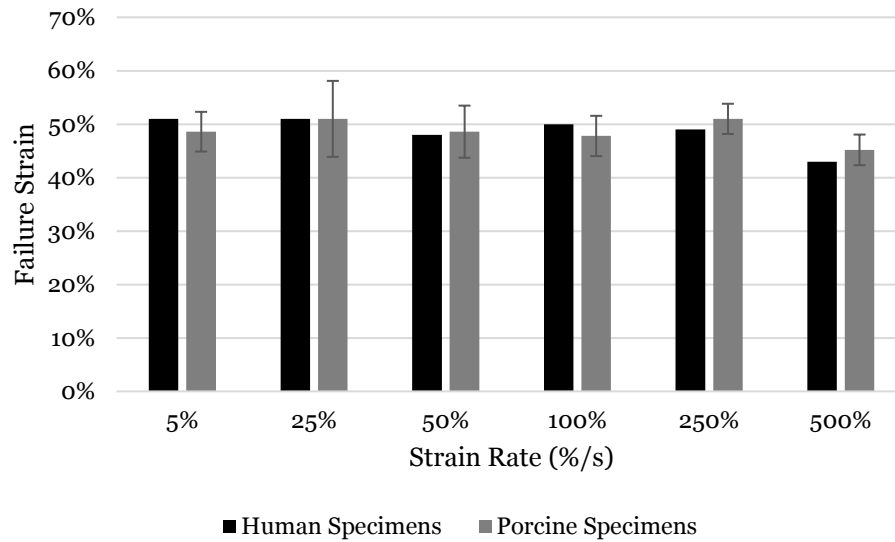


Figure 4-20: Failure strain for both human and porcine specimens measured at various rates

4.2.3.2 Liver

4.2.3.2.1 Stress versus strain

In each of the types of testing a different profile was observed (Figure 4-21). In the compression testing the human livers had a shorter toe region before the inflection point, that was matched with a lower level of stress before the yield point than the porcine samples. Similarly, the human specimens had shorter toe regions than the porcine specimens in the probe testing. However, the human probe tests resulted in much higher elastic modulus and higher stress before the yield point than the compression tests. This is contrary to the porcine specimens where the probing and compression test results were more similar to each other.

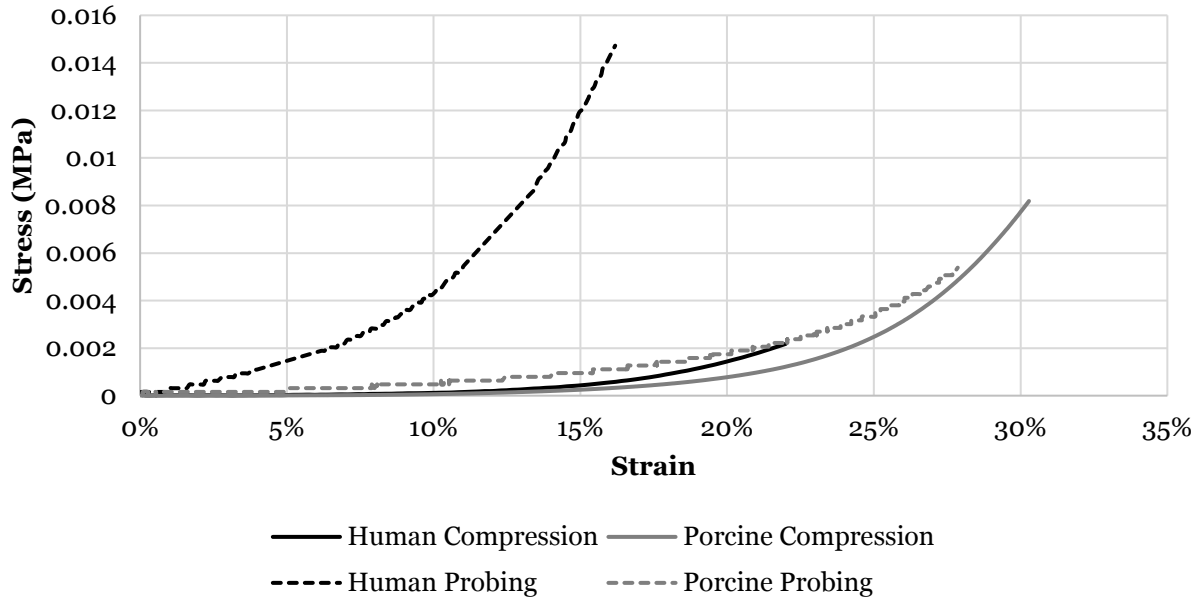


Figure 4-21: Stress versus strain of representative samples from the compression and probing protocols for both human and porcine liver specimens at 1%/s strain rate

Eq. 5 was also used to describe the stress versus strain behavior of the human and porcine liver specimens between the rates of 1%/s to 25%/s. The values found for all four parameters at the tested strain rates for livers of both human and porcine hosts are shown in Table 4-9. An effect of strain rate was observed for all four parameters for both human and porcine specimens only after the strain rate was increased to 25%/s. The E_{toe} term tripled from rates of 5%/s to 25%/s for the human host and but only increased by 40% for the porcine host. An increase of 20% was observed for the E_{term} parameter between the rates of 5%/s and 25%/s for the modeled human stress-strain curve, but a 75% increase was measured for the modeled porcine results. Little to no changes were observed between the rest of the parameters between the rates of 5%/s to 25%/s for both human and porcine modeled results. On average the R^2 for the fit

between model and experimental results was above 0.9 for all rates and hosts. An example of experimental and modeled stress strain curve is shown in Figure 4-22.

Table 4-9: Model parameters for liver at tested strain rates for each host

Human	Strain Rate		
	1 %/s	5 %/s	25 %/s
E_{toe} (MPa)	0.0006 (± 0.0008)	0.0003 (± 0.0004)	0.0003 (± 0.0004)
E_{term} (MPa)	0.06 (± 0.015)	0.065 (± 0.019)	0.079 (± 0.028)
ϵ_c	0.192 (± 0.015)	0.19 (± 0.023)	0.19 (± 0.05)
Ψ	15.76 (± 1.08)	17.04 (± 1.65)	17.33 (± 2.92)
R^2	0.9958 (± 0.002)	0.9971 (± 0.003)	0.9767 (± 0.015)
Porcine			
E_{toe} (MPa)	0.0002 (± 0.0001)	0.0002 (± 0.0001)	0.00034 (± 0.0002)
E_{term} (MPa)	0.025 (± 0.012)	0.024 (± 0.018)	0.042 (± 0.028)
ϵ_c	0.211 (± 0.007)	0.211 (± 0.008)	0.214 (± 0.006)
Ψ	17.46 (± 2.13)	18 (± 2.44)	17.27 (± 2.85)
R^2	0.9973 (± 0.001)	0.9947 (± 0.005)	0.9939 (± 0.003)

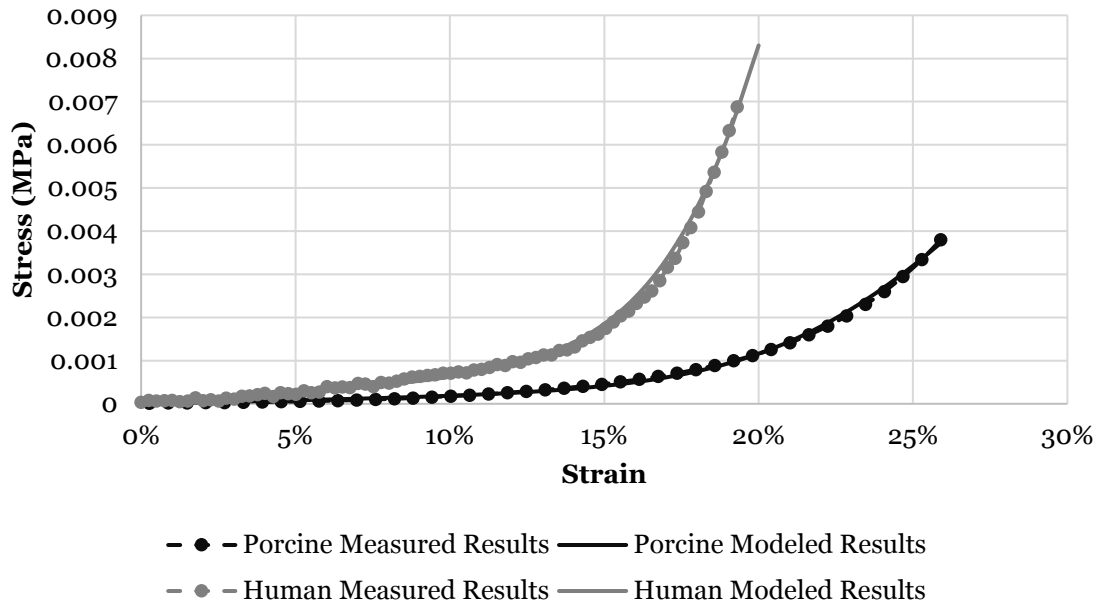


Figure 4-22: Experimental and modeled stress-strain curve for both human and porcine kidney specimens

4.2.3.2.2 Elastic Modulus

Small differences were observed in the elastic modulus between human and porcine hosts tested under compression at the rates of 1%/s, 5%/s, and 25%/s. Porcine hosts were only stiffer by 0.004 MPa, 0.013 MPa, and 0.002 MPa for the rates of 1%/s, 5%/s, and 25%/s respectively (Figure 4-23). The average elastic modulus for the human specimens ranged from 0.04 MPa at 1%/s to 0.06 MPa at 25%/s. Porcine specimens became stiffer with every increase in strain rate starting at 0.032 MPa at 1%/s and increased to 0.065 MPa at 500%/s ($p=0.016$). Only the rates above 100%/s were statistically significantly greater than the elastic modulus measured at 1%/s (Figure 4-24).

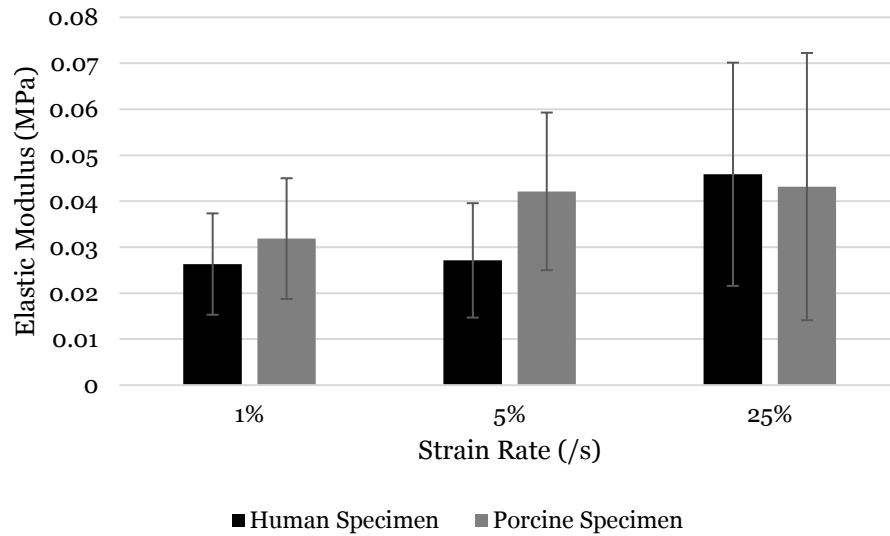


Figure 4-23: Elastic modulus of both human and porcine livers at various strain rates

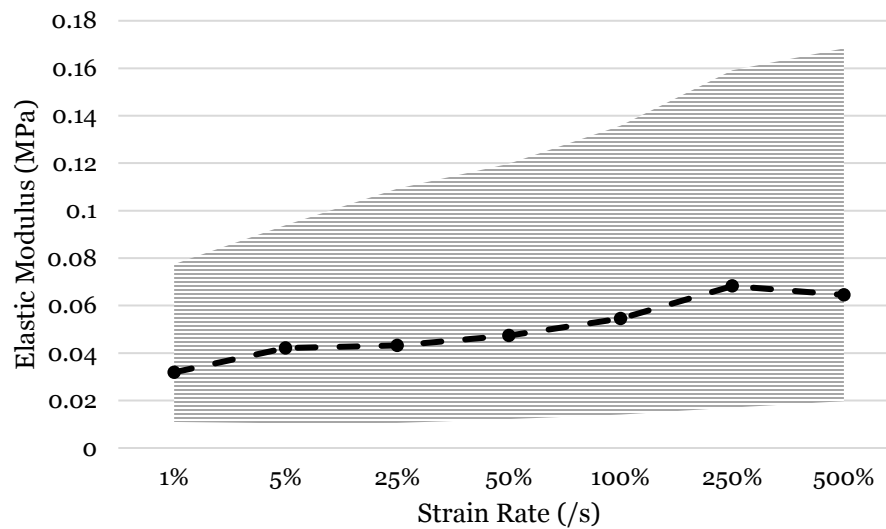


Figure 4-24: Average and range of elastic modulus for the porcine livers at all rates investigated

The model (Equation 5, Table 4-10) is plotted against the measured porcine results (Figure 4-25) and has an R^2 of 0.87. Human results were not modeled due to the limited number of specimens. The behavior of the porcine liver elastic modulus is sensitive to the strain rate between the rates of 5%/s and 50%/s. As the rates increase

above 50%/s, the material property dependency on strain rate becomes linear. Through this model and the parameters found in Table 4-10, an estimate of the elastic modulus can be obtained for both low and high dynamic strain rates.

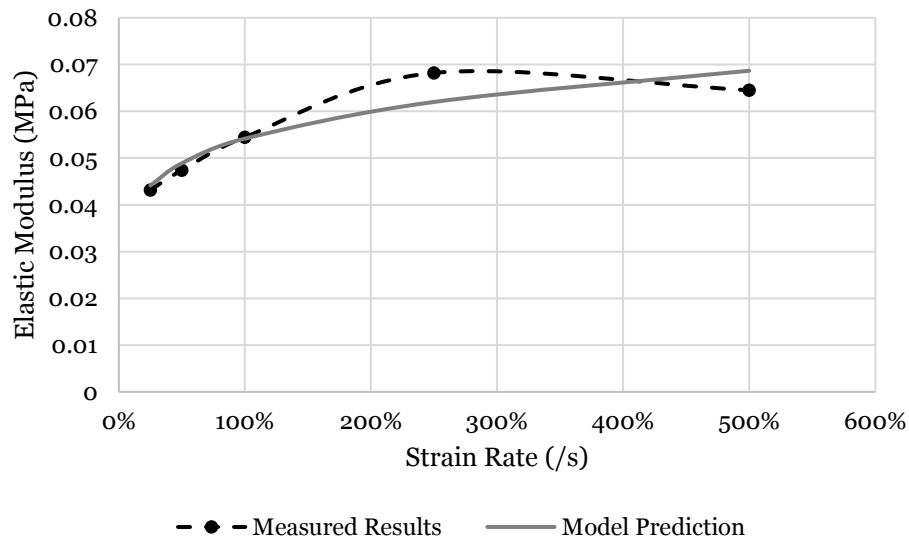


Figure 4-25: Measured and model predicted elastic modulus of the porcine liver

Table 4-10: Parameters for the material model that describes the relationship between strain rate and porcine liver elastic modulus

Variable	a	b	c	d	ϵ
Value	0	0.054	0.14	2070615	Strain Rate

Human livers were approximately 0.15 MPa stiffer at 1%/s and 0.22 MPa stiffer at 25%/s strain rate ($p=0.027$ and 0.033). Stiffness increased by 33% from the rate of 1%/s to 25%/s for the porcine hosts and 55% for the human liver but both increases were not statistically significant ($p>0.05$) (Figure 4-26).

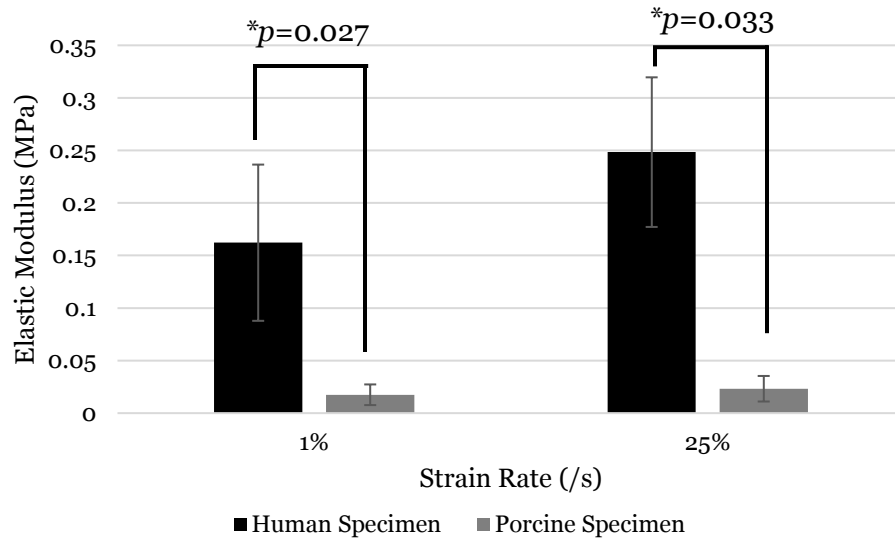


Figure 4-26: Elastic modulus measured in the probing protocol for both human and porcine liver specimens at various rates

4.2.3.2.3 Failure Stress

Human livers had a higher failure stress than the porcine specimens at every tested strain rate. The largest difference, a 135% increase, was observed at the rate of 25%/s, and the smallest difference, a 62% increase, was observed at 500%/s. Strain rate dependency was observed for the failure stress in both human and porcine livers (Figure 4-27). Human livers tested at a rate of 25%/s had a failure stress of 0.11 MPa which increased by 54% to 0.17 MPa when tested at 500%/s. Similarly, the porcine specimen failure stress increased from 0.04 MPa to 0.11 MPa from the rate of 25%/s to 500%/s. Failure stress dependence on strain rate was statistically significant ($p=0.011$) for the porcine results.

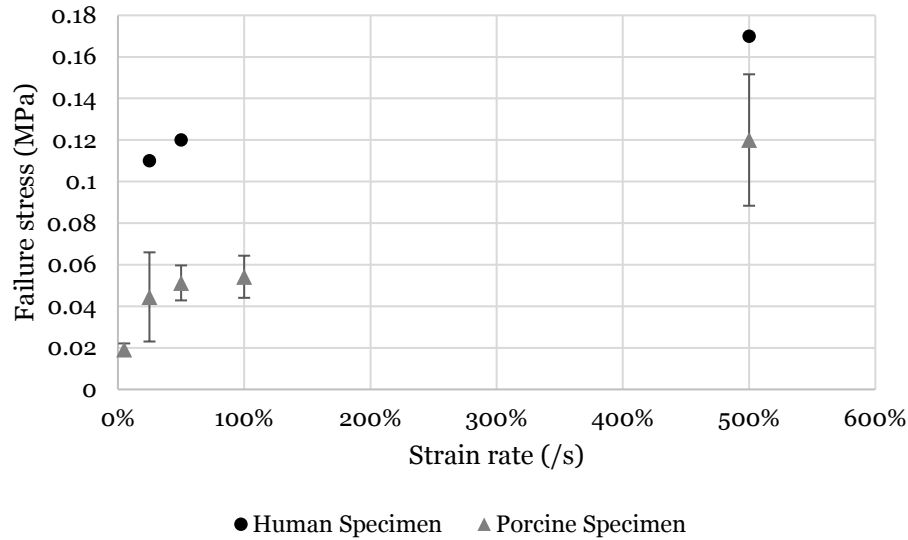


Figure 4-27: Failure stress of the human and porcine liver measured at various rates

The strain rate dependence model of the porcine failure stress results (Equation 5, Table 4-11) is plotted against the measured results (Figure 4-28) and has an R^2 of 0.98. Due to limited human specimens, only the porcine results were modeled. The liver failure stress is sensitive to the strain rate between the rates of 5%/s to 500%/s. A slight pause is observed between the rates of 25%/s to 100%/s but then a slight increase of failure stress was observed from 100%/s to 500%/s. Through this model and the parameters found in Table 4-11, an estimate of the failure stress can be estimated for both low and high dynamic strain rates.

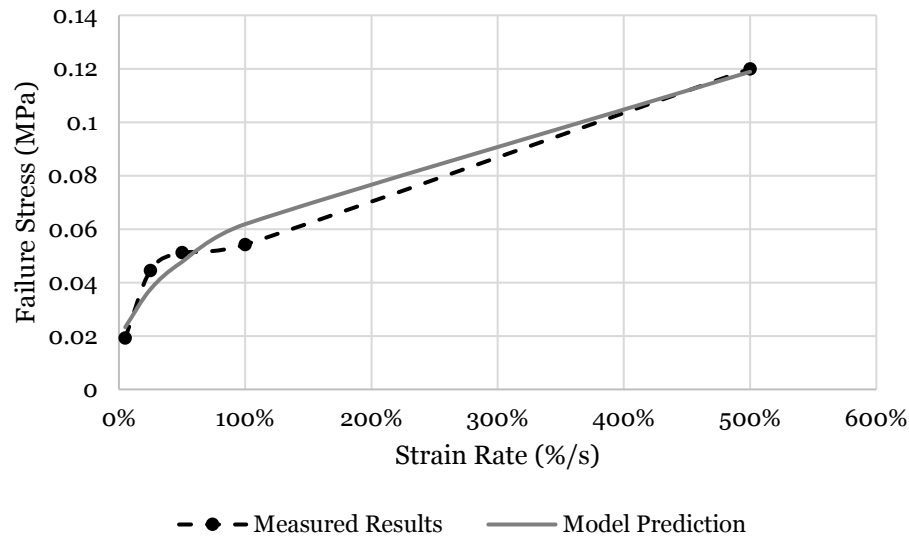


Figure 4-28: Measured and model predicted failure stress of the porcine liver

Table 4-11: Parameters for the material model that describes the relationship between strain rate and porcine liver failure stress

Variable	a	b	c	d	ϵ
Value	0.011	0.05	0.46	2075789	Strain Rate

A strain rate dependency was observed for failure strain of human and porcine liver (Figure 4-29). No differences were observed between the rates of 25%/s and 50%/s but the failure strain increased 20% when tested at 500%/s. Clearer differences were observed in the failure strain of the porcine livers. More specimens, and therefore more rates, were able to be tested from the porcine hosts. It was found that failure strain increased with each incremental increase of strain rate ranging from 50% strain at 5%/s to 75% strain at 500%/s ($p=0.01$). Failure strain at rates of 100%/s and 500%/s were statistically higher than at a rate of 5%/s, and only 500%/s was statistically higher than at the rate of 25%.

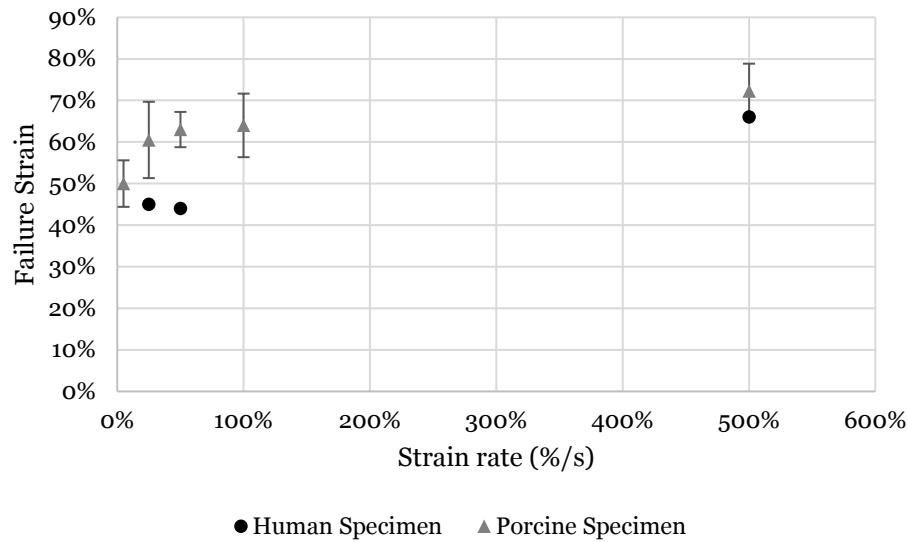


Figure 4-29: Failure strain for both human and porcine liver specimens measured at various rates

The model (Equation 5, Table 4-12) is plotted against the measured results (Figure 4-30) and has an R^2 of 0.96. Due to limited human specimens, only the porcine results were modeled. The behavior of the liver failure strain is sensitive to the strain rate between the rates of 5%/s to 50%/s. As the rates increase above 50%/s, the material property dependency on strain rate starts to saturate. Through this model and the parameters found in Table 4-12, an estimate of the failure strain can be estimated for both low and high dynamic strain rates.

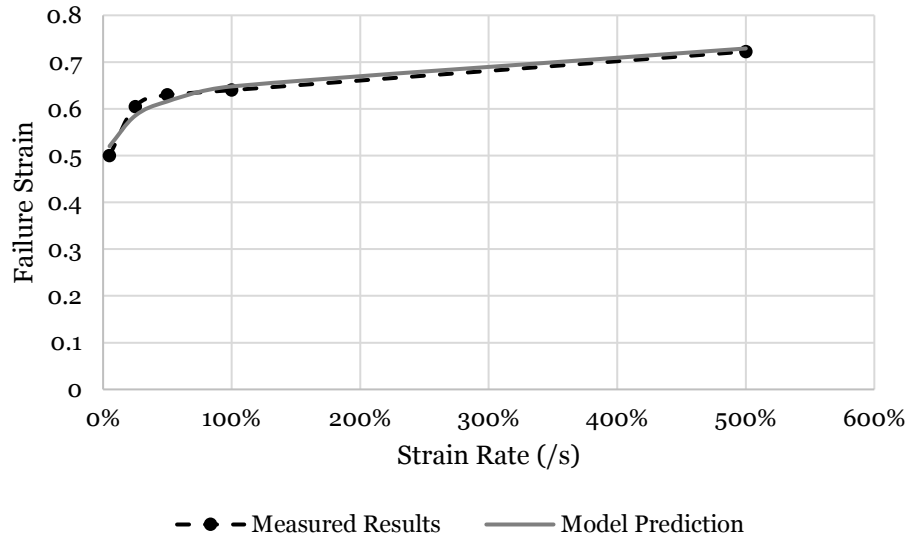


Figure 4-30: Measured and model predicted failure strain of the porcine liver

Table 4-12: Parameters for the material model that describes the relationship between strain rate and porcine liver failure strain

Variable	a	b	c	d	$\dot{\epsilon}$
Value	0	0.65	0.07	2510543	Strain Rate

4.2.4. DISCUSSION

4.2.4.1 Kidney

An unconfined compression and probing protocol were used to characterize the mechanical properties of the intact human and porcine kidney. The results from the unconfined compression protocol determined that porcine tissue was measured to be 4 times stiffer than the human kidneys, however little to no differences were observed in failure stress and failure strain between the two hosts. Snedeker et al., found similar elastic modulus and failure stress for human and porcine kidney tissue capsules [34].

One difference between the two studies is that Snedeker et al. only tested the kidney capsule in tension. It is possible the parenchyma has a greater influence on the elastic modulus of the entire kidney than the capsule and thus Snedeker did not find differences between the two hosts for the elastic modulus [34]. It is also possible that the large disparity in elastic modulus between the two hosts is due to the relative age of the specimens, as researchers have previously identified many anatomical similarities between human and porcine kidneys [35]. The porcine kidneys were obtained from subjects that were within the first 2% of their average lifespan whereas the human specimens were obtained from cadavers that died of causes related to old age. It has been previously determined that aging has a significant impact on the elastin content within tissue which effects stiffness [36].

Only a few other studies have investigated the material properties of the kidney in fashion similar to this study. Umale quasi-statically compressed only the cortex of the porcine kidney and determined the stiffness to be 15 kPa, which is lower than what was found in the current study [14]. The same study determined that the stiffness of the kidney capsule to be 7.1 MPa in tension, far stiffer than what was measured in this study. Overall it appears that the stiffness is more of a function of the renal cortex than the capsule. A researcher only using the capsule for the material properties of the kidney would vastly overestimate the stiffness. Testing the kidney as a whole undamaged organ should provide the most realistic properties as the kidney is a combination of all of its components.

No previous studies have directly compared the resulting elastic modulus from two different methods applied to the same human and porcine kidneys. A similar

relationship with strain rate was observed between the two protocols, however the elastic modulus in the probing protocol was slightly higher for both hosts. The human and porcine kidneys geometries are identical, thus the similar trend in elastic modulus and its variation with strain rate was expected. The small increase in elastic modulus seen in the probing protocol could be due to compressing a smaller area of the tissue and the activation of surrounding tissue is not directly addressed in the calculation of modulus.

Although the porcine kidneys were much stiffer than the human kidneys, the tissue behavior in relation to strain rate were similar. An increase in stiffness with an increase in strain rate was observed for both specimen types. Compression tests were performed at higher rates for the porcine specimens due to the availability of specimens, and the effect of strain rate on stiffness was determined. Strain rate increased stiffness linearly at a rate of 0.05 MPa per 1%/s increase in strain rate, but after 50%/s this dependence started to saturate. From the rates of 100%/s to 1000%/s the stiffness increase was 0.006 MPa per 1%/s increase in strain rate. This demonstrates that the kidney tissue is more sensitive to strain rates at lower rates. A similar relationship between strain rate and failure stress was observed. A linear relationship with an increase of 0.16MPa with every 1%/s increase in strain rate was found up to 50%/s. This strain rate dependency saturates at this point and as the rate increases to 500%/s and 1000%/s there is no difference observed in failure stress. Snedeker performed a similar study but performed tension testing on the kidney capsule only. A relationship similar to that from this study was found, but the saturation occurred at a higher rate of 150%/s

[34]. The differences could be due to the kidney capsule having a different dependence on strain rate than the entire kidney.

No differences in failure strain were observed in this study between human and porcine kidneys. The tissue structures are very similar, which is why porcine kidneys are widely used as a model for the human kidney. In contrast to failure stress and stiffness, increasing the compression rate did not impact the measured failure strain. Snedeker found a different result with failure strain being inversely related to strain rate; however this affect was not observed until rates were faster than 5,000%/s [24]. Snedeker only tested the renal capsule, which has a higher elastin content, potentially contributing to the strain rate/failure strain relationship, whereas the current study utilized the whole intact kidney and factoring in the parenchyma could modify this relationship.

4.2.4.2 Liver

The material properties of an intact liver were characterized for both human and porcine specimens. No observable differences were found between the stiffness and failure strain of the human liver and the porcine liver in unconfined compression. On a biological level the porcine and human liver are similar [37] and thus it is not unexpected that similar results were found. The similar results also suggest that the relative age of the two hosts was not a factor for stiffness and failure strain in the liver, since the porcine specimens were much younger than the human hosts. This is could be due to the lack of elastin in the liver which is present in the kidney [38]. It has been previously found that elastin, which impacts the material properties, changes with age of the host [36]. A lack of elastin could translate to a diminished effect of age.

A large difference was found between the probing and unconfined compression results for the human liver, while a small difference was found for the porcine specimens. This resulted in a large difference between human and porcine liver elastic modulus in the probing protocol versus no difference in the compression protocol elastic modulus. The reason for this discrepancy could be due to the differences in geometry. In the unconfined compression protocol, the entire organ was compressed at once and thus the geometrical differences have little influence. However, in the probing protocol only a small portion of the liver is being compressed. For both specimens, the highest point of the liver was probed. The human liver has two lobes of which the right lobe is often larger, thus the probe compressed the right. For porcine livers, there are four lobes that are all connected at the center. The area where the porcine liver lobes conjoin is where the highest spot of the tissue is located. Compressing the porcine liver via probe allows for the four lobes to move somewhat relative to each other as the pressure increases, thus lowering the measured stiffness.

Another difference found between the two hosts was that the failure stress was much higher in the human specimens versus the porcine specimens. The difference in failure stress could be contributed to the dietary factors of the two hosts. Alcohol can have a significant effect on the collagen content of the liver [39] which is only consumed by the human hosts. Although it was previously reported that the porcine liver has more collagen content [40], the influence of alcohol over a lifetime could alter this and make the human liver stronger than the porcine host. A direct comparison of the material properties from human and porcine liver has not been done previously. This study highlights that the use of porcine liver is a feasible substitute for investigating human

liver material properties using unconfined compression testing. Porcine tissue could even be a better representative of a healthy human as the liver will be less likely to be damaged from poor health and won't have scarring from years of alcohol consumption.

A strain rate dependency was observed for the elastic modulus, failure stress, and failure strain. In all three parameters the dependency on strain rate saturates after 50%/s for both hosts. The strain rate effect is greatest going from quasi-static to slow dynamic rates. A material model was derived to numerically describe this relationship. A reason for the lack of material models that incorporate the changes due to strain rate could be due to the lack of investigated strain rates. This study tested at several different rates which allowed for the model development that describes the point at which the strain rate dependency saturates. The model can increase the ability for research to predict the stress-strain relationships and modulus at different rates.

4.2.5 LIMITATIONS

One of the limitations in this study is the number of rates used in the probing protocol. Due to instrument limitations, a larger range of rates were not able to be used. However, an impact of strain rate, similar to that in unconfined compression, was still able to be identified. Another limitation regarding the probing is the differences between human and porcine liver geometry as discussed previously. Testing at the high point of one lobe of the human specimen, and at the juncture of all four lobes for the porcine specimen, could have influenced the differences observed. Probing each lobe individually may produce more consistent results (Figure 4-31). The last limitation is the lack of human specimens. This study stresses the importance of using whole, undamaged organs and the lack of human specimens meant that obtaining statistical

significance was not possible. Thus, in order to gain some insight into the behavior of human organs, comparison between human and porcine organs was performed and the strain rate dependency on porcine organs were fully characterized.

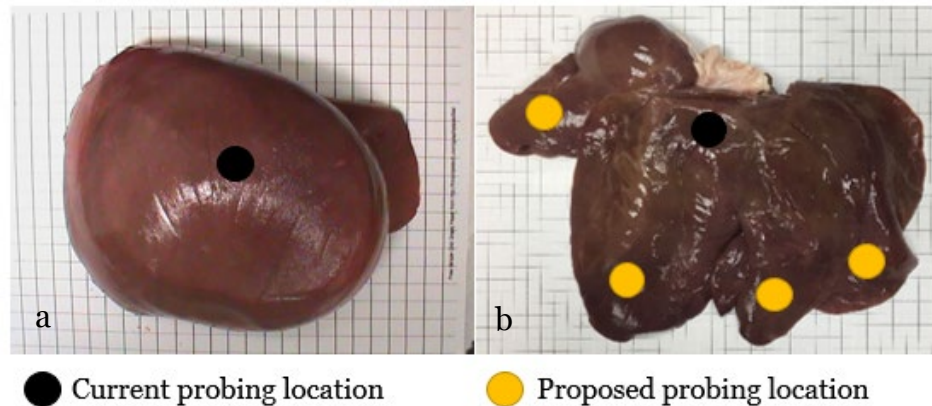


Figure 4-31: Current probing locations for the a) human liver and b) porcine liver and proposed probing location to address limitation

4.2.6 CONCLUSION

Testing for the mechanical properties of kidney and liver has been performed on both human and porcine hosts. Probing stiffness and unconfined compression stiffness, failure stress, and failure strain was found at varying strain rates for the liver and kidney. Both porcine kidney and liver tissue were determined to be an appropriate substitute for human tissue. Material properties were similar between the two hosts, with only the elastic modulus of the kidney differing significantly, and indicates that use of porcine tissue properties may be feasible for the liver and kidneys in the absence of acceptable human tissue testing results. However, this difference could be contributed the factor of age of the porcine hosts were relatively much younger at the time of death. The probing protocol resulted in an increase in elastic modulus for all tissue except the

porcine liver. The geometry of the liver differed greatly between the human and porcine hosts, and changes in motion due to geometric effects could have resulted in the probing protocol not demonstrating an increase in stiffness for the porcine liver. Furthermore, the strain rate dependency has been identified and characterized for both organs. A model has been derived that will enable researchers to estimate the changes in the measured material properties when the compressive strain rate is changed. It was also identified at what strain rate, if any, this relationship starts to saturate and increasing the rate of load application has a diminishing affect. Overall valuable information for researchers in the fields that require the material properties of liver and kidney has been revealed. The results provided will aid in the development of more accurate and more comprehensive finite element models.

4.2.7 REFERENCES

- [1] Asensio, J. A., Trunkey, D. D. (2008). Current Therapy of Trauma and Surgical Critical Care E-Book. *Elsevier Health Sciences*.
- [2] Chauhan, N., Badgurjar, M. K., Saxena, P. (2019). A Prospective Study of Assessment of Solid Organs in Cases of Blunt Abdominal Trauma. *International Journal of Scientific Research*, 8 (3): 48-50.
- [3] Loftis, K. L., Mazuchowski, E. L., Clouser, M. C., Gillich, P. J. (2019). Prominent Injury Types in Vehicle Underbody Blast. *Military medicine*, 184 (Sup1), S261-S264.
- [4] Lizee, E., Robin, S., Song, E., Bertholon, N., Le Coz, J. Y., Besnault, B., Lavaste, F. (1998). Development of a 3D Finite Element Model of the Human Body. *SAE Transactions*, 107(6): 2760-2782.
- [5] Bass, C., Davis, M., Rafaels, K., Rountree, M., Harris, R. M., Sanderson, E., ... Zielinski, M. (2005). A Methodology for Assessing Blast Protection in Explosive Ordnance Disposal Bomb Suits. *International Journal of Occupational Safety and Ergonomics*, 11(4), 347-361.
- [6] Roberts, J. C., Merkle, A. C., Biermann, P. J., Ward, E. E., Carkhuff, B. G., Cain, R. P., O'Connor, J. V. (2007). Computational and Experimental Models of the Human Torso for Non-Penetrating Ballistic Impact. *Journal of Biomechanics*, 40(1), 125-136.
- [7] Ward, E., Merkle, A., Harrigan, T., Roberts, J. (2010). Comparing Blast Effects on Human Torso Finite Element Model Against Existing Lethality Curves. *Defense Technical Information Center*, <https://apps.dtic.mil/docs/citations/ADA532225>.
- [8] Chen, Z., Joli, P., Feng, Z. Q. (2011, May). Finite Element Modeling of Interactions Between Pelvic Organs Due to Pressure. *Proceedings from 10e Colloque National En Calcul Des Structures* (1-7). Giens, France. <https://hal.archives-ouvertes.fr/hal-00592691/document>.
- [9] Gayzik, F. S., Moreno, D. P., Vavalle, N. A., Rhyne, A. C., Stitzel, J. D. (2011). Development of the Global Human Body Models Consortium Mid-Sized Male Full Body Model. *Injury Biomechanics Research: Proceedings from the 39th International Workshop on Human Subjects for Biomechanical Research*, https://www.nrd.nhtsa.dot.gov/Pdf/BIO/Proceedings/2011_39/39-12.pdf.
- [10] Beillas, P., Berthet, F. (2012). Performance of a 50th Percentile Abdominal Model for Impact: Effects Of Size And Mass. *Journal of Biomechanics*, 45(sup1), S83.
- [11] Golman, A. J., Danelson, K. A., Miller, L. E., Stitzel, J. D. (2014). Injury Prediction in A Side Impact Crash Using Human Body Model Simulation. *Accident Analysis & Prevention*, 64, 1-8.

- [12] Schwartz, D., Guleyupoglu, B., Koya, B., Stitzel, J. D., Gayzik, F. S. (2015). Development of A Computationally Efficient Full Human Body Finite Element Model. *Traffic Injury Prevention*, 16 (sup1), S49-S56.
- [13] Umale, S., Deck, C., Bourdet, N., Dhumane, P., Soler, L., Marescaux, J., Willinger, R. (2013). Experimental Mechanical Characterization of Abdominal Organs: Liver, Kidney & Spleen. *Journal of the Mechanical Behavior of Biomedical Materials*, 17, 22-33.
- [14] Tamura, A., Omori, K., Miki, K., Lee, J. B., Yang, K. H., King, A. I. (2002). Mechanical Characterization of Porcine Abdominal Organs. *Stapp Car Crash Journal*, 46, 55-69.
- [15] Kemper, A. R., Santago, A. C., Stitzel, J. D., Sparks, J. L., Duma, S. M. (2012). Biomechanical Response of Human Spleen in Tensile Loading. *Journal of Biomechanics*, 45(2), 348-355.
- [16] Rosen, J., Brown, J. D., De, S., Sinanan, M., Hannaford, B. (2008). Biomechanical Properties of Abdominal Organs In-Vivo and Postmortem Under Compression Loads. *Journal of Biomechanical Engineering*, 130(2), 1-17.
- [17] Snedeker, J. G., Barbezat, M., Niederer, P., Schmidlin, F. R., Farshad, M. (2005). Strain Energy Density as a Rupture Criterion for the Kidney: Impact Tests on Porcine Organs, Finite Element Simulation, and a Baseline Comparison Between Human and Porcine Tissues. *Journal of Biomechanics*, 38(5), 993-1001.
- [18] Roberts, J. C., O'Connor, J. V., Ward, E. E. (2005). Modeling the Effect of Nonpenetrating Ballistic Impact as a Means of Detecting Behind-Armor Blunt Trauma. *Journal of Trauma and Acute Care Surgery*, 58(6), 1241-1251.
- [19] Hollenstein, M., Nava, A., Valtorta, D., Snedeker, J. G., Mazza, E. (2006). Mechanical Characterization of the Liver Capsule and Parenchyma. *Proceedings from International Symposium on Biomedical Simulation* Springer, Berlin, Heidelberg, 150-158.
- [20] Chui, C., Kobayashi, E., Chen, X., Hisada, T., Sakuma, I. (2007). Transversely Isotropic Properties of Porcine Liver Tissue: Experiments and Constitutive Modelling. *Medical & Biological Engineering & Computing*, 45(1), 99-106.
- [21] Karimi, A., Shojaei, A. (2017). Measurement of the Mechanical Properties of the Human Kidney. *IRBM*, 38(5), 292-297.
- [22] Santago, A., Kemper, A., McNally, C., Sparks, J., Duma, S. (2009). The Effect of Temperature on the Mechanical Properties of Bovine Liver. *Biomedical Science Instrumentation*, 45, 376-81.
- [23] Brunon, A., Bruyere-Garnier, K., Coret, M. (2010). Mechanical Characterization of Liver Capsule Through Uniaxial Quasi-Static Tensile Tests Until Failure. *Journal of Biomechanics*, 43(11), 2221-2227.

- [24] Gao, Z., Lister, K., Desai, J. P. (2010). Constitutive Modeling of Liver Tissue: Experiment and Theory. *Annals of Biomedical Engineering*, 38(2), 505-516.
- [25] Kemper, A. R., Santago, A. C., Stitzel, J. D., Sparks, J. L., Duma, S. M. (2010). Biomechanical Response of Human Liver in Tensile Loading. *Association for the Advancement of Automotive Medicine Annual Scientific Conference*, (54): 15.
- [26] Chatelin, S., Oudry, J., Périchon, N., Sandrin, L., Allemann, P., Soler, L., Willinger, R. (2011). In Vivo Liver Tissue Mechanical Properties by Transient Elastography: Comparison with Dynamic Mechanical Analysis. *Biorheology*, 48(2), 75-88.
- [27] Lu, Y. C., Untaroiu, C. D. (2013). Effect of Storage Methods on Indentation-Based Material Properties of Abdominal Organs. *Journal of Engineering in Medicine*, 227(3), 293-301.
- [28] Lu, Y. C., Kemper, A. R., Untaroiu, C. D. (2014). Effect of Storage on Tensile Material Properties Of Bovine Liver. *Journal of the Mechanical Behavior of Biomedical Materials*, 29, 339-349.
- [29] Dương, M. T., Nguyễn, N. H., Trần, T. N., Tolba, R. H., Staat, M. (2015). Influence of Refrigerated Storage on Tensile Mechanical Properties of Porcine Liver and Spleen. *International Biomechanics*, 2(1), 79-88.
- [30] Miller, K. (2000). Constitutive Modelling of Abdominal Organs. *Journal of Biomechanics*, 33(3), 367-373.
- [31] Tay, B. K., Kim, J., Srinivasan, M. A. (2006). In Vivo Mechanical Behavior of Intra-Abdominal Organs. *IEEE Transactions on Biomedical Engineering*, 53(11), 2129-2138.
- [32] Kemper, A. R., Santago, A. C., Stitzel, J. D., Sparks, J. L., Duma, S. M. (2013). Effect of strain rate on the material properties of human liver parenchyma in unconfined compression. *Journal of biomechanical engineering*, 135(10): 1-8.
- [33] Campbell-Kyureghyan, N., W. Marras (2009). Combined Experimental and Analytical Model of the Lumbar Spine Subjected to Large Displacement Cyclic Loads Part II – Model Validation. *International Journal of Computational Vision and Biomechanics* 2(1): 95-104.
- [34] Snedeker, J. G., Niederer, P., Schmidlin, F. R., Farshad, M., Demetropoulos, C. K., Lee, J. B., Yang, K. H. (2005). Strain-rate dependent material properties of the porcine and human kidney capsule. *Journal of Biomechanics*, 38(5), 1011-1021
- [35] Giraud, S., Favreau, F., Chatauret, N., Thuillier, R., Maiga, S., Hauet, T. (2011). Contribution of Large Pig for Renal Ischemia-Reperfusion and Transplantation Studies: The Preclinical Model. *Journal of Biomedicine and Biotechnology*, 2011: 1-14.

- [36] Roan, E., Vemaganti, K. (2007). The Nonlinear Material Properties of Liver Tissue Determined From No-Slip Uniaxial Compression Experiments. *Journal of Biomechanical Engineering*, 129(3), 450-456.
- [37] Sherratt, Michael J. (2009). Tissue Elasticity and the Ageing Elastic Fibre. *Age* 31 (4): 305-325.
- [38] Nykonenko, A., Vavra, P., Zonča, P. (2017). Anatomic Peculiarities of Pig and Human Liver. Experimental and Clinical transplantation: Official Journal of the Middle East Society for Organ Transplantation, 15(1), 21-26.
- [39] Neuman, R. E., Logan, M. A. (1950). The Determination of Collagen and Elastin in Tissues. *Journal of Biological Chemistry*, 186(2), 549-556.
- [40] Rojkind, M., Giambrone, M. A., Biempica, L. (1979). Collagen Types in Normal and Cirrhotic Liver. *Gastroenterology*, 76(4), 710-719.

4.3 Spleen Manuscript

CHARACTERIZING THE MATERIAL PROPERTIES OF HUMAN AND PORCINE SPLEEN WITH SPECIAL REFERENCE TO CHANGES IN STRAIN

ABSTRACT

Splenic injuries resulting from blunt force trauma, blast, and other dynamic loads commonly life threatening. Finite element modeling is a tool used to aid in the prediction of these injuries, but the use of accurate material properties is essential to obtaining useful results. Further characterization of spleen material properties is needed as current data are limited and often not appropriate for the intended purpose. Three human and 32 porcine spleens were procured for this study. All specimens were subjected to a nondestructive unconfined compression protocol at the rates of 1%/s to 1000%/s, a destructive unconfined compression protocol at the rates 1%/s to 500%/s, and a nondestructive probing protocol at the rates of 1%/s and 25%/s. The elastic modulus was calculated for both nondestructive protocols and the failure stress and strain was measured in the destructive protocol. Numerical models were developed that describe the stress-strain relationship and the strain rate dependence of the material properties. No differences were found between human and porcine spleens for the elastic modulus, which was found to be strain rate dependent and increased from 0.008 MPa at 1%/s to 0.036 MPa at 1000%/s. On average, a 136% increase in stiffness was observed for the probing as opposed to the unconfined compression protocol. Failure stress was found to be strain rate dependent for both human and porcine spleens ranging from 0.083 MPa at 1%/s to 0.28 MPa at 500%/s for the porcine specimens. No strain rate dependency was observed for failure strain for either porcine or human specimens. Overall, the results found from this study can be used to improve the understanding of spleen response to maximal and submaximal loading at different rates.

4.3.1 INTRODUCTION

Abdominal injuries can put victims of traumatic situations into grave danger as they can be hard to diagnosis. In a study observing patients admitted for abdominal trauma the spleen was the second most frequently injured organ [1]. One way to better diagnose and predict abdominal injuries is through a more thorough understanding of the injury mechanism during these blunt force impact events, which can involve both experimental and analytical studies. Finite element modeling is a tool that is widely used in the field of trauma biomechanics. Detailed finite element models are used to predict injury due to car crashes, blunt force trauma, and blast loading, to help plan surgeries, and in forensic biomechanics etc. [2-13].

Finite element models require accurate material properties in order to produce accurate simulations. However, accurate material properties for many of the human abdominal organs are scarce or nonexistent in the literature. Additionally, given the dynamic nature of many of the intended applications, the effects of strain rate on the mechanical behavior should be considered. Only three articles have identified strain rate effects on the material properties of the spleen and a numerical relationship has yet to be identified. Stingl et al. and Kemer et al. only tested the spleen capsule under tension, while Tamura et al. tested samples of the parenchyma under compression [14-16]. These studies investigated the different structures that together make up the spleen, but have not looked at the entire organ as a unit. These studies also used different methodologies that yielded results that are not similar, making it impossible to draw any overarching conclusions.

In order to characterize the complete structure of the spleen, the whole intact organ must be studied in a similar fashion than that of a traumatic situation. The spleen is housed within the abdominal cavity on the left-hand side in between the 9th and 11th thoracic vertebrae. If force is applied directly to the abdomen the spleen is compressed by the surrounding structures. To determine material properties for models that simulate traumatic loading the intact organ must be tested intact under compression. Furthermore, in order to allow for damage predictions, the load or deformation at which failure occurs is also required and has not been studied in the literature.

Due to the challenges in obtaining specimens for studying human spleen material properties porcine spleens are often used instead [17-20]. Only one study [15] has investigated the tensile material properties of the human spleen and compared them to a study that was conducted in a similar manner using porcine specimens [21]. The study concluded that the properties obtained from human specimens differed from porcine, however it is also pointed out within the article that there were some assumptions made in order to compare the two studies. No research has been conducted that fully investigated the feasibility of using porcine specimens instead of human spleens to determine a range of material properties through a direction comparison of the two hosts using an identical methodology.

The goal of this study is to characterize the elastic modulus of the intact spleen using a probing protocol and the elastic modulus, failure stress, and failure strain using an unconfined compression protocol at various loading rates. A specific aim is to estimate the relationship between spleen material properties and strain-rate. It is hypothesized that the probing elastic modulus will differ from the elastic modulus found

using an unconfined compression protocol. It is further hypothesized that failure stress, failure strain, and elastic modulus will increase as strain-rate increases for an intact spleen subjected to compression loading.

4.3.2 METHODS

4.3.2.1 Specimens

Material testing was performed on spleens from two different hosts, humans and porcine. Three cadavers were procured from the Medical College of Wisconsin. A splenectomy was performed on all three cadavers within 48 hours after death. All donors were screened and were free of any transmittable diseases. Porcine spleens were received from a government inspected local slaughterhouse. Professional butchers performed the splenectomy on the spleens leaving the entire organ intact. Organs received from the slaughterhouse were obtained from porcine being slaughtered for other purposes and thus no animals were required to be euthanized for research purposes. Testing was completed as soon as possible after harvesting with specimens being stored in a cooler set at 4 degrees Celsius prior to testing.

4.3.2.2 Experimental Protocol

Two types of testing were performed: unconfined compression testing and probing testing. Unconfined compression testing was performed using two separate methods, a nondestructive method and a destructive method. Nondestructive testing involved compressing the spleen between two compression plates while simultaneously measuring force and displacement using an MTS (Figure 4-32). The spleen was oriented with the posterior surface resting on the compression plate and the force was

applied to the anterior surface of the organ. This orientation is similar to how compression would be applied in a blunt impact to the abdomen. The compressive force was applied to the spleen up to 35% strain using the rates in Table 1. Once 35% strain was reached the plates released the applied force at the same rate it was applied. Specimens were allowed to return to their original height and then retested for each rate of interest. Destructive testing followed the same protocol; however the compressive force was applied until the specimen failed. Failure was defined as a 5% drop in applied force or no increase of force after a 3% increase in strain. Rates that were tested in nondestructive testing and destructive testing for all protocols are outlined in Table 4-13.

Table 4-13: Strain rates used in each of the protocols in the spleen experimental testing (✓ represents that only elastic modulus was measured, and x represents that failure properties were also measured)

Strain Rate	Human		Porcine	
	Compression	Probing	Compression	Probing
1 %/s	x	✓	x	✓
25 %/s	x	✓	x	✓
50 %/s	x	-	x	-
100 %/s	-	-	x	-
250 %/s	-	-	✓	-
500 %/s	x	-	x	-
1000 %/s	-	-	✓	-



Figure 4-32: Human spleen placed between the compression plates of an MTS

The other testing method, the probing protocol, took place either before or after the nondestructive compression protocol and before the destructive testing protocol. Similar to the nondestructive compression protocol, a force was applied to the organ at a constant rate (Table 1) up to 31% strain and then relaxed at the same rate. The spleen was placed in the same orientation as for the compression protocol but force was applied with a flat end probe that has a surface area of 126.7 mm² (Figure 4-33). The probe was placed at the center point of the spleen, in between inferior, superior, medial, and lateral walls. Probe placement was consistent for all spleens tested. Force and displacement were measured using the Mark 10-EML test stand.

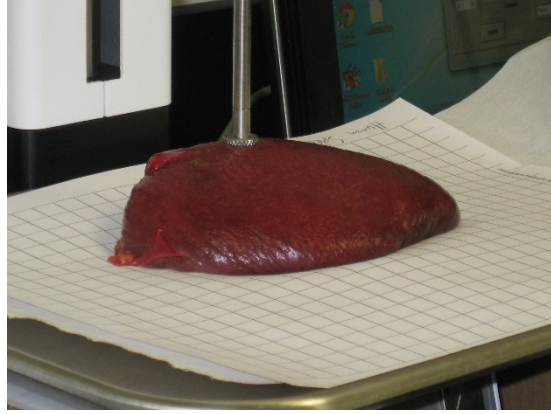


Figure 4-33: Human spleen placed on the Mark 10-EML test stand for the probing protocol

2.3 Data Analysis

In both protocols the force and displacement were measured simultaneously during the tests. Stress was computed using Eq 1 in the unconfined compression protocol and Eq 2 for the probing protocol. Strain was calculated using Eq 3. Stiffness was determined by calculating the slope of the stress-strain curve at the highest measured strain.

$$\sigma_{ND} = \frac{Force}{Surface\ Area_{specimen}} \quad (1)$$

$$\sigma_P = \frac{Force}{Surface\ Area_{probe}} \quad (2)$$

$$\varepsilon = \frac{\Delta Height}{Height_{Initial}} \quad (3)$$

A mathematical model (Eq. 4) was used to describe the stress-strain relationship that was observed in the experimental testing [22]. The variables used within the model are the elastic modulus in the toe region (E_{toe}), the elastic modulus in the terminal region (E_{term}), the center strain of the inflection region (ε_c), and a parameter describing the curvature of the inflection region (ψ). For each of the trials the parameter values

that best fit the experimental curves were determined. An equation was also developed to determine the relationship between the material properties with strain rate (Eq. 5).

$$E = \{1.0 + \tanh(\psi[\varepsilon - \varepsilon_c])\}(E_{term} - E_{toe})/2.0 + E_{toe} \quad (4)$$

where E is the current elastic modulus and ε is the current strain.

$$Property = a + b\dot{\varepsilon}^c \quad (5)$$

where a , b , and c are parameters that vary with each property type, and $\dot{\varepsilon}$ is the strain rate.

Changes in the material model parameters between different strain-rates were analyzed. A one-way ANOVA was used to test the factor of strain rate for all tests for each host. A two sample t-test was conducted at each of the strain rates that were tested on both hosts to test whether or not human and spleen material properties were statistically different. An alpha value of 0.05 was set for both statistical tests that were performed.

4.3.3 RESULTS

4.3.3.1 Stress-Strain Behavior

Human and porcine spleens were observed to have different stress strain curves (Figure 4-34). Human spleens had a shorter toe region (maxed out at 5% strain) before the inflection point than the porcine hosts (maximum of 20% strain). A numerical material model (Eq. 4) was used to describe the stress-strain curves of both human and porcine spleens. Five different variables were used in the model which consisted of the elastic modulus in the toe region (E_{toe}), the elastic modulus in the terminal region (E_{term}), the center strain of the inflection region (ε_c), and a parameter describing the

curvature of the inflection region (ψ). Table 4-14 contains the values of all parameters between a quasi-static rate, 1%/s, and a dynamic rate, 25%/s, for both human and porcine spleens. An example of the stress strain curve of the experimental versus the modeled results are in Figure 4-34.

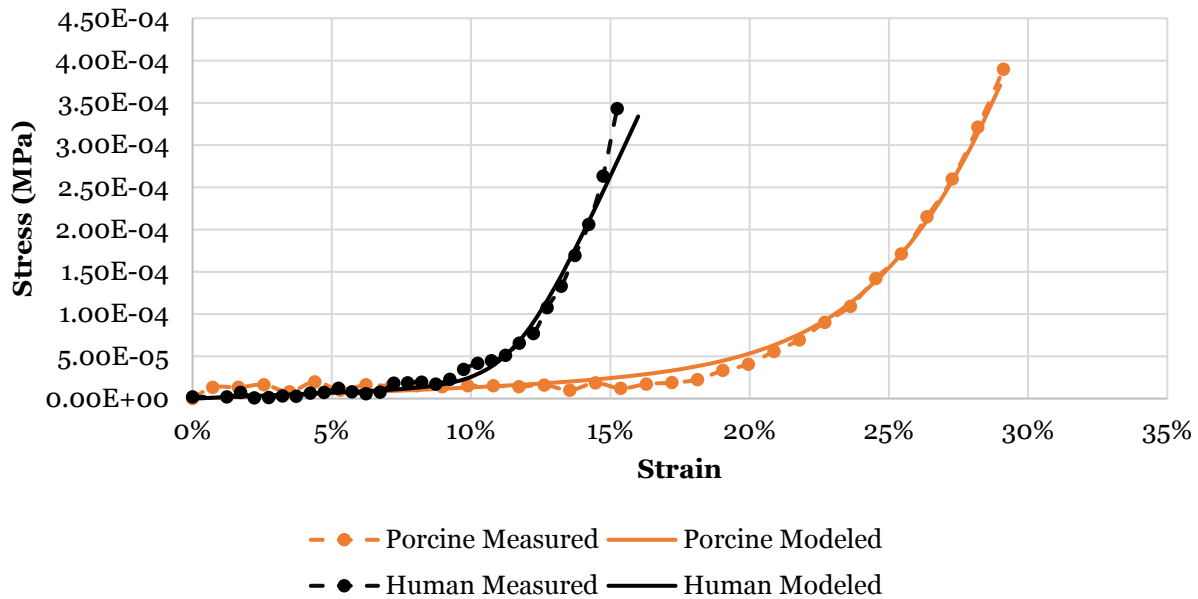


Figure 4-34: Representative measured and modeled stress-strain curves of the human and porcine spleen in unconfined compression at a rate of 25%/s

Table 4-14: Average and standard deviation of the modeled variables for both human and porcine specimens in unconfined compression

Human	1 %/s	25 %/s
E_{toe} (MPa)	0.0002 (± 0.0001)	0.0002 (± 0.0002)
E_{term} (MPa)	0.004 (± 0.0012)	0.007 (± 0.004)
ϵ_c	0.09 (± 0.02)	0.12 (± 0.03)
Ψ	48.1 (± 28.9)	28.1 (± 10.1)
R^2	0.94 (± 0.02)	0.95 (± 0.02)
Porcine		
E_{toe} (MPa)	0.0001 (± 0.00026)	0.0001 (± 0.00016)
E_{term} (MPa)	0.008 (± 0.005)	0.010 (± 0.004)
ϵ_c	0.27 (± 0.05)	0.27 (± 0.01)
Ψ	12.9 (± 6.77)	12.9 (± 2.87)
R^2	0.98 (± 0.007)	0.96 (± 0.03)

Virtually no differences were observed between the human and porcine spleen elastic modulus in both probing and unconfined compression protocols ($p > 0.05$). In both rates, the standard deviations overlap between the two organ hosts (Figure 4-34. Human spleen specimens averaged 0.004 MPa and 0.007 MPa at 1%/s and 25%/s in unconfined compression respectively. Porcine spleen averages 0.008 MPa and 0.01 MPa for the rates of 1%/s and 25%/s in unconfined compression respectively. Human spleen specimens averaged 0.014 MPa and 0.018 MPa at 1%/s and 25%/s in the probing protocol respectively. Porcine spleen averages 0.015 MPa and 0.02 MPa for the rates of 1%/s and 25%/s in the probing protocol respectively. The elastic modulus was increased from the unconfined compression to probing protocol for both hosts in both quasi-static and dynamic rates. Human spleen became 220% and 160% stiffer from the unconfined

compression protocol to the probing protocol in the 1%/s and 25%/s respectively (Figure 4-35). Porcine spleen became 73% and 90% stiffer from the unconfined compression protocol to the probing protocol in the 1%/s and 25%/s respectively (Figure 4-35).

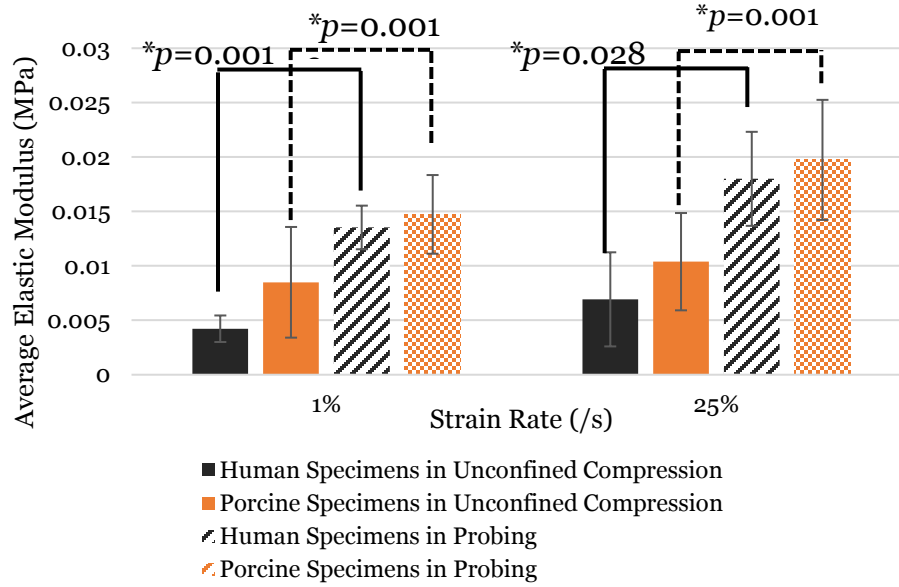


Figure 4-35: Average elastic modulus for both human and porcine spleen tissue under full unconfined compression at a quasi-static and dynamic rate

Both human and porcine elastic modulus of the spleen were observed to be strain rate dependent. Strain rate was found to be a statistically significant factor ($p=0.001$) for the porcine specimens as an increase in stiffness was observed as the rate increased (Figure 4-36). The post-hoc tukey test revealed that the statistically significant increase in elastic modulus was observed only after the rate was above 100%/s ($p<0.05$). From the rates of 1%/s to 100%/s the elastic modulus only increased by 57%, but as the rate doubled from 500%/s to 1000%/s a 58% increase was observed (Figure 4-35). A model (Eq 6) that was fit to the measured results with an R^2 of 0.98 was created to describe the

relationship between the elastic modulus and strain rate. The b parameter shows how the elastic modulus changes with each percent strain increase in rate, while c parameter shows how this relationship changes as the rate increases. Through the modeled results (Figure 4-37), it is seen that there is a slight inflection point at the rate of 100%/s. The rates of 100%/s and lower were statistically different than the rate of 500%/s ($p < 0.05$).

$$E_{term} = a + b\dot{\epsilon}^c \quad (6)$$

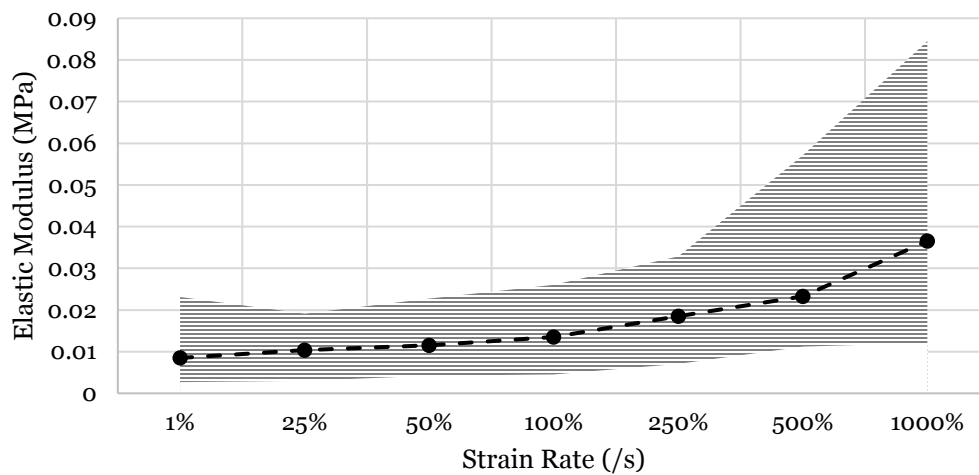


Figure 4-36: Average and range of elastic modulus results for porcine spleen under full unconfined compression at each strain rate

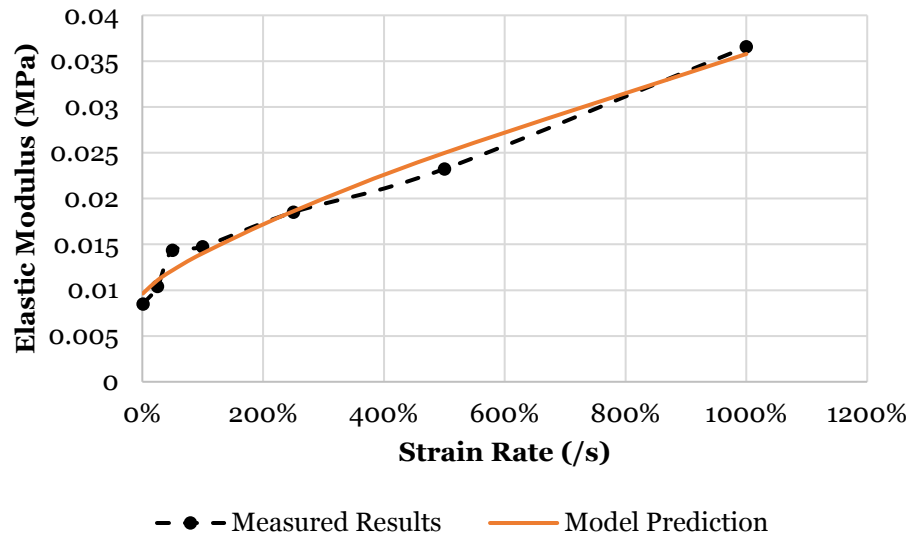


Figure 4-37: Measured and modeled elastic modulus of the porcine specimens at different strain rates

Table 4-15: Values for the parameters of Eq. 5

Variable	a	b	c	$\dot{\epsilon}$
Value	0.009	0.004	0.76	Strain Rate

4.3.3.2 Failure Properties

Failure stress of the porcine spleen was consistently higher than that of the human hosts (Figure 4-38). Although, only one specimen at each rate was tested of the human specimen, both hosts exhibited strain rate dependent behavior with an increase in failure stress with each increase of strain rate. The factor of strain rate was statistically significant for the porcine organ ($p=0.001$). Similar to the elastic modulus results, only the failure stress at a rate of 500%/s was statistically different than at the other tested rates. The rate of 100%/s is also observed as an inflection point where the relationship strain rate has with failure stress changes slightly. The model fit of failure

stress (Figure 4-39) versus strain rate using Eq 7 showed that the parameter c was lower than the same parameter for the elastic modulus. Parameter c is the variable that determines the saturation of the strain rate dependency for the material property.

$$F_{stress} = a + b\dot{\epsilon}^c \quad (7)$$

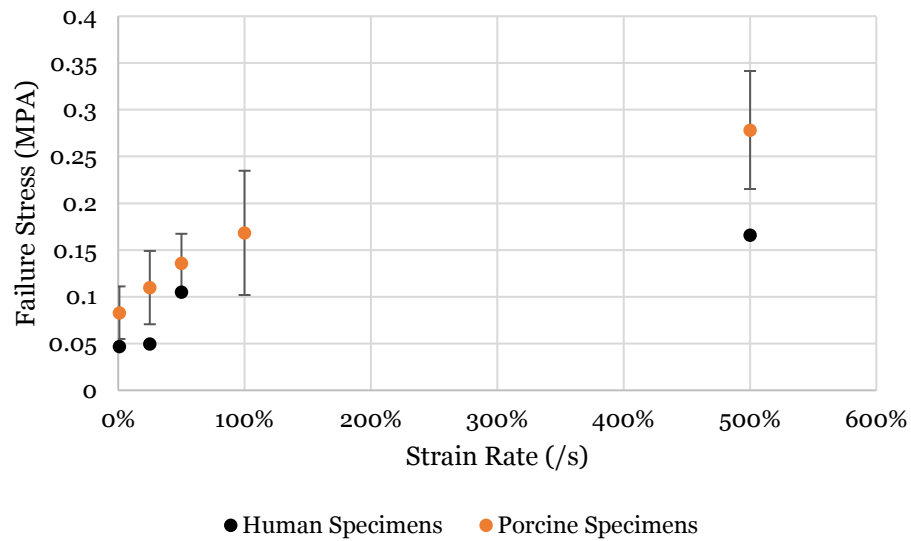


Figure 4-38: Failure stress of human and porcine spleen at various rates under unconfined compression

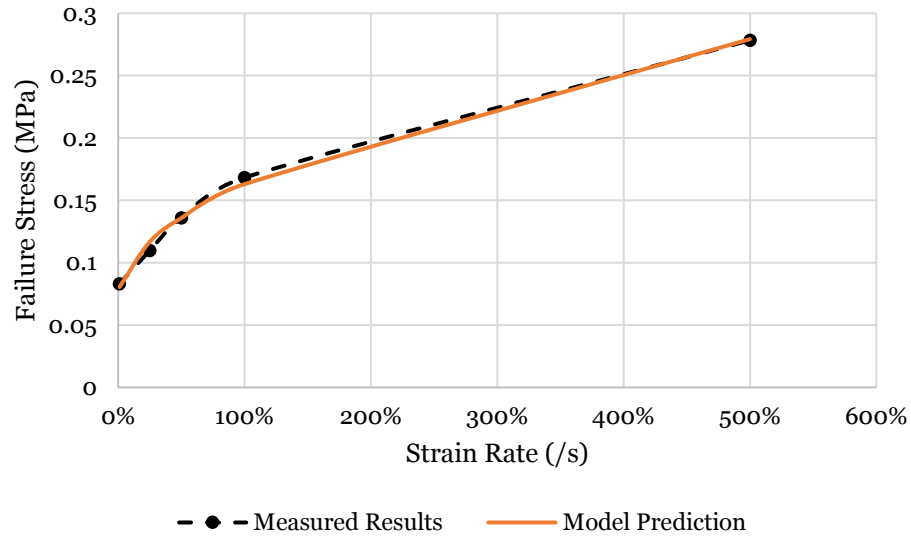


Figure 4-39: Measured and modeled failure stress at various strain rates

Table 4-16: Values for the parameters of Eq. 5

Variable	a	b	c	ϵ
Value	0.072	0.091	0.51	Strain Rate

No strain rate dependency was found for the parameter of failure strain (Figure 4-40) for either the human or porcine specimens. Between the rates of 1%/s and 500%/s only a 6% increase in failure strain was observed and the rates of 1%/s, 25%/s, and 50%/s were within 1% strain of each other on average. The ANOVA determined that the factor of strain rate was not statistically significant for failure stress ($p > 0.05$).

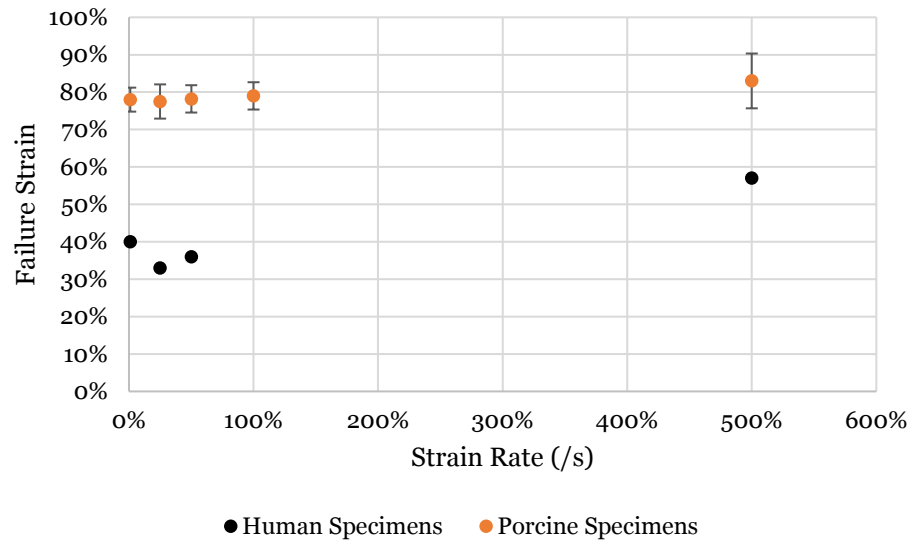


Figure 4-40: Failure strain of porcine spleen at various rates under unconfined compression

4.3.4 DISCUSSION

In both probing and unconfined compression protocols the stress-strain curves were experimentally determined for both human and porcine spleens. Although different studies have researched the mechanical properties of spleens and published varying results [14-21], no studies have directly compared different protocols. In this study it is found that using different testing methodologies on the same specimens results in different elastic moduli. For example, in the probing condition a small area of the spleen is being compressed but the resistance to the force still draws on the surrounding structure. In contrast, for unconfined compression testing the entire organ is being compressed at once.

For both testing protocols the human and porcine spleens were observed to have similar stiffness. No previous research has directly compared the stiffness of human

and porcine spleens using identical compression protocols. The results from this study highlights that using porcine elastic modulus is a potentially viable option for use in finite modeling of the human spleen in the absence of appropriate human specimen data.

Two previous studies investigated the elastic modulus of the spleen tissue [14,18]. Stingl et al. performed dynamic tension testing of the human spleen capsule and found the elastic modulus to be 10x the stiffness value obtained at any loading rate in the current study [14]. Umale et al. performed a probing compression test on porcine spleens using a quasi-static rate. Umale et al. found the modulus to be about slightly higher (7%) than the current study results for quasi-static probing testing [18]. The difference in modulus found between these studies highlights that effect that the testing methodology can produce. The difference between testing only a portion of the specimen (either via only the capsule for the tension tests or a small surface area for the probing test) and testing the entire intact specimen is also seen as a factor in the results. It is expected that the material properties found from the current research would not necessarily reflect these of other studies due to the differences in testing methodology and specimens. The current study testing methodology more accurately reflects the conditions for *in-vivo* blunt force trauma.

Although the elastic modulus of the spleen was found to be similar between the two hosts, differences were observed in the stress-strain curves. A numerical model was used to describe the behavior of spleen in unconfined compression testing for both the human and porcine. As seen in Figure 3, the toe region of the porcine spleen is longer than that of the human spleen, leading to a lower value of the E_{toe} parameter for the

porcine spleen. One possible reason for the differences between the two hosts is their relative age. The porcine hosts were within 2% of their average lifespan whereas the human host had reached the end of their natural life. It has been previously determined that aging has a significant impact on the elastin content within solid abdominal organ tissue, which effects stiffness [23].

The effect of strain rate on the elastic modulus is obvious for the porcine specimens, with modulus increasing with strain rate. The strain rate-elastic modulus relationship shows no sign of saturating, with modulus continuing to increase as strain rate increases. Thus, the spleen is sensitive to strain rate, even at higher rates, and when modeling dynamic loading this effect must be taken into account.

The failure stress for the human and porcine spleen were similar. No statistical testing was completed due to a limited number of human specimens, but the largest difference in this study (68%) was smaller than in a study that compared human and porcine spleen failure stress in a tension testing protocol (150%) [15]. Failure stress was observed to be strain rate dependent. As the strain rate increased an increase in failure stress was observed for both human and porcine tissue. The strain rate dependence continued through the largest rate tested with no apparent saturation

The strain rate was not observed to have an effect on failure strain. In both human and porcine spleen specimens, the failure strain remained fairly consistent through all strain rates of interest. The porcine spleen failure strain was double that of the human spleen, but since only one specimen per rate was obtained for the human testing it is not possible to generalize the results. Similar results were obtained from studies that performed tension testing on the capsule of the spleen. Kemper et al.

performed tension testing on human spleen and compared the results to Uhere et al. which was performed on porcine spleen [15,21]. Failure strain was approximately double for the porcine specimens versus the human specimens in these studies, as in the current study. Kemper et al. suggests the reason for the differences observed between the human and porcine spleens could be due the differing cellular structure [15]. Porcine spleens have thicker collagen walls and interwoven smooth muscle cells in the capsule which could result in the increase in failure strain [24-27].

4.3.5 LIMITATIONS

A limitation of this study is that, due to probing equipment limitations, only a quasi-static and one dynamic rate were used in the probing protocol whereas multiple rates were able to be used in the unconfined compression protocol. However, a comparison between the probing and unconfined compression protocols was able to be completed for the tested rates. Another limitation is the number of human spleen specimens that were available for this study.

4.3.6 CONCLUSION

Probing stiffness and stiffness, failure stress, and failure strain from an unconfined compression protocol was characterized for both human and porcine spleens. The feasibility of using porcine spleen material properties as a substitute for human properties was investigated, as well as the dependence of the material properties on strain rate. Mathematical models were created to describe the stress-strain curve and the relationship between strain rate and the measured material properties. The results of this study will aid in the development of more accurate and more

comprehensive finite element models that capture the actual spleen behavior when subjected to dynamic loads.

4.3.7 REFERENCES

- [1] Smith, J., Caldwell, E., D'Amours, S., Jalaludin, B., & Sugrue, M. (2005). Abdominal Trauma: A Disease in Evolution. *ANZ Journal of Surgery*, 75(9), 790-794.
- [2] Schwartz, D., Guleyupoglu, B., Koya, B., Stitzel, J. D., & Gayzik, F. S. (2015). Development of a Computationally Efficient Full Human Body Finite Element Model. *Traffic Injury Prevention*, 16(sup1), S49-S56.
- [3] Golman, A. J., Danelson, K. A., Miller, L. E., & Stitzel, J. D. (2014). Injury Prediction in a Side Impact Crash Using Human Body Model Simulation. *Accident Analysis & Prevention*, 64, 1-8.
- [4] Roberts, J. C., Merkle, A. C., Biermann, P. J., Ward, E. E., Carkhuff, B. G., Cain, R. P., & O'Connor, J. V. (2007). Computational and Experimental Models of the Human Torso For Non-Penetrating Ballistic Impact. *Journal of Biomechanics*, 40(1), 125-136.
- [5] Bass, C., Davis, M., Rafaels, K., Rountree, M., Harris, R. M., Sanderson, E., ... & Zielinski, M. (2005). A Methodology for Assessing Blast Protection in Explosive Ordnance Disposal Bomb Suits. *International Journal of Occupational Safety and Ergonomics*, 11(4), 347-361.
- [6] Beillas, P., & Berthet, F. (2012). Performance of a 50th Percentile Abdominal Model for Impact: Effects of Size and Mass. *Journal of Biomechanics*, 45(sup1), S83.
- [7] Chen, Z., Joli, P., & Feng, Z. Q. (2011, May). Finite Element Modeling of Interactions Between Pelvic Organs Due to Pressure. *Proceedings from 10e colloque national en calcul des structures* (1-7). Giens, France. <https://hal.archives-ouvertes.fr/hal-00592691/document>.
- [8] Gayzik, F. S., Moreno, D. P., Vavalle, N. A., Rhyne, A. C., & Stitzel, J. D. (2011). Development of the Global Human Body Models Consortium Mid-Sized Male Full Body Model. *Injury Biomechanics Research: Proceedings from the 39th International Workshop on Human Subjects for Biomechanical Research*, https://www.nrd.nhtsa.dot.gov/Pdf/BIO/Proceedings/2011_39/39-12.pdf.

- [9] Ward, E., Merkle, A., Harrigan, T., & Roberts, J. (2010). Comparing Blast Effects on Human Torso Finite Element Model Against Existing Lethality Curves. *Defense technical information center*, <https://apps.dtic.mil/docs/citations/ADA532225>.
- [10] Lizee, E., Robin, S., Song, E., Bertholon, N., Le Coz, J., Besnault, B., & Lavaste, F. (1998). Development of a 3D Finite Element Model Of The Human Body. *SAE Transactions*, 107(6), 2760-2782.
- [11] Shen, W., Niu, Y., Mattrey, R. F., Fournier, A., Corbeil, J., Kono, Y., & Stuhmiller, J. H. (2008). Development and Validation of Subject-Specific Finite Element Models for Blunt Trauma Study. *Journal of Biomechanical Engineering*, 130(2), 1-13.
- [12] Wu, X., Wang, Y., Huang, C., Liu, Y., & Lu, L. (2015). Experiment and Numerical Simulation on the Characteristics of Fluid–Structure Interactions of Non-Rigid Airships. *Theoretical and Applied Mechanics Letters*, 5(6), 258-261.
- [13] Tang, Z., Tu, W., Zhang, G., Chen, Y., Lei, T., & Tan, Y. (2012). Dynamic Simulation and Preliminary Finite Element Analysis of Gunshot Wounds to the Human Mandible. *Injury*, 43(5), 660-665.
- [14] Stingl, J., Báçã, V., Čech, P., Kovanda, J., Kovandova, H., Mandys, V., ... & Sosna, B. (2002). Morphology and Some Biomechanical Properties of Human Liver and Spleen. *Surgical And Radiologic Anatomy*, 24(5), 285-289.
- [15] Kemper, A., Santago, A., Stitzel, J., Sparks, J., & Duma, S. (2012). Biomechanical Response of Human Spleen in Tensile Loading. *Journal of Biomechanics*, 45(2), 348-355.
- [16] Tamura, A., Omori, K., Miki, K., Lee, J., Yang, K., & King, A. (2002). Mechanical Characterization of Porcine Abdominal Organs. *Stapp Car Crash Journal*, 46, 55-69.
- [17] Lu, Y. C., & Untaroiu, C. D. (2013). Effect of Storage Methods on Indentation-Based Material Properties of Abdominal Organs. *Proceedings of the Institution of Mechanical Engineers, Part H: Journal of Engineering in Medicine*, 227(3), 293-301.
- [18] Umale, S., Deck, C., Bourdet, N., Dhumane, P., Soler, L., Marescaux, J., & Willinger, R. (2013). Experimental Mechanical Characterization of Abdominal

Organs: Liver, Kidney & Spleen. *Journal of the Mechanical Behavior of Biomedical Materials*, 17, 22-33.

- [19] Carter, F. J., Frank, T. G., Davies, P. J., McLean, D., & Cuschieri, A. (2001). Measurements and Modelling Of The Compliance Of Human And Porcine Organs. *Medical Image Analysis*, 5(4), 231-236.
- [20] Dương, M., Nguyễn, N., Trần, T., Tolba, R., & Staat, M. (2015). Influence of Refrigerated Storage on Tensile Mechanical Properties of Porcine Liver And Spleen. *International Biomechanics*, 2(1), 79-88.
- [21] Uehara, H. (1995). A Study on the Mechanical Properties of the Kidney, Liver, and Spleen, by Means Of Tensile Stress Test with Variable Strain Velocity. *Journal of Kyoto Prefectural University of Medicine*, 104 (1), 439–451.
- [22] Campbell-Kyureghyan, N. and W. Marras (2009). Combined Experimental and Analytical Model of the Lumbar Spine Subjected to Large Displacement Cyclic Loads Part II – Model Validation. *International Journal of Computational Vision and Biomechanics*, 2(1), 95-104.
- [23] Sherratt, Michael J. (2009). Tissue Elasticity and The Ageing Elastic Fibre. *Age* 31(4), 305-325.
- [24] Dellmann, H. (1971). *Veterinary Histology: An Outline Text-Atlas*. Lea & Febiger, Philadelphia, PA.
- [25] Fawcett, D.W. (1986). *Bloom and Fawcett: A Textbook of Histology*, 11th ed. W.B. Saunders Company, Philadelphia, PA.
- [26] Eurell, J., Frappier, B. (2006). *Dellmann's Textbook of Veterinary Histology*, 6th ed. Blackwell Publishing, Ames.
- [27] Bacha, W., Bacha, L., (2000). *Color Atlas of Veterinary Histology*, 2nd ed. Lippincott Williams & Wilkins, Baltimore.

Chapter 5 : Tension Testing

5.1 Tension Testing Manuscript

Biomechanical Properties of Abdominal Organs Under Tension with Special Reference to Increasing Strain Rate

Abstract

Currently, abdominal finite element models overlook the organs such as gallbladder, bladders, and intestines, and instead are modeled as a simple bag which is then not included in the analysis. Further characterization of the material properties is required in order for researchers to include these organs into these models. This study characterized the mechanical properties of human and porcine gallbladder, bladder, and intestines using uniaxial tension loading from the rates of 25%/s to 500%/s. Little differences were observed between human and porcine gallbladder elastic modulus, failure stress, and failure strain. Strain rate was determined to be a significant factor for predicting gallbladder elastic modulus and failure strain which was found to be 9.03 MPa and 1.83 MPa at the 500%/s, respectively. Human bladder was observed to be slightly stiffer with a slightly lower failure stress than porcine specimens. Both hosts, however, demonstrated a strain rate dependency with the elastic modulus and failure stress increasing and the rate increase with the highest elastic modulus (2.16 MPa) and failure stress (0.65 MPa) occurring at 500%/s. Only the porcine intestine was found to be strain rate dependent, but only a small number of human specimens were available. Both human and porcine intestines were observed to be affected by the strain rate. Failure stress was found to be 1.6 MPa and 1.42 MPa at 500%/s for the human and porcine intestines respectively. None of the organs of interests exhibited a strain rate dependency for the property of failure strain. For all properties found to be strain rate dependent, a numerical model was created to quantify the impact. The results from this study will enable researchers to create more detailed finite element models that include the gallbladder, bladder, and intestines.

5.1.1 INTRODUCTION

Injury to human abdominal organs can occur in many types of accidents, for instance; car crashes, explosions, or even during athletic activity. These types of traumatic accidents are not rare and affect many people. According to the Center for Diseases Control and Prevention (CDC), more than 2.5 million Americans went to the emergency department and nearly 200,000 people were then hospitalized for crash injuries in 2012 [1]. A two-decade long study of bombing events by Kapur et al. (2005) revealed that about 5931 bomb-related injuries in the United States occurred between the years of 1983 and 2002 [2-5]. The CDC also estimated that nearly 2.7 million young people are treated in the emergency room every year for sports-related injuries, of which 21.9% were abdominal injuries [6].

The degree of injury depends on the magnitude and duration of the impact, and absorption of induced forces by the body. The impact wave itself can cause displacement, tearing, and rupturing of the internal abdominal organs. However, the exact mechanisms for injuries are still not fully understood. Modeling has been a widely used tool to gain insight on the mechanism of injury. There are currently finite element models for all three of these accident types [7-11]. However, the existing models use material properties that were determined from testing that do not replicate the loading conditions and rates of the accident scenarios. For instance, some FEA models use other materials such as clay, gel simulants, and rubber [9; 12-13], while other studies used material properties derived from animal organs [8;14-15].

Accurate modeling of the induced forces on abdominal organs is an urgent topic for all researchers who are working to produce realistic simulations or developing

appropriate protection. Achieving accurate simulation through a model requires representative material properties of the organs targeted by the incident. While many of these properties have already been widely studied in quasi static situations [16-18], some are left unexamined at higher dynamic rates. Previous literature has demonstrated the viscoelastic nature of biological tissue and its strain rate dependency [19-20]. However, most research has not expanded this concept far enough, specifically for the bladder, gallbladder, stomach, and intestines, to investigate the material properties at rates that better reflect traumatic accidents. Investigating the organ mechanical properties as a function of high strain rate loading and the correlation between loading rate and response can provide insight into how much damage can be caused by such a load and can better classify which organs are most vulnerable.

Only a few studies have investigated the material properties of the bladder. Martins (2011) investigated the age, BMI, and menopausal effects on stiffness and maximum stress for the female urinary bladder under quasi-static loads [21]. Barnes (2015) studied the viscoelastic properties of porcine bladders through a cyclic tensile experiment with a maximum rate of 55 mm per second [22]. Coolaset (1975) investigated the material properties during stimulation [23]. No studies have determined material properties at high dynamic rates.

The gallbladder is an organ that has been understudied. Although traumatic gallbladder injury occurs in about 2% of blunt trauma victims, no injury models include this organ [24], and only a few studies even investigated the material properties. Genovese (2014) determined the material properties of a lamb gallbladder under quasi-static conditions [25]. Rosen (2008) determined the material properties of a bovine gallbladder in vivo using a grasping technique [26]. Neither of these studies have

researched the material properties of the human gallbladder and under dynamic loading in tension.

Limited research on the material properties of the stomach is available to date. Saraf has tested the stomach tissue at extremely high rates using the Kolsky bar technique, however these rates were not controlled [27]. Rosen (2008) investigated the material properties of the porcine stomach under quasi-static conditions using a grasping technique [26]. Egrov (2002) tested the human stomach under tensile loading but used quasi-static conditions [28].

The intestines are the most extensively researched of the organs of interest in this paper. Gregersen (1998) quasi-statically filled guinea pig intestines with air to determine the cyclic loading properties [29]. In a similar study by Stockholm (1995), the passive properties of the guinea pig were found through pressurizing the organ [30]. Another study by Duch et al., 1996, used the pressurized balloon technique to measure the circumferential elastic properties of rat intestines [31]. Bourgouin (2012) studied the human small intestine under dynamic tensile loading at a constant rate of 1 m/s [32]. Gao (2000) measured the stress and strain of rat intestine through inflating and relaxing the organ under quasi-static conditions [33].

A limited variety of research has been conducted on the mechanical properties of the gallbladder, bladder, intestines, and stomach, which is one reason why finite element models might neglect including these organs. A lack of consistency in methodology and differences between the organs make it difficult to determine which material properties are the most appropriate for an abdominal traumatic injury model. Either researchers use material properties investigating the material properties at quasi-

static rates or use non-human hosts for the source of the organ tissue without determining the feasibility of using animal tissues as a substitute.

The goal of this study is to quantify the mechanical properties (modulus of elasticity, failure stress and failure strain) of the abdominal organs including the stomach, intestines, bladder, and gallbladder *in-vitro* at multiple loading rates for both human and porcine hosts. The material properties of the two hosts will be compared in order to determine the feasibility of using porcine animal organs as a substitute for human organs. It is hypothesized that the elastic modulus, failure stress, and failure strain will increase as strain rate increases for all organs.

5.1.2 METHODS

5.1.2.1 Specimen Preparation

Abdominal organs from two different hosts were used in this study; porcine and human. Stomachs, intestines, bladders, and gallbladders were harvested from fresh postmortem human male cadavers with the mean age of 87 ± 11 years. All cadavers were screened to be sure there were no pathological diseases and then preserved in a refrigerator maintained at a temperature of 4°C. Porcine specimens were obtained from a local government inspected slaughterhouse. Professional butchers surgically removed the organs from porcine that were euthanized for other purposes and not solely for this study.

The bladder, gallbladder, stomach, and small intestines were sliced into individual specimens. Slicing was performed in one smooth slow pass through the tissue to avoid damaging or deforming the tissue while minimizing downward force. Figure 5-1 shows a “dog-bone” shaped specimen used for uniaxial tension testing.

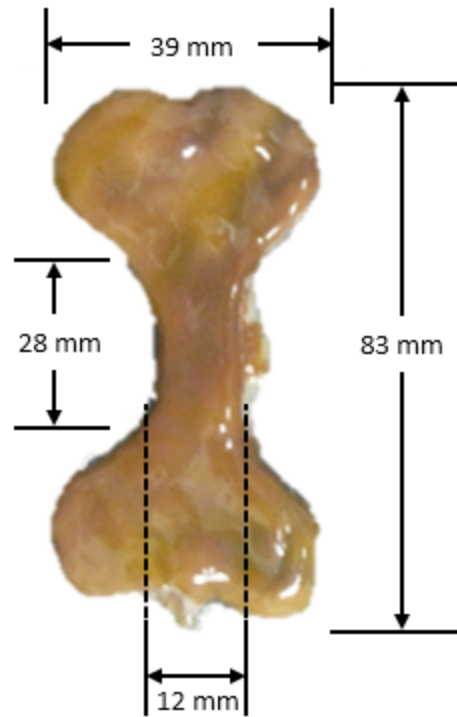


Figure 5-1: A dog-bone shaped specimen from the stomach

5.1.2.2 Experimental Protocol

Mechanical property testing was conducted using a servo hydraulic Material Testing System (MTS, Minnesota) with a 15 kN load cell. Specimens were mounted in the MTS system using a set of standard grips (Figure 5-2). To prevent unwanted bending moments, the specimen was aligned in between upper and lower grips so that its longitude axis coincided with the centerline of the load train and clamped in place. Sandpaper was placed on the clamping surface to prevent any slipping throughout the trials. The specimen height, width, and thickness were measured using a caliper set.

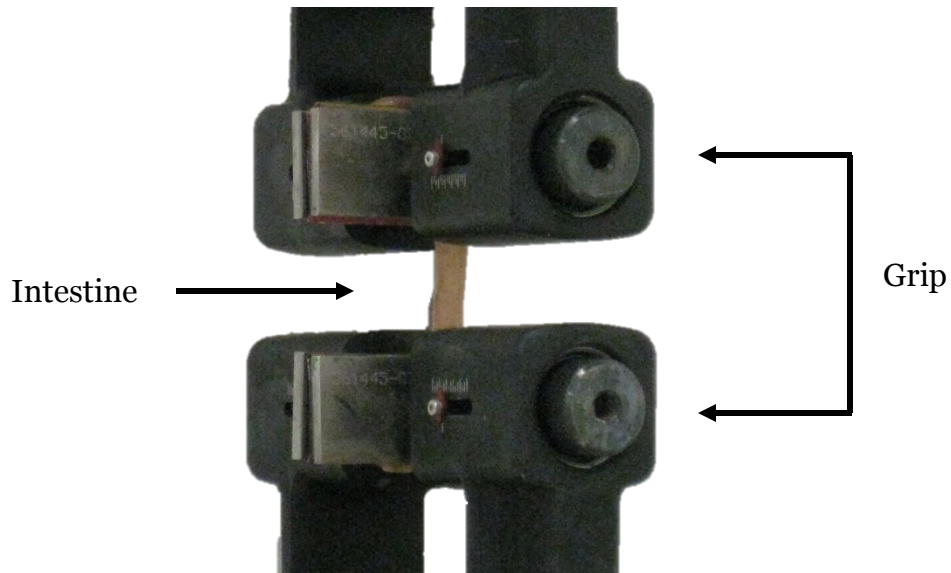


Figure 5-2: Intestine mounted in MTS system

The organs were tested at various strain rates ranging from quasi-static to dynamic. A summary of different strain rates that were utilized in the study for testing both human and porcine specimens is presented in Table 5-1. Human stomachs were tested only at 25%/s and 50%/s due to a limited number of specimens.

Table 5-1: Testing strain rates utilized for different organs and hosts

Strain Rate	Gallbladder		Bladder		Intestine	
	Human	Porcine	Human	Porcine	Human	Porcine
25 %/s	✓	✓	✓	✓	✓	✓
50 %/s	✓	✓	✓	✓	✓	✓
100 %/s	✓	✓	✓	✓	✓	✓
500 %/s	✓	✓	✓	✓	✓	✓

Forces and displacements were sampled at a rate of 4,096 Hz. Stress and strain were calculated using Equations 1 and 2 respectively. To measure the modulus of elasticity of each organ, the slope of the stress strain curve was calculated at the most linear section of the curve (Figure 5-3). Failure was defined as a complete reduction of force (when the specimen separated into two pieces). Failure stress and failure strain were recorded.

$$Stress = \frac{Force}{Area} \dots\dots\dots(1)$$

$$Strain = \frac{Height}{Height_{Initial}} \dots\dots\dots(2)$$

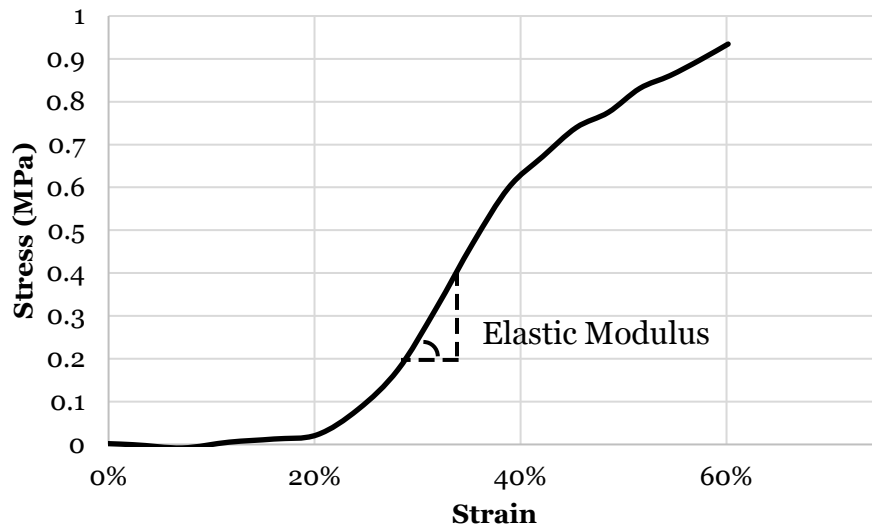


Figure 5-3: Intestines tested at 50%/s

5.1.2.2 Analysis

This manuscript provides a full description of the measured material properties of the human specimens as not enough specimens were available to perform statistical analysis. A one-way ANOVA with a post-hoc tukey test was performed on all porcine

material properties of interest to determine if the factor of strain rate was statistically significant. Equation 3 was used to model the relationship of strain rate with each of the material properties of interest. Parameter a describes the value of the material property at a static state, parameter b represents the effect strain rate has on the material property of interest, parameter c indicates the rate of saturation of the strain rate relationship with said material property, and $\dot{\epsilon}$ is the strain rate. An optimization process was used to determine the parameters that would maximize the R^2 of the line created from plotting the measured results with the predicted results, which would best numerically describe the relationship of strain rate with the material properties of interest.

$$\text{Material property} = a + b\dot{\epsilon}^c \dots\dots\dots(3)$$

5.1.3 RESULTS

5.1.3.1 Gallbladder Material Properties

Due to the limited number of sample size and the variation that can be seen, a clear effect of strain rate was not observed for the human gallbladder. All measured elastic modulus was stiffer than the slowest rate measured however the rates of 50%/s and 100%/s were higher than 500%/s. The largest difference observed between the two hosts were 150% increase in stiffness for the porcine gallbladder versus the human gallbladder. A difference of less than 20% was observed at the rates of 25%/s and 100%/s between the two hosts. With more samples of porcine specimens, a clear strain rate effect was observed ($p=0.001$). The post-hock tukey test on the elastic modulus results revealed that the rate of 500%/s was the only rate statistically different than the rest of the rates ($p<0.05$), but all elastic modulus averages increased with each increase

in strain rate (Figure 5-4). Eq. 3 was used to aid in the description of the relationship between elastic modulus and strain rate. An optimization process was utilized to maximize the R2 of the line formed by the modeled results and experimental results. The relationship between the elastic modulus and strain rate appears to have little saturation (Figure 5-4) as the c parameter (Table 5-2) is close to one.

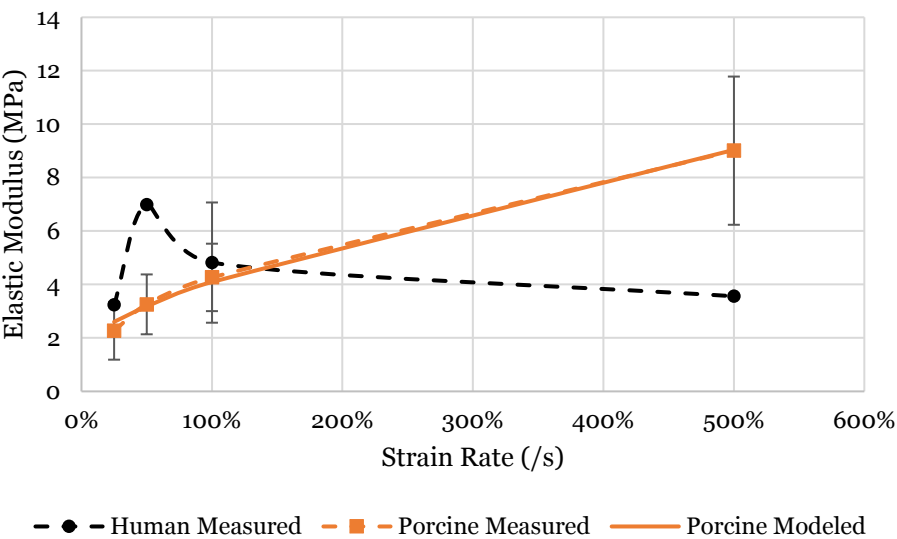


Figure 5-4: Predicted porcine and measured human and porcine gallbladder elastic modulus at each rate tested

Table 5-2: Values of the model parameters that most accurately predicted elastic modulus

Variable	a	b	c	$\dot{\epsilon}$
Value	1.68	2.41	0.69	Strain Rate

The failure stress results mimicked the elastic modulus results for both human and porcine specimens. Once again, the failure stress of the human specimens was higher at the rates of 50%/s and 100%/s than 25%/s and 500%/s. For the human gallbladders, the failure stress was still 25% higher at the of 500%/s than 25%/s. Porcine gallbladders failure stress increased with each increase in strain rate ($p=0.001$). The rates of 500%/s, 100%/s, and 50%/s were statistically different than all other rates ($p<0.05$). The largest difference between hosts was a 75% increase in failure stress for the human host versus the porcine specimens at 100%/s. Human specimens were consistently stronger than porcine specimens, except for the rate of 500%/s. Eq. 3 was also used to aid in the description of the relationship between failure stress and strain rate. The parameters for failure stress (Table 5-3) were not similar to that of elastic modulus (Table 5-2). The failure stress (Figure 5-5) has a relatively low value for c which demonstrates that the effect of strain rate (parameter b) saturates as the rate increases (Figure 5-5), whereas the elastic modulus has a value closer to one representing little saturation of this effect.

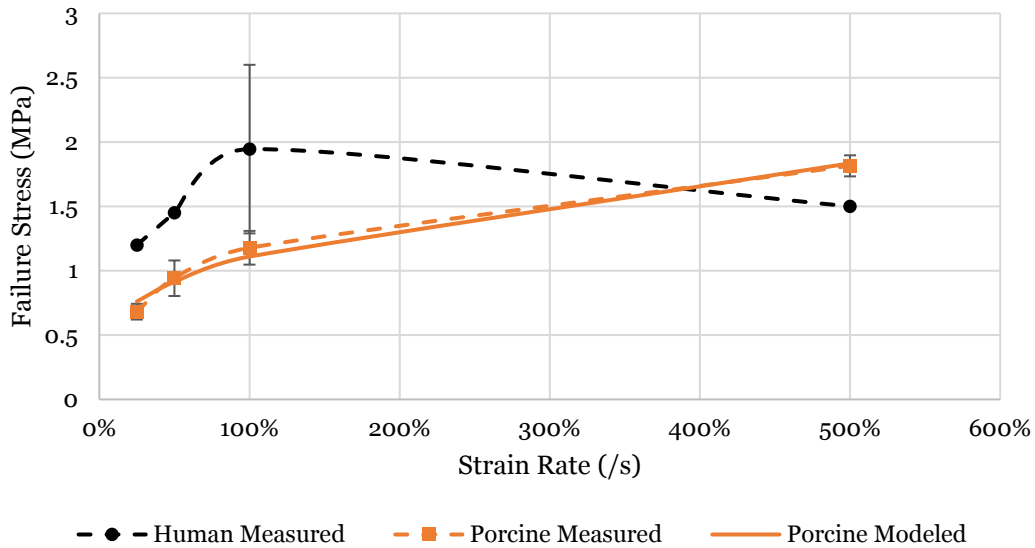


Figure 5-5: Predicted porcine and measured human and porcine gallbladder failure stress at each rate tested

Table 5-3: Values of the model parameters that most accurately predicted failure stress

Variable	a	b	c	$\dot{\epsilon}$
Value	0.27	0.85	0.38	Strain Rate

Human and Porcine failure strain showed no dependence ($p=0.382$) on strain rate (Figure 5-6). The largest difference between any of the rates for the human host was 5% and for the porcine gallbladders it was 20%. All human failure strain results fell within the standard deviation of the porcine gallbladder failure strain results.

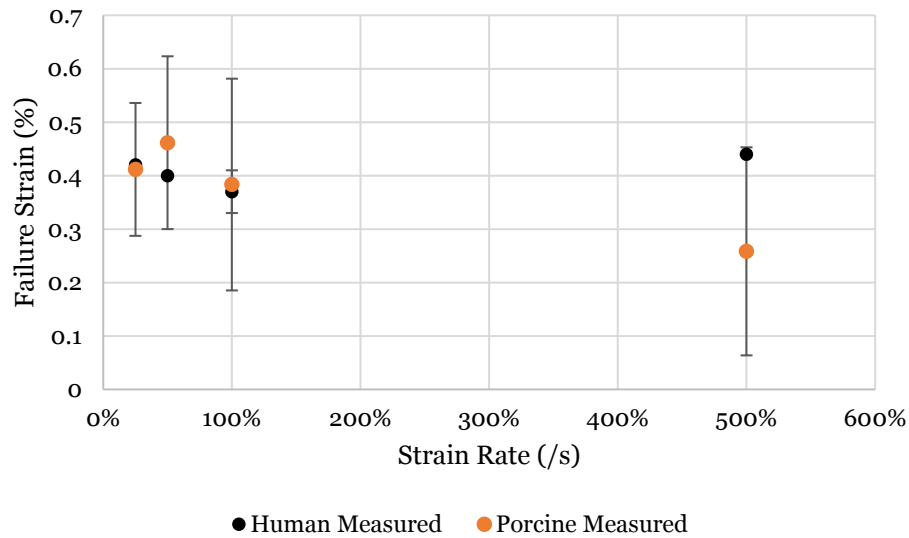


Figure 5-6: Average human and porcine gallbladder failure strain at each rate tested

5.1.3.2. Bladder Material Properties

The elastic modulus of both human and porcine specimens were observed to be effected by strain rate (Figure 5-7). An increase was observed for increase in strain rate for the human specimens start at 0.51 MPa at 25%/s and going to 2.16 MPa at 500%/s. Strain rate had a similar effect on the material properties of the porcine bladders as to the human bladders. A one-way ANOVA determined that the factor of strain rate was a significant factor in predict elastic modulus ($p=0.001$). The rates of 500%/s produced statistically higher elastic modulus than the rest of the rates (Figure 5-7). Human bladders were consistently stiffer than porcine bladders with the largest difference being 75%. However, at the fastest rate measured the human bladder elastic modulus fell within the standard deviation of the porcine stiffness. A model was created to describe the effect of strain rate on the elastic modulus. The model described the strain rate effect

as the elastic modulus increases by 0.29 MPa for every 0.01 strain increase in rate (Table 5-4). Little saturation of this effect was observed as the parameter c is closer to 1.

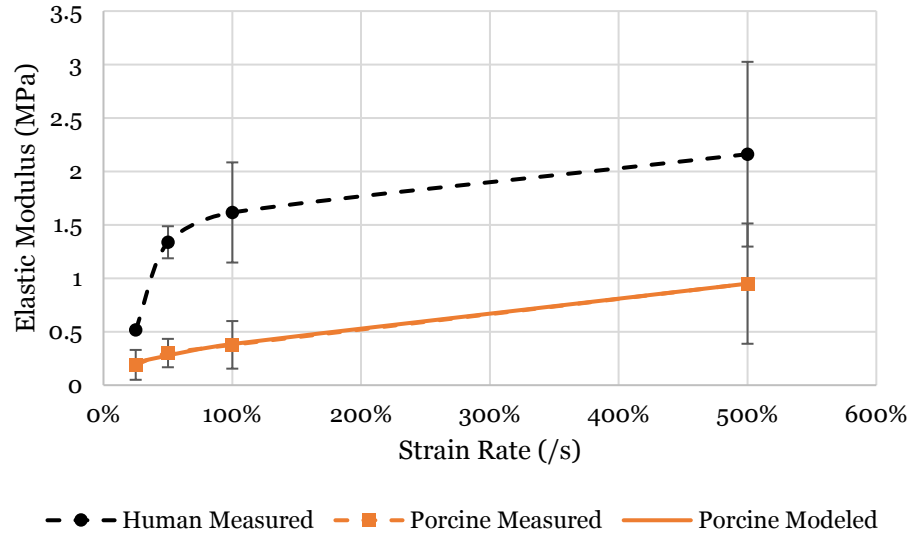


Figure 5-7: Predicted porcine and measured human and porcine bladder elastic modulus at each rate tested

Table 5-4: Values of the model parameters that most accurately predicted elastic modulus

Variable	a	b	c	ϵ
Value	0.09	0.29	0.68	Strain Rate

Human bladder failure stress almost doubled from the rate of 25%/s to 500%/s. Failure stress was observed to consistently increase as the strain rate increased (Figure 5-8). Porcine failure stress observed a similar affect to strain rate ($p=0.001$) as human specimens but were consistently 40% higher than the human results. The model (Eq. 3) determined that failure stress increases by 0.82 MPa for 100% increase in rate. This

effect appears to saturate around 100%/s (Figure 5-8) which is described through the value of parameter c being close to 0 (Table 5-5).

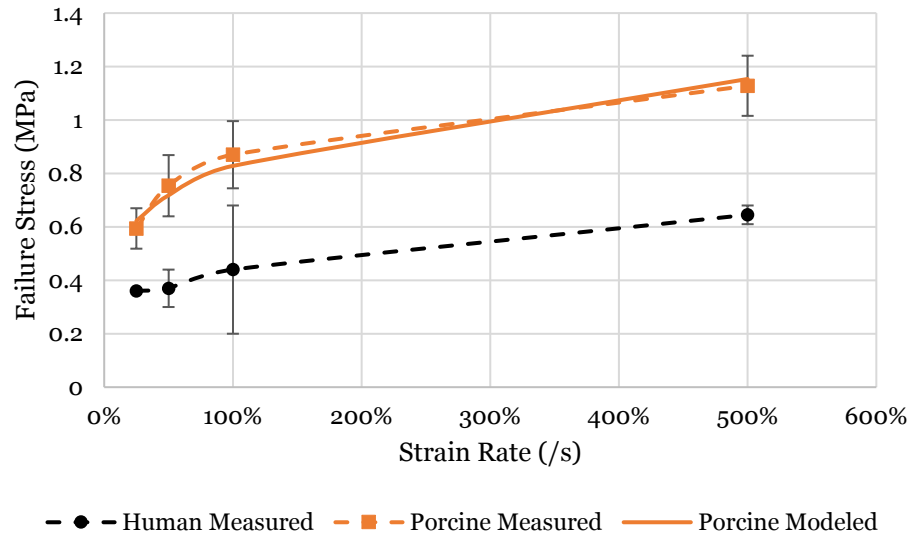


Figure 5-8: Predicted porcine and measured human and porcine bladder failure stress at each rate tested

Table 5-5: Values of the model parameters that most accurately predicted the failure stress of porcine bladder at various rates

Variable	a	b	c	ϵ
Value	0	0.82	0.2	Strain Rate

Human specimens were observed to have a slight relationship to strain rate with a reduction in failure strain being associated with an increase in strain rate. This was mimicked for the porcine samples (Figure 5-9) however, this factor was not statistically

significant. Porcine failure strain was consistently almost a factor of 4 higher than that of human specimens with an average of 203% versus 58% respectively.

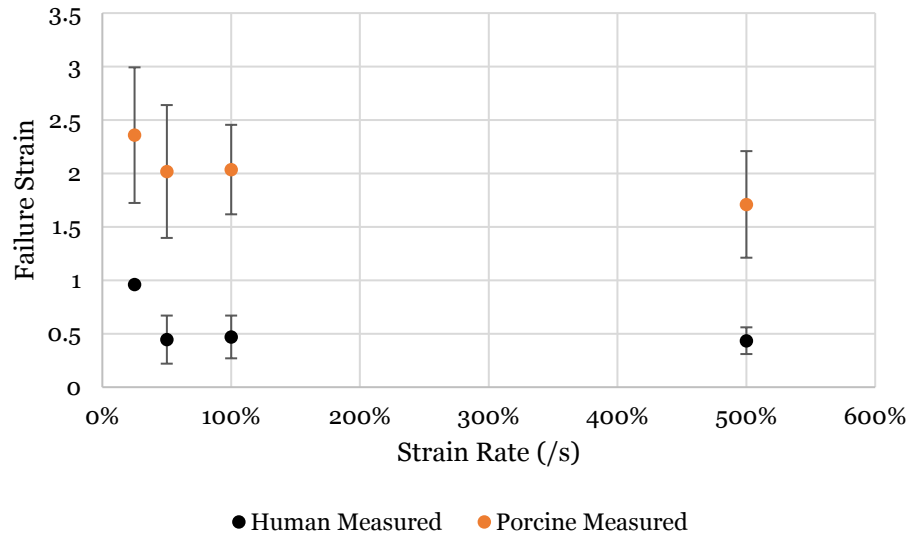


Figure 5-9: Average failure strain of human and porcine bladder specimens performed in uniaxial tension testing

5.1.3.3 Intestines Material Properties

The experimentally derived and modeled elastic modulus is displayed in Figure 10. No strain rate dependency was observed for the human specimens as only an 18% increase in stiffness was observed between 50%/s and 500%/s. On the other hand, strain rate was found to have a significant effect on the porcine intestine elastic modulus ($p=0.001$). The elastic modulus of porcine specimens more than doubled from 25%/s to 500%/s with an increase in stiffness observed for each increase in strain rate. Porcine measured results were consistently stiffer than human specimens. As rate increase, the difference between the two hosts increased. From the parameters of the numerical model that described the relationship between strain rate and the elastic modulus

(Table 5-6), it is observed that the porcine intestine gets stiffer by 7.54 MPa with each strain rate increase of 100%. However, this rate saturates as the c parameter is 0.2 which reduces the strain rate effect as the rate increases. The saturation is observed to occur between the rates of 100%/s and 500%/s (Figure 5-10).

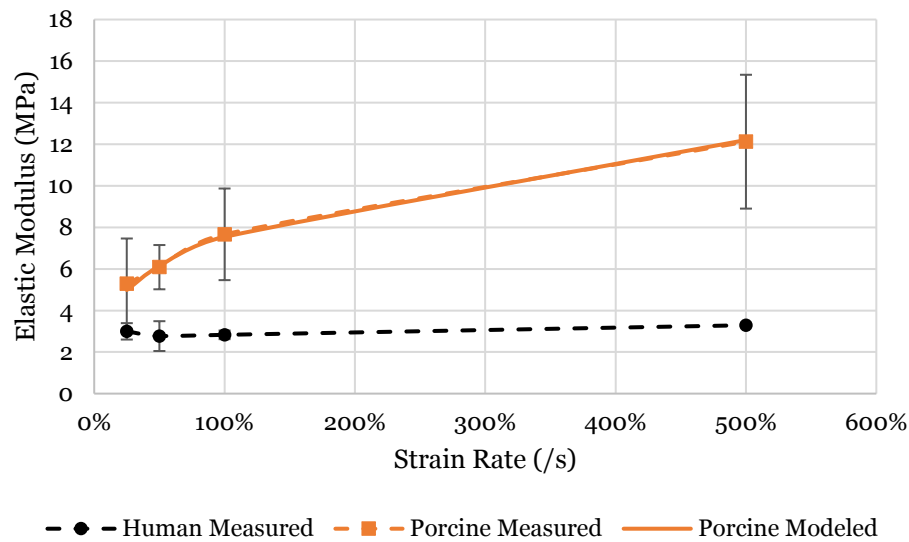


Figure 5-10: Predicted porcine and measured human and porcine intestine elastic modulus at each rate tested

Table 5-6: Values of the model parameters that most accurately predicted the elastic modulus of porcine intestine at various rates

Variable	a	b	c	ϵ
Value	0	7.54	0.29	Strain Rate

The failure stress of both porcine and human specimens was observed to have a similar relationship with strain rate as the elastic modulus for the porcine intestine specimens (Figures 5-10 and 5-11). Human specimens failure stress almost tripled from the rates of 25%/s to 100%/s and then plateaued as only a small increase was observed

between 100%/s to 500%/s. Porcine intestines followed a similar pattern with the failure stress almost doubling from 25%/s to 100%/s and then only a 50% increase from the rates of 100%/s to 500%/s. Human specimens were consistently stronger than porcine intestines with the largest difference (0.42 MPa) occurring at 100%/s.

Parameter c , the saturation effect, of the numerical model for the failure stress (Table 5-7) is 0.23 versus 0.29, the value for the elastic modulus model, and thus has a higher saturation effect that was observed to also occur around 100%/s.

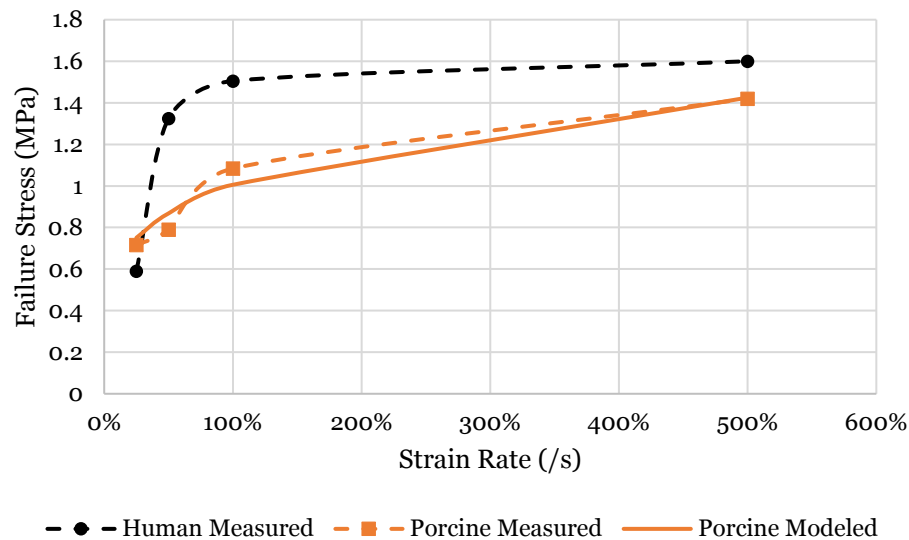


Figure 5-11: Predicted porcine and measured human and porcine intestine failure stress at each rate tested

Table 5-7: Values of the model parameters that most accurately predicted the failure stress of porcine intestine at various rates

Variable	a	b	c	ϵ
Value	0.08	0.93	0.23	Strain Rate

Both human and porcine intestines were observed to not be dependent on strain rate (Figure 5-12). Only a difference of 10% was observed between the rates of 25%/s to 500%/s for the porcine specimens ($p>0.05$). This difference was even smaller (1.5%) for human specimens. Overall, porcine intestine failure strain was consistently over 4 times higher than that of the human specimens.

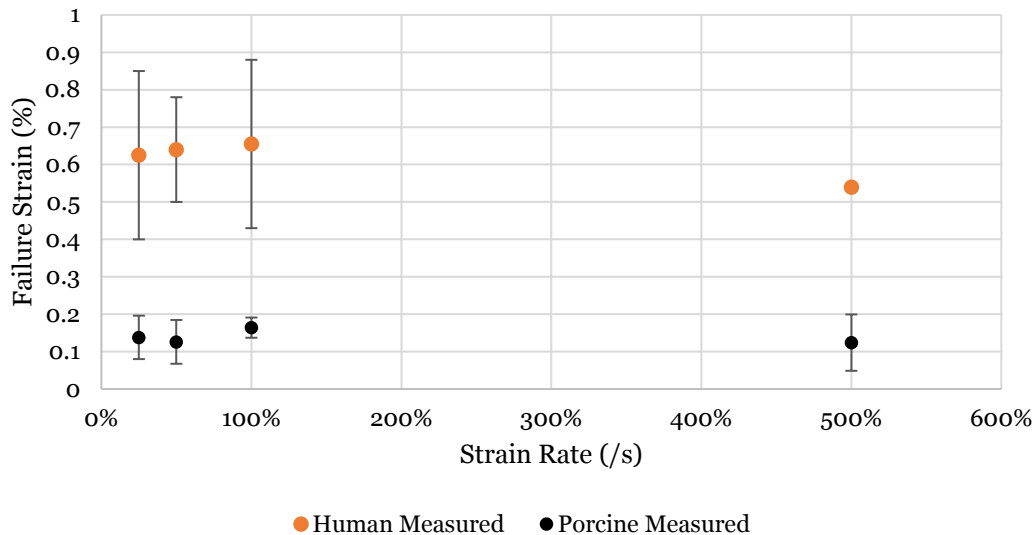


Figure 5-12: Average failure strain of porcine and human intestine specimens performed in uniaxial tension testing

5.1.4 Discussion

This paper describes the material properties of the human and porcine gallbladder, bladder, and intestine at increasingly higher dynamic tensile strain rates. Abdominal organ models used for impact, blunt force, or blast simulations often oversimplify the parameters used within the model. Many of the torso models exclude the analysis of fluid filled/ pressurized organs such as those studied in this paper.

Instead, the organs are modeled as a simple bag to cover the space and not included in the analysis [34]. The organ material properties that have been established in this study could fill a knowledge gap on the mechanical characteristics of abdominal organs.

The material properties of the human and porcine gallbladder were mechanically characterized in this study. Very few studies have measured the material properties of the gallbladder, and only one published the elastic modulus found using numerical modeling combined with ultrasound analysis. The results from the current study are 100x stiffer than what was found in the previous study [35]. Large differences were expected as an imaging methodology was used versus a uniaxial tension test. Human gallbladder specimens were found to be similar to the porcine specimens, and thus porcine gallbladder material properties could be a useful substitute. More specimens from porcine gallbladders were available to be tested and thus statistically analyzed, and a clearer dependency on strain rate was observed from the porcine results. Through the numerical model developed it is found that the elastic modulus of the gallbladder has a close to linear relationship with strain-rate. However, the effect of strain rate on the failure stress shows a rate, 100%/s, where the impact of strain rate starts to saturate. This characteristic of strain rate dependency saturation is shared among other organ tissue such as the spleen and renal capsule of saturation [36; 37]. Current blunt trauma finite element models of the torso usually considers organs like the gallbladder as a simple bag to fill the space and the structure is not analyzed computationally [34]. However, with newly derived material properties, researchers can incorporate this organ into their models. Although injury is rare because of the placement of the organ [38,39], gallbladder trauma does occur in blunt force incidents such as car accidents [40].

The tension testing of the bladder organ revealed that this was the least stiff abdominal organ investigated in this study. Physiologically, it would be expected that the bladder is one of the most flexible organs as it expands, and contracts more rapidly based on the amount of urine that is being held.

Very few studies have quantified the material properties of human bladder tissue [16,18,21,22,25,] and only two have tested in tension, but both used a quasi-static strain rate [16, 21]. Only one of the two studies published elastic modulus was similar to what was found in the current study [21]. However, previous research has yet to quantify not only the human bladder tissue at such high strain rates, but porcine tissue as well. The stiffness found at strain rate of 25%/s was over double that found under quasi-static conditions for both human and porcine results [16]. With limited specimens available for human bladder tensile testing, only the porcine specimens were statistically analyzed. Comparatively, the human results were stiffer, had higher failure stress, and lower failure strains than the porcine specimens. This discrepancy between material property values between hosts could be due to the differences in relative age of the specimens. The human specimens came from hosts that had naturally reached the end of their life whereas the porcine specimens were euthanized within just 20% of their life expectancy. However, even with the differences in age, the two hosts had a similar effect from strain rate.

The strain rate dependency of the bladder tissue was fully characterized for the porcine hosts as well. Two studies have uniaxial tested porcine bladder tissue. One study tested using quasi-static rates and published the elastic modulus, failure stress, and failure strain to be lower than what was found in this study [16]. Another study

using dynamic rates found the elastic modulus to be similar to what was found in this study [22]. However, only the current study investigated strain rate as a factor that effects the material properties. It was found that failure stress and the elastic modulus had strain rate as a statistically significant factor. Similar to the gallbladder, the bladder also demonstrated little saturation of the strain rate effect on the elastic modulus while a larger saturation for the failure stress. The rate has a continued effect on the elastic modulus while as the rate increases the failure stress has diminishing increases. Numerically estimating this effect through a model will help researchers understand how the bladder tissue reacts in situations of traumatic loading. Taken together, the stress-strain properties and strain rate effects will be useful in generating models of high rate impact trauma on the bladder. These models will have the potential to expand the knowledge of the injury mechanism for this organ beyond the current research on how to manage the injuries from a clinical point of view [41-43].

The intestine also demonstrated multilinear behavior. Similar behavior was also found in a study by Bourgouin et al. (2012), who proposes that this behavior is due to the multilayer structure of the intestines [32]. Different layers fail at different strains and thus the stress-strain curve is not linear. Additionally, the viscoelastic behavior of the tissue is observed to have a toe region and an inflection point at which the intestine tissue has different elastic modulus. Thus, the shape of the stress-strain curves can differ based on when and which of the intestine layers fail, making development of a single material model difficult.

The stiffness of the intestine found in a study by Bourgouin et al (2012) are slightly higher than the highest stiffness of the human results reported in this study

[32]. However, Bourgouin et al. (2012) tested at a higher rate of 1 m/s, and the results of this study demonstrate that higher strain rates increase the stiffness of the intestines. Contrary to the human results, the porcine intestine specimens reported higher elastic modulus at lower rates. This difference between the hosts could be due to the differences in age between human and porcine specimens.

In a study by Ergorov et. al (2002) similar magnitudes of failure stress and strains to the current study were found [17]. In another study that performed material testing on porcine intestines by Rosen et. al (2008), similar failure strains were also observed [27]. In both studies failure of the tissue occurred between 60%-70% strain, even for the porcine specimens. The similarities found between the human and porcine specimens in this study highlights the feasibility using data from porcine specimens as a substitute for human intestines.

In this study, the effect of strain rate was fully characterized for the porcine intestine specimens. A clear strain rate dependency was observed for the properties of elastic modulus and failure stress. The numerical model was able to quantify the rate of which the increase in strain rate impacts these properties. It was also found in the numerical model that both failure stress and elastic modulus have a point where the relationship with strain rate saturates. The knowledge obtained from this study helps further characterize the material properties of the intestinal tissue. In a review spanning over 50 years looking at human body numerical models not a single abdominal model used intestine material properties, but instead the intestines were modeled as bags to fill space and were not included in the computational simulation of car accidents [22]. Thus, there have been no attempts to predict injuries to the intestines, and the

availability of material properties at appropriate strain rates will make such modeling possible.

These newly established material properties determined with the current testing methodology will provide a better understanding of the mechanical behavior of these organs under high loading rates and the feasibility of using porcine tissue properties instead of human where limited human data are available. Currently, most abdominal finite element models do not include all organs within the simulation [34]. The reason for excluding these organs within the model could be because there is a lack of accurate material properties at higher strain rates for the organs of interest in this study.

Inclusion of all abdominal organs would increase the accuracy of these models and improve the information that could be extracted from them. However, this study has not only studied these tissues from human hosts, but also investigated the feasibility of using porcine tissues. Although limited data from human specimens prevents any definitive answers, the gallbladder, and intestines appear to be suitable candidates for the substitute use of porcine material properties while this is still undetermined for the bladder as the human results were double of the porcine results. Using the material properties from this study, models can now be extended to include these rarely studied organs.

5.1.5 References

- [1] *CDC VitalSigns - Motor Vehicle Crash Injuries*. (2014). *Centers for Disease Control and Prevention*. Retrieved 8 November 2016, from <http://www.cdc.gov/vitalsigns/crash-injuries>
- [2] Kapur G, Hutson H, Davis M, Rice P. (2005). The United States Twenty-Year Experience with Bombing Incidents: Implications for Terrorism Preparedness and Medical Response. *Journal of Trauma*, 59(6):1436–1444.
- [3] Bridges, E. J. (2006). Blast Injuries: From Triage to Critical Care. *Critical Care Nursing Clinics*, 18(3), 333-348.
- [4] Mozingo, D. W., Barillo, D. J., & Holcomb, J. B. (2005). The Pope Air Force Base Aircraft Crash and Burn Disaster. *The Journal of Burn Care & Rehabilitation*, 26(2), 132-140.
- [5] Cairns, B. A., Stiffler, A., Price, F., Peck, M. D., & Meyer, A. A. (2005). Managing a Combined Burn Trauma Disaster in the Post-9/11 World: Lessons Learned from the 2003 West Pharmaceutical Plant Explosion. *The Journal of Burn Care & Rehabilitation*, 26(2), 144-150.
- [6] Johnson, B., & Comstock, R. (2017). Epidemiology of Chest, Rib, Thoracic Spine, and Abdomen Injuries Among United States High School Athletes, 2005/06 To 2013/14. *Clinical Journal of Sport Medicine*, 27(4), 388-393.
- [7] Roberts, J., Merkle, A., Biermann, P., Ward, E., Carkhuff, B., Cain, R., O'Connor, J. (2007). Computational and Experimental Models of the Human Torso for Non-Penetrating Ballistic Impact. *Journal of Biomechanics*, 40(1), 125-136.

- [8] Shen, W., Niu, Y., Mattrey, R. F., Fournier, A., Corbeil, J., Kono, Y., Stuhmiller, J. H. (2008). Development and validation of subject-specific finite element models for blunt trauma study. *Journal of Biomechanical Engineering*, 130(2), 1-13.
- [9] Dominiak, J., Stempień, Z. (2012). Finite-Element-Based Modeling of Ballistic Impact on a Human Torso Protected by Textile Body Armor. *Innovative Materials & Technologies in Made-Up Textile Articles, Protective Clothing and Footwear*, DOI: 10.13140/2.1.2463.1687.
- [10] Gupta, R., Przekwas, A. (2013). Mathematical Models of Blast-Induced TBI: Current Status, Challenges, and Prospects. *Frontiers in Neurology*, 4(59), 1-21.
- [11] Vavalle, N., Moreno, D., Rhyne, A., Stitzel, J., Gayzik, F. (2013). Lateral Impact Validation of a Geometrically Accurate Full Body Finite Element Model for Blunt Injury Prediction. *Annals of Biomedical Engineering*, 41(3), 497-512.
- [12] Saraf, H., Ramesh, K. T., Lennon, A. M., Merkle, A. C., Roberts, J. C. (2007). Mechanical Properties of Soft Human Tissues Under Dynamic Loading. *Journal of Biomechanics*, 40(9), 1960-1967.
- [13] Shen, W., Niu, Y., Bykanova, L., Laurence, P., Link, N. (2010). Characterizing the Interaction Among Bullet, Body Armor, and Human and Surrogate Targets. *Journal of Biomechanical Engineering*, 132(12), 1-11.
- [14] Shao, Y., Zou, D., Li, Z., Wan, L., Qin, Z., Liu, N., Chen, Y. (2013). Blunt Liver Injury with Intact Ribs Under Impacts on the Abdomen: A Biomechanical Investigation. *PloS One*, 8(1), 1-8.
- [15] Umale, S., Deck, C., Bourdet, N., Dhumane, P., Soler, L., Marescaux, J., Willinger, R. (2013). Experimental Mechanical Characterization of Abdominal Organs:

- Liver, Kidney, Spleen. *Journal of the Mechanical Behavior of Biomedical Materials*, 17, 22-33.
- [16] Dahms, S. E., Piechota, H. J., Dahiya, R., Lue, T. F., Tanagho, E. A. (1998). Composition and Biomechanical Properties of the Bladder Acellular Matrix Graft: Comparative Analysis In Rat, Pig and Human. *British Journal of Urology*, 82, 411-419.
- [17] Egorov, V., Schastlivtsev, I., Prut, E., Baranov, A., Turusov, R. (2002). Mechanical Properties of the Human Gastrointestinal Tract. *Journal of Biomechanics*, 35(10), 1417-1425.
- [18] Rubod, C., Brieu, M., Cosson, M., Rivaux, G., Clay, J. C., de Landsheere, L., Gabriel, B. (2012). Biomechanical Properties of Human Pelvic Organs. *Urology*, 79(4), 17-22.
- [19] Snedeker, J., Barbezat, M., Niederer, P., Schmidlin, F., Farshad, M. (2005). Strain Energy Density as a Rupture Criterion for the Kidney: Impact Tests on Porcine Organs, Finite Element Simulation, and a Baseline Comparison Between Human and Porcine Tissues. *Journal of Biomechanics*, 38(5), 993-1001.
- [20] Kemper, A., Santago, A., Stitzel, J., Sparks, J., Duma, S. (2012). Biomechanical Response of Human Spleen in Tensile Loading. *Journal of biomechanics*, 45(2), 348-355.
- [21] Martins, P., Silva Filho, A., Fonseca, A., Santos, A., Santos, L., Mascarenhas, T., Ferreira, A. (2011). Uniaxial Mechanical Behavior of the Human Female Bladder. *International Urogynecology Journal*, 22(8), 991-995.

- [22] Barnes, S., Shepherd, D., Espino, D., Bryan, R. (2015). Frequency Dependent Viscoelastic Properties of Porcine Bladder. *Journal of the Mechanical Behavior of Biomedical Materials*, 42, 168-176.

- [23] Coolsaet, B., Van Duyl, W., Van Mastrigt, R., Van der Zwart, A. (1975). Visco-Elastic Properties of the Bladder Wall. *Urologia Internationalis*, 30(1), 16-26.

- [24] Sharma, O. M. (1995). Blunt Gallbladder Injuries: Presentation of Twenty-Two Cases with Review of the Literature. *Journal of Trauma and Acute Care Surgery*, 39(3), 576-580.

- [25] Genovese, K., Casaletto, L., Humphrey, J. D., & Lu, J. (2014). Digital Image Correlation-Based Point-Wise Inverse Characterization of Heterogeneous Material Properties of Gallbladder In Vitro. *Proceedings of the Royal Society A: Mathematical, Physical and Engineering Sciences*, 470, 1-20.

- [26] Rosen, J., Brown, J. D., De, S., Sinanan, M., Hannaford, B. (2008). Biomechanical Properties of Abdominal Organs In-Vivo and Postmortem Under Compression Loads. *Journal of Biomechanical Engineering*, 130(2), 1-17.

- [27] Saraf, H., Ramesh, K. T., Lennon, A. M., Merkle, A. C., Roberts, J. C. (2007). Mechanical Properties of Soft Human Tissues Under Dynamic Loading. *Journal of Biomechanics*, 40(9), 1960-1967.

- [28] Egorov, V. I., Schastlivtsev, I. V., Prut, E. V., Baranov, A. O., Turusov, R. A. (2002). Mechanical Properties of the Human Gastrointestinal Tract. *Journal of Biomechanics*, 35(10), 1417-1425.

- [29] Gregersen, H., Emery, J. L., McCulloch, A. D. (1998). History-Dependent Mechanical Behavior of Guinea-Pig Small Intestine. *Annals of Biomedical engineering*, 26(5), 850-858.
- [30] Storkholm, J. H., Villadsen, G. E., Jensen, S. L., Gregersen, H. (1995). Passive Elastic Wall Properties in Isolated Guinea Pig Small Intestine. *Digestive Diseases and Sciences*, 40(5), 976-982.
- [31] Duch, B. U., Petersen, J. A. K., Vinter-Jensen, L., Gregersen, H. (1996). Elastic Properties in the Circumferential Direction in Isolated Rat Small Intestine. *Acta Physiologica*, 157(2), 157-163.
- [32] Bourgouin, S., Bège, T., Masson, C., Arnoux, P., Mancini, J., Garcia, S., Berdah, S. (2012). Biomechanical Characterization of Fresh and Cadaverous Human Small Intestine: Applications for Abdominal Trauma. *Medical & Biological Engineering & Computing*, 50(12), 1279-1288.
- [33] Gao, C., Gregersen, H. (2000). Biomechanical and Morphological Properties In Rat Large Intestine. *Journal of Biomechanics*, 33(9), 1089-1097.
- [34] Yang, K., Hu, J., White, N., King, A. (2006). Development of Numerical Models for Injury Biomechanics Research: A Review of 50 Years of Publications in the Stapp Car Crash Conference. *Stapp Car Crash Journal*, 50, 429-490.
- [35] Li, W. G., Luo, X. Y., Hill, N. A., Ogden, R. W., Smythe, A., Majeed, A. W., & Bird, N. (2012). A Quasi-Nonlinear Analysis of The Anisotropic Behavior of Human Gallbladder Wall. *Journal of Biomechanical Engineering*, 134(10), 1-9.

- [36] Snedeker, J., Niederer, P., Schmidlin, F., Farshad, M., Demetropoulos, C., Lee, J., Yang, K. (2005). Strain-Rate Dependent Material Properties of the Porcine and Human Kidney Capsule. *Journal of Biomechanics*, 38(5), 1011-1021.
- [37] Kemper, A., Santago, A., Stitzel, J., Sparks, J., Duma, S. (2012). Biomechanical Response of Human Spleen in Tensile Loading. *Journal of Biomechanics*, 45(2), 348-355.
- [38] Ball, C. G., Dixon, E., Kirkpatrick, A. W., Sutherland, F. R., Laupland, K. B., Feliciano, D. V. (2010). A Decade of Experience with Injuries to the Gallbladder. *Journal of Trauma Management & Outcomes*, 4(1), 1-4.
- [39] Soderstrom, C. A., Maekawa, K. A. Z. U. H. I. K. O., DuPriest Jr, R. W., Cowley, R. A. (1981). Gallbladder Injuries Resulting from Blunt Abdominal Trauma: An Experience and Review. *Annals of Surgery*, 193(1), 60-66.
- [40] Wirth, G., Peter, R., Poletti, P., Iselin, C. (2010). Advances in the Management of Blunt Traumatic Bladder Rupture: Experience with 36 Cases. *BJU International*, 106(9), 1344-1349.
- [41] Hsieh, C., Chen, R., Fang, J., Lin, B., Hsu, Y., Kao, J., ... Kang, S. (2002). Diagnosis and Management of Bladder Injury by Trauma Surgeons. *The American Journal of Surgery*, 184(2), 143-147.
- [42] Quagliano, P. V., Delair, S. M., Malhotra, A. K. (2006). Diagnosis of Blunt Bladder Injury: A Prospective Comparative Study of Computed Tomography Cystography and Conventional Retrograde Cystography. *Journal of Trauma and Acute Care Surgery*, 61(2), 410-422.

- [43] Watts, D. D., Fakhry, S. M., EAST Multi-Institutional HVI Research Group. (2003). Incidence of Hollow Viscus Injury in Blunt Trauma: An Analysis From 275,557 Trauma Admissions from The East Multi-Institutional Trial. *Journal of Trauma and Acute Care Surgery*, 54(2), 289-294.

Chapter 6 : Conclusion

6.1 Summary

This research has investigated the material properties of human and porcine abdominal organs, resulting in an expansion of knowledge of the abdominal organ material properties and a framework for more accurately modeling their behavior under dynamic loading conditions. Through a comprehensive literature review, gaps in the existing knowledge were identified and specific research goals were created. The feasibility of substituting porcine tissue for human tissue and quantifying the relationship of strain rate dependency for all organs of interest were investigated. For the organs that require compression testing, the effect of using a probing protocol versus an unconfined compression protocol were compared. The end result of this research is that the material properties for the investigated organs were either established or further characterized. A summary of the results for each posed research question is provided in Table 6-1.

The elastic modulus, failure stress, and failure strain of the prostate organ has been characterized for the human and porcine hosts. An unconfined compression protocol and probing protocol were used to derive the elastic modulus of the prostate, which found no differences between the methods. Porcine prostates were measured to be slightly stiffer than the human hosts, which is a difference that could be contributed to the age of the host. A strain rate dependency was found for the property of elastic modulus and this dependency was observed to saturate at the rate of 100%/s.

Table 6-1: Results to all research objectives for each organ.

Paper	Organ	Porcine Feasible Substitute	Strain Rate Dependent			Strain Rate Saturates			Probing Vs. Compression
			Elastic Modulus	Failure Stress	Failure Strain	Elastic Modulus	Failure Stress	Failure Strain	
Paper 1	Prostate	Yes	Yes	No	No	Yes	N/A	N/A	Not Equal
Paper 2	Liver	Yes	Yes	Yes	Yes	Yes	Yes	Yes	Equal
	Kidney	Yes	Yes	Yes	No	Yes	Yes	N/A	Not Equal
Paper 3	Spleen	Yes	Yes	Yes	No	No	Yes	N/A	Not Equal
Paper 4	Bladder	Undetermined	Yes	Yes	No	No	Yes	N/A	N/A
	Gallbladder	Yes	Yes	Yes	No	No	Yes	N/A	N/A
	Intestines	Yes	Yes	Yes	No	Yes	Yes	N/A	N/A

Similar testing was performed on the liver for both human and porcine hosts that was conducted on the prostate. A large number of studies have characterized the material properties of this organ, but this is the first study that directly compares the properties resulting from different methodologies and different hosts. With little differences measured between the material properties of the liver, the porcine host was determined to be a feasible substitute for human tissue in the unconfined compression protocol. However, due to the differing geometry between the human and porcine liver the elastic modulus from the probing protocol was not similar between the two hosts. A dependency on strain rate was observed for the elastic modulus, failure stress, and failure strain, but the strain rate dependence started to saturate at a rate of 100%/s. A model was derived to describe this effect to aid in model development.

The kidney mechanical properties have also been extensively studied using various protocols and with various hosts. However, a direct comparison of the results from methodologies using the same tissue and a comparison using identical protocols with different hosts had yet to be performed. It was found that porcine kidney material properties are similar to those of human kidneys and thus a feasible substitute. The probing protocol resulted in slightly higher elastic modulus highlighting how different methods can yield different results. A strain rate dependency was found for the elastic modulus and failure stress with this effect starting to saturate at a rate of 100%/s.

Human and porcine spleens were also tested using the compression protocols. Porcine spleens were found to be a feasible substitute for human tissue in both probing and unconfined compression protocols. The probing protocol resulted in a higher stiffness than what was found using unconfined compression, highlighting how the

testing protocol can affect the results obtained. A strain rate dependency for the elastic modulus and failure stress was found and numerically modeled. The failure stress and elastic modulus increased as strain rate increased, but the relationship starts to saturate at a rate of 100%/s.

Three more organs were investigated using a tension testing protocol. Due to the structure of the gallbladder, bladder, intestine a uniaxial tension protocol was most suitable to mimic the *in-vivo* loading conditions. The elastic modulus, failure stress, and failure strain was determined for all four organs from both human and porcine hosts at varying rates. Porcine tissue was determined to be a feasible substitute for human tissue as similar results were found for elastic modulus and the failure properties for almost all organs investigate. Further research is required for the bladder as the elastic modulus and failure stress was doubled, and failure strain was half that of human specimens as they for porcine. A strain rate dependency was observed in the gallbladder, bladder, intestine. The failure stress of the gallbladder, bladder, and intestine exhibited a saturation in strain rate dependency above the rates of 100%/s. However, only the elastic modulus of the intestines were observed to have a diminishing effect of strain rate above the rates of 100%/s.

Overall, valuable information was gathered that expands the knowledge of material properties for researchers in this field. The results can be used to improve the accuracy and expand the abilities of finite element models regarding the human abdomen. A better understanding of the mechanism of various injuries to the abdomen in high force traumatic situations can thus be achieved using higher fidelity models that more accurately capture the material behavior at varying strain rates. Improved finite

element models will aid the fields of forensics, diagnostics, injury prediction, personal protective equipment development, and many other fields.

6.2 Future Work

Possible continuation of this research could include further testing of human specimens. Currently, the number of specimens tested for most of the human organs is too small for statistical testing of the failure properties. Also, rates were tested up to 1000%/s in tension and unconfined compression tested, but only 25%/s for probing testing. Further characterizations at rates higher could be considered for future testing.

Only probing and unconfined compression testing protocols were compared through this research. Other protocol comparisons could be made such as tension testing and inflation testing or the Kolsky Bar Technique versus compression. Further comparisons between different techniques will enable researchers to fully understand the mechanical behavior of organs under different loading scenarios.

Future research extending from this work is to incorporate the measured material properties into finite element models and determine the effect this has on the results. With material properties characterized at several different rates, a sensitivity analysis can be performed on existing models to determine the effects of varying material properties due to strain rates on a model. The properties determined in this research can also lead to more detailed models that factor in previously ignored organs such as the intestines, bladder, and gallbladder. Incorporating these organs into the models will enable more research on the mechanism of injuries for the intestines,

bladder, and gallbladder as well as improve the understanding of other organs interaction with these surrounding tissues.

Furthermore, this work is the first of its kind to do such comprehensive work on characterizing the material properties of several organs within the abdominal cavity. One challenge for researchers is finding the most appropriate material properties to use within their model. A future step for this research is organizing an easily accessible database that will enable researchers in the field of modeling to have a resource which will increase their efficiency in being able to complete their work.

6.3 Research Significance/Contributions to the Field

The results of this research will make a significant impact in several different fields. Establishing and further characterizing the material property of abdominal organs is fundamental research that can be translated into many areas. First, the failure testing establishes threshold limits and provides an understanding of how much pressure the tissue can withstand which is significant in understanding that tolerance each organ has to resist force. Second, these material properties can be used within models that can provided a better understanding of the mechanism of injury for these organs. This better understanding of failure limits and improved models will aid fields such as injury prediction, personal protective equipment assessment, forensics, medical diagnosis, and many others.

The development of a numerical model to quantify the relationship between strain rate and material properties adds substantial knowledge to the field of abdominal organ material behavior. Through this research, not only is the strain rate dependency

established, it is measured and quantified. This information will aid researchers who create models for situations involving higher velocity impacts to the abdomen.

It has been a long unanswered question as to whether or not the material properties from an animal host is comparable to a human host for the purposes of mechanical modeling. This question was addressed for several abdominal organs within this dissertation. Previously, no research has been conducted that makes a direct comparison between porcine and human hosts using identical protocols. From the results of this research, an understanding is gained regarding which porcine organ material properties might be feasible substitutes for human material properties. This knowledge will help assess the accuracy of current models that often resort to using material properties derived from porcine organs as resources are limited for conducting this research on humans.

The knowledge gained from the work for this dissertation is intended to be published as technical reports to the funding agency, in peer-reviewed journals and presented at the scientific conferences. A total of 4 publications, which have already been written and constitute different portions of this dissertation, are under review, or planned for submission. The titles and status of these submission are in Table 6-1. This research has also resulted in several scientific conference presentations and a technical report that are also summarized in Table 6-1. Furthermore, concurrent with my dissertation research, other papers, conferences, and technical reports have been completed throughout the PhD program, and these are also summarized in Table 6-1. Honors and awards that are a result of the research performed are detailed in 6-2.

Table 6-2: List of peer-reviewed publications, conference presentations/abstracts/papers and technical reports *presented in this dissertation

PEER REVIEWED JOURNAL PAPERS STATUS	
<i>*The Differences in Measured Prostate Material Properties Between Probing and Unconfined Compression Testing Methods</i>	In Review (MEP)
<i>*Characterizing the Material Properties of The Kidney and Liver in Unconfined Compression and Probing Protocols with Special Reference to Varying Strain Rate</i>	In Review (JMBBM)
<i>*Characterizing the Material Properties of Human and Porcine Spleen with Special Reference to Changes in Strain Rate</i>	In Prep.
<i>*Biomechanical Properties of Abdominal Organs Under Tension with Special Reference to Increasing Strain Rate</i>	In Prep.
<i>*Johnson, B., Campbell-Kyureghyan, N. “A Comparison Of Strain Rate Dependency Between Human Prostate And Other Solid Organs In Unconfined Compression.”</i>	BSI, 2019
<i>Tomasiewicz, H. G., Johnson, B. A., & Liu, X. C. (2017). Development Of Zebrafish (Danio Rerio) As A Natural Model System For Studying 10 Scoliosis.</i>	JOSR, 2017
Conference Presentations	
<i>“The Strain Rate Dependency on the Elastic Modulus, Failure Stress, and Failure Strain of Human and Porcine Stomach Tissue”</i>	In Prep.
<i>*Johnson, B., Campbell-Kyureghyan, N. “The Effect of Strain Rate on the Mechanical Properties of the Human Liver Under Unconfined Compression.”</i>	Poster, ISB, 2019

*Johnson, B., Campbell-Kyureghyan, N. "A Comparison Of Strain Rate Dependency Between Human Prostate And Other Solid Organs In Unconfined Compression."	Podium, RMBS, 2019
Johnson, B., Campbell-Kyureghyan, N. "Dynamic Response Of The Human Penis To Tensile Loading At Various Strain Rates."	Poster, ASB, 2017
*Johnson, B., Campbell-Kyureghyan, N. "Dynamic Response Of Human Spleen To Various Compression Strain Rates."	Podium, GLBC, 2017
Wang, Y., Johnson, B., Campbell-Kyureghyan, N. "The effect of K-Tape on knee flexion/extension performance in a fatiguing task." 2017 IEEE Great Lakes Biomedical Conference	Poster, GLBC, 2017
*Johnson, B., Campbell, S., Campbell-Kyureghyan, N., "Comparison of Kidney Elastic Modulus Using Full Unconfined Compression and Probing Methods."	Poster, ASB, 2016
Porter, Q., Johnson, B., Campbell-Kyureghyan, N. "Comparison of Upper Arm Muscle Activity and User Tool Preference During Wrenching Task."	Poster, ASB, 2016
Johnson, B., Campbell-Kyureghyan, N., Otieno, W., O'Connor, K., "Influence of Jackhammer Weight on Hand Arm Vibration Transmission."	Podium, ASB, 2015
Johnson, B., Tomasiewicz, H., Campbell-Kyureghyan, N., "Towards the Development of a Testable Model for Spinal Deformities using Zebrafish."	Podium, GLBC, 2015
Technical Reports	
Kyureghyan-Campbell, N., Johnson, B. "Injury and Safety Hazard Prevention in the Oil and Gas Production Industry: Final Closeout Report", p1-56, Chicago, IL. March, 2019.	2019
*Kyureghyan-Campbell, N., Johnson, B. "Pelvic Model with Multi-Sensory Data Acquisition (ELVIS)." Physical Optics Corporation, p1-93, Torrence, CA. February, 2016.	2016

Table 6-3: List of honors and awards since the start of PhD

Honors and Awards	Year
Rocky Mountain Biomechanics Symposium Presidents Award	2019
Chancellor's Graduate Student Award	2019
Distinguished Graduate Student Fellowship	2014
Deans Doctoral Fellowship	2014

Chapter 7 : Curriculum Vitae

Blake Johnson, BS, MS, PhD

PROFESSIONAL PREPARATION

Undergraduate:

Marquette University	Exercise Physiology	B.S.	2012 (gpa: 3.37)
----------------------	---------------------	------	------------------

Graduate:

University of Wisconsin-Milwaukee	Industrial Engineering	M.S.	2014 (gpa: 3.97)
-----------------------------------	------------------------	------	------------------

University of Wisconsin-Milwaukee	Engineering	Ph.D.	2019 (gpa: 3.925)
-----------------------------------	-------------	-------	-------------------

APPOINTMENTS

Academic:

8/15 – 12/15	Instructor, Industrial and Manufacturing Engineering Department, UWM
6/12 - pres	Research Assistant, Bioengineering Imaging and Testing Laboratory, UWM
8/13 – 12/13	Teaching Assistant, Industrial and Manufacturing Engineering Department, UWM
8/11 – 5/12	Research Assistant, Mechanical Engineering Department, Marquette University

HONORS AND AWARDS

2019	Rocky Mountain Bioengineering Symposium President's Award
2019	Chancellor's Graduate Student Award (University of Wisconsin-Milwaukee)
2015	Chancellor's Graduate Student Award (University of Wisconsin-Milwaukee)
2014	Academic Excellence Award (University of Wisconsin-Milwaukee)
2014	Deans Doctoral Fellowship (University of Wisconsin-Milwaukee)
2014	Distinguished Graduate Student Fellowship (University of Wisconsin-Milwaukee)
2014	Honorable Mention in CEAS Poster Competition (University of Wisconsin-Milwaukee)
2013	Chancellor's Graduate Student Award (University of Wisconsin-Milwaukee)
2013	1st Place IEEE Larry Hause Student Poster Competition
2012	Chancellor's Graduate Student Award (University of Wisconsin-Milwaukee)

2011	Big East All Academic Team (Marquette University)
2010	USTFCCA National All-Academic Team (Marquette University)
2010	Big East All Academic Team (Marquette University)
2009	USTFCCA National All-Academic Team (Marquette University)
2009	Big East All Academic Team (Marquette University)
2008	Ignatious Scholarship Recipient for Academics (Marquette University)

REFEREED PUBLICATIONS AND PRESENTATIONS

- **Johnson, B.**, Campbell-Kyureghyan, N. “The Effect of Strain Rate on the Mechanical Properties of the Human Liver Under Unconfined Compression.” Poster presentation, International Society of Biomechanics Conference. Calgary, AB. August 4th, 2019.
- **Johnson, B.**, Campbell-Kyureghyan, N. “A Comparison Of Strain Rate Dependency Between Human Prostate And Other Solid Organs In Unconfined Compression.” Biomedical Science Instrumentation. April, 2019; 55(2):285-291.
- **Johnson, B.**, Campbell-Kyureghyan, N. “A Comparison Of Strain Rate Dependency Between Human Prostate And Other Solid Organs In Unconfined Compression.” 2019 IEEE Rocky Mountain Biomechanics Symposium (RMBS). April 12th, 2019.
- **Johnson, B.**, Campbell-Kyureghyan, N. “Dynamic Response Of The Human Penis To Tensile Loading At Various Strain Rates.” Poster presentation, American Society of Biomechanics Conference. Boulder, CO. August 10th, 2017.
- Tomasiewicz, H.G., **Johnson, B.A.** and Liu, X.C., 2017. Development of Zebrafish (*Danio rerio*) as a natural model system for studying 10 scoliosis. *J Orthop Surg Rehabil* 2017; 1 (1): 9-14.
- **Johnson, B.**, Campbell-Kyureghyan, N. “Dynamic Response Of Human Spleen To Various Compression Strain Rates.” 2017 IEEE Great Lakes Biomedical Conference (GLBC). April 6th, 2017.
- Wang, Y., **Johnson, B.**, Campbell-Kyureghyan, N. “The effect of K-Tape on knee flexion/extension performance in a fatiguing task.” 2017 IEEE Great Lakes Biomedical Conference (GLBC). April 6th, 2017.
- **Johnson, B.**, Otieno, W., Campbell-Kyureghyan, N. “Quantitative and Qualitative Evaluation of the Lift-assist Device during Jackhammering Task.” *Journal of Ergonomics*. July 27th, 2017.

- **Johnson, B.**, Otieno, W., Campbell-Kyureghyan, N. “Influence of Jackhammer Weight On Grip Pressure, Muscle Activity, and Hand-Arm Vibration Of The Operator.” IIE Transactions of Occupational Ergonomics and Human Factors. January 31st, 2017.
- **Johnson, B.**, Campbell, S., Campbell-Kyureghyan, N., “Comparison of Kidney Elastic Modulus Using Full Unconfined Compression and Probing Methods.” ASB Conference, Raleigh, NC. August 5th 2016.
- Porter, Q., **Johnson, B.**, Campbell-Kyureghyan, N. “Comparison of Upper Arm Muscle Activity and User Tool Preference During Wrenching Task.” ASB Conference, Raleigh, NC. August 5th 2016.
- **Johnson, B.**, Campbell-Kyureghyan, N., Otieno, W., O’Connor, K., “Influence of Jackhammer Weight on Hand Arm Vibration Transmission.” ASB Conference, Columbus, OH. August 8th 2015.
- **Johnson, B.**, Tomasiewicz, H., Campbell-Kyureghyan, N., “Towards the Development of a Testable Model for Spinal Deformities using Zebrafish.” GLBC, Milwaukee, WI. May 14th 2015.
- **Johnson, B.**, Campbell-Kyureghyan, N., “Biomechanical Evaluation of a Lift Assist Device Using a Lightweight Jackhammer.” HFES Conference, Chicago, IL. October 29th 2014.
- **Johnson, B.**, Campbell-Kyureghyan, N., “3D Geometric Model of Zebrafish to Study Spinal Deformities Using CT Imaging.” CEAS Conference, Milwaukee, WI. April 18th 2015.
- **Johnson, B.**, Campbell-Kyureghyan, N., “Response to Muscle Activity to a Jackhammering Task with and without a Lift Assist.” ISOES Conference, El Paso, TX. June 5th 2014.
- Campbell-Kyureghyan, N., **Johnson, B.** “Ergonomic Evaluation of Lift Assist Device During Jackhammering Task.” AGA Operations Conference, Pittsburg, PA. May, 22 2014.
- **Johnson, B.**, Campbell-Kyureghyan, N.(2013). “Evaluation of Grip Pressure and Hand-Arm Vibration in Jackhammering Task with and without a Lift Assist.” Poster presentation, American Society of Biomechanics Conference. Omaha, NE.
- **Johnson, B.**, Dix, P., Campbell-Kyureghyan, N.(2013). “Biomechanical Evaluation of a Jackhammer Lift Assist.” Poster presentation, College of Engineering, Arts, and Sciences Poster Competition. Milwaukee, WI.

- **Johnson, B.**, Dix, P., Campbell-Kyureghyan, N. (2013). “Benefits of Jackhammering with a Lift Assist.” Poster presentation, 36th GLBC. Milwaukee, WI.
- **Johnson, B.**, Dix, P., Campbell-Kyureghyan, N.(2013). “Biomechanical Evaluation of a Jackhammer Lift Assist.” Poster presentation, IEEE Larry Hause Student Poster Competition. Milwaukee, WI.
- Lomo-Tettey, D., Campbell-Kyureghyan, N., **Johnson, B.** Beschorner, K. (2013). “Leg and Torso Response to Prolonged Kneeling.” Poster presentation, American Society of Biomechanics Conference. Omaha, NE.
- Lomo-Tettey, D., **Johnson, B.**, Campbell-Kyureghyan, N., Beschorner, K., (2013). “Muscle Co- Activation During Prolong Kneeling.” Poster presentation, 36th GLBC. Milwaukee, WI.
- Hernandez-Principe, A., **Johnson, B.**, Campbell-Kyureghyan, N., Beschorner, K. (2013). “Application Of Near Infrared Spectroscopy to Detect Changes During and After the Keeling Task.” Poster presentation, 36th GLBC. Milwaukee, WI.
- Hernandez-Principe, A., **Johnson, B.**, Campbell-Kyureghyan, N., Beschorner, K. (2013). “Application Of Near Infrared Spectroscopy to Detect Changes During and After the Keeling Task.” Poster presentation, College of Engineering, Arts, and Sciences Poster Competition. Milwaukee, WI.
- Hernandez-Principe, A., **Johnson, B.**, Campbell-Kyureghyan, N., Beschorner, K. (2013). “Application Of Near Infrared Spectroscopy to Detect Changes During and After the Keeling Task.” Poster presentation, IEEE Larry Hause Student Poster Competition. Milwaukee, WI.
- Lomo-Tettey, D., **Johnson, B.**, Campbell-Kyureghyan, N., Beschorner, K., (2013). “Muscle Co- Activation During Prolong Kneeling.” Poster presentation, College of Engineering, Arts, and Sciences Poster Competition. Milwaukee, WI.

TECHNICAL REPORTS

- Kyrueghyan-Campbell, N., **Johnson, B.** "Injury and Safety Hazard Prevention in the Oil and Gas Production Industry: Final Closeout Report", p1-56, Chicago, IL. March, 2019.
- Kyrueghyan-Campbell, N., **Johnson, B.** "Pelvic Model with Multi-Sensory Data Acquisition (ELVIS)." Physical Optics Corporation, p1-93, Torrence, CA. February, 2016.
- Aurit, C., **Johnson, B.** "Evaluation of Accessibility: Microsoft Office 365 and Google Apps for Education." University of Wisconsin-Milwaukee, p1-4, Milwaukee, WI. December 2013.
- **Johnson, B.**, Campbell-Kyureghyan, N. "Jackhammer Study: Phase II. Technical Report." Gas Technologies Institute, p1-86, Chicago, IL. July, 2013.
- Adamo, M., Bubaris, J., Jarnecke, D., Daniels, N. Campbell-Kyureghyan, N., **Johnson, B.** "GTI/OTD Quarterly Report: Light Weight Jackhammer, Phase II." Gas Technology Institute, p1-3. Chicago, IL. April 2013.

INDUSTRY PROJECTS

- Gas Technology Institute
- Snap-On Tools
- Iron Clad Gloves
- Ringer Gloves

PROFESSIONAL MEMBERSHIP

2013 - present Member, American Society of Biomechanics (ASB)

2012 - present Member, Human Factors and Ergonomics Society (HFES)

SERVICE

- 2015 - 2018 Volunteer, Special Olympics Triathlon
- 2013 – 2017 Treasurer, Human Factors and Ergonomics Society and Student Chapter at UWM
- 2013 (Fall) Community Outreach, Organization Festival Informational Display, HFES at UWM
- 2013 (Fall) Community Outreach, Party at the Plaza Informational Display, HFES at UWM
- 2012 - 2013 Secretary, Human Factors and Ergonomics Society and Student Chapter at UWM
- 2010 Volunteer, Hunger Task Force, Marquette University Track and Field
- 2009 – 2010 Volunteer, Teaching Assistant for Milwaukee School of Chinese Learning, Marquette University

TEACHING

2017	Teaching Assistant	Introduction to Ergonomics
2016	Teaching Assistant	Design of Experiments
2016	Teaching Assistant	Ergonomic Job Evaluation Techniques
2015	Instructor	Introduction to Ergonomics
2013	Teaching Assistant	Introduction to Ergonomics

SYNERGISTIC ACTIVITIES

- Mentored undergraduate students in various research activities
- Helped organized CARGI Train the Trainer event
- Helped organizational sponsored speakers